FUNCTIONAL ANALYSIS OF RACK1 AS A NOVEL INTERACTION PARTNER OF BMPRII IN PULMONARY ARTERIAL HYPERTENSION

ANNA ZAKRZEWICZ

Functional analysis of RACK1 as a novel interaction partner of BMPRII in pulmonary arterial hypertension

Inaugural-Dissertation

zur Erlangung des Grades eines
Doktors der Humanbiologie
des Fachbereichs Medizin der
Justus-Liebig-Universität Gießen

vorgelegt von

Anna Zakrzewicz

aus Skarzysko-Kamienna, Polen

Gießen, 2006

Aus dem Zentrum für Innere Medizin

des Klinikums der Justus-Liebig-Universität Gießen

Director: Prof. Dr. W. Seeger

I Table of contents

II List of figures

III List of tables

IV Abbreviations

AA	Amino acid
ActR	Activin receptor
AD	Activation domain
ALK1	Activin like kinase type one
APS	Ammonium persulfate
APAH	Pulmonary arterial hypertension related to associated conditions
BAMBI	BMP and activin membrane bound inhibitor
BD	Binding domain
BISC	BMP-induced signalling complexes
BMP	Bone morphogenetic proteins
BMPRII	Bone morphogenetic protein receptor type two
BRE	BMP-responsive element
CD	Cytoplasmic domain
cDNA	Complementary deoxyribonucleic acid
CHAPS	3-[3-chloramidopropyl)dimethylammonio]-1-propanesulfonate
Co-Smad	Common Smad
DAPI	4´,6´-diamidino-2-phenylindole
DMSO	Dimethyl sulfoxide
DTT	Dithiothreitol
ECD	Extracellular domain
EDTA	Ethylendinitrilo-N,N,$N´,N´$,-tetra-acetate
ERK1	Extracellular-signal regulated kinase 1
FACS	Fluorescence-activated cell sorting
FBS	Foetal bovine serum
FPAH	Familial pulmonary arterial hypertension
GDF	Growth-differentiation factor
GFP	Green fluorescent protein
GST	Gluthathione S-transferase
HEPES	2-(-4-2-hydroxyethyl)-piperazinyl-1-ethansulfonate
HHT	Hereditary haemorrhagic telangiectasia
HIV	Human immunideficiency virus
IB	Immunoblot
ICCH	Immunocytochemistry
ID	Intracellular domain

IHCH	Immunohistochemistry
IP	Immunoprecipitation
IPAH	Idiopathic pulmonary arterial hypertension
IPTG	Isopropyl β-thiogalactopyranoside
I-Smad	Inhibitory Smad
KD	Kinase domain
LB	Luria-Bertani
MAPK	Mitogen-activated protein kinase
MCT	Monocrotaline
MCTP	Monocrotaline pyrole
MH1	Mad homology domain
NIH	National Institutes of Health
NLK	Nemo-like kinase
OD	Optical density
OP	Osteogenic protein
ORF	Open reading frame
PAH	Pulmonary arterial hypertension
PAP	Pulmonary arterial preassure
paSMC	Pulmonary arterial SMC
PBGD	Porphobilinogen deaminase
PBS	Dublecco' s phosphate buffered saline
PCR	Polymerase chain reaction
PDE	Phosphodiesterase
PEG	Polyethylene glycol
PFC	Preformed oligomeric receptor complexes
PH	Plekstrin homology domain
PIASy	Protein inhibitor of activated STAT4
PKC	Protein kinase C
RACK1	Receptor for activated protein kinase C
R-Smad	Receptor Smad
RT-PCR	Reverse transcription polymerase chain reaction
RV/LV+S	Right ventricle to left ventricle plus septum ratio
SD	Synthetic dropout solution
SDS	Sodium dodecyl sulfate
SDS-PAGE	SDS polyacrylamide gel electrophoresis
SH2	Src homology domain

siRNA	Small interfering RNA
Smurf1	Smad-ubiquitination regulatory factor 1
SMA	Smooth muscle actin
SMC	Smooth muscle cell
SP	Signalling peptide
SUMO	Small ubiquitin related modifire
TA	Transcriptional activator
TAK1	TGFβ activated kinase 1
TAB1	Tak1 binding proteins
TAE	Tris acetate EDTA
TE	Tris/EDTA
TBST	Tris-buffered saline + 0.1% Tween 20
TCF	T-cell-specific transcription factor
TGFβ	Transforming growth factor beta
TM	Transmembrane
UAS	Upstream activating sequences
UTR	Untranslated region
WT	Wild type
XIAP	X-linked inhibitor of apoptosis
YPDA	Yeast extract/peptone/dextrose/adenine medium.

III Summary

Pulmonary arterial hypertension (PAH) is characterised by selective elevation of pulmonary arterial pressure. The pathological hallmark of PAH is the occlusion of pulmonary arterioles due to proliferation and dysfunction of smooth muscle and endothelial cells. Heterozygous mutations in *BMPR2*, encoding the type II BMP receptor (BMPRII), were identified in PAH suggesting that alterations to BMPRII function are involved in disease onset and/or progression.

To further elucidate the function of BMPRII, we sought to identify novel interaction partners of BMPRII by yeast two-hybrid analysis using the kinase domain of BMPRII as a bait. Using this technology, several novel interaction partners of BMPRII were identified. Among these, the receptor for activated protein kinase C (RACK)-1 was selected for further investigation. The interaction between RACK1 and the BMPRII kinase domain was confirmed by Glutathione S-transferase (GST)-pull-down and co-immunoprecipitation. Immunofluorescent staining of human pulmonary artery smooth muscle cells (paSMC), as well immunohistochemistry of human lungs from healthy donors and PAH patients, demonstrated the co-localisation of BMPRII and RACK1 *in vitro* and *in vivo.* Overexpression of RACK1 in paSMC led to a two-fold increase in induction of a BMP-responsive promoter in a luciferase-based promoter reporter assay, indicating that the BMPRII-RACK1 interaction may potentiate BMP signalling. RACK1 depletion using small interfering RNA (siRNA) technology resulted in enhanced proliferation of paSMC, thus implicating a role for RACK1 and the RACK1-BMPRII interaction in paSMC growth regulation. In contrast, overexpression of RACK1 led to enhanced proliferation of paSMC.

Several BMPRII variants that contained amino acid substitutions present in PAH patients exhibited a reduced affinity for RACK1. Furthermore, in the monocrotaline-induced rat model of PAH, the expression of RACK1 was significantly down-regulated at the RNA and protein level, two and four weeks after monocrotaline administration.

Thus, the novel interaction of RACK1 with BMPRII is functionally significant in BMP signal transduction. The reduced affinity of RACK1 for BMPRII variants that are peculiar to PAH patients, and the reduced levels of RACK1 evident in the pulmonary vasculature in an animal model of PAH, suggest a potential role for RACK1, and the RACK1-BMPRII interaction, in the pathogenesis of PAH.

IV Zusammenfassung

Die Pulmonalarterielle Hypertonie (PAH) ist charakterisiert durch eine selektive Erhöhung des pulmonalarteriellen Blutdrucks. Das pathologische Korrelat der PAH ist ein Verschluss der pulmonalen Arteriolen durch eine Proliferation/Fehlfunktion der glatten Gefässmuskelzellen und des Endothels. Heterozygote Keimbahnmutationen im Bone Morphogenetic Receptor Type II (BMPRII) kodierenden Genlokus zeigen eine Assoziation mit PAH, was für einen Einfluss des BMPRII auf die Pathogenese der PAH spricht.

Um die Funktion von BMPRII zu charakterisieren, war es das Ziel unserer Arbeit, neue potentielle Interaktionspartner dieses Rezeptors mittels Yeast Two-Hybrid Analyse zu identifizieren. Unter den vielen bisher unbekannten Interaktionspartnern von BMPRII wurde RACK (receptor for activated protein kinase C)-1 für weitergehende Untersuchungen ausgewählt. Glutathion S-Transferase (GST)-pulldown Experimente sowie Ko-Immunopräzipitationen bestätigten die Interaktion von RACK1 und der BMPRII Kinasedomäne. Immunohistochemische Analysen von Lungenschnitten und Immunofluoreszenzanalysen isolierter glatter Muskelzellen aus der Pulmonalarterie zeigten eine Ko-Lokalisation von BMPRII und RACK1 *in vitro* und *in vivo*. Für weitere funktionelle Analysen wurde das RACK1 Gen kloniert und in einem BMP-Reportergenassay überexprimiert. RACK1 Expression führte zu einer zweifach erhöhten Reportergenaktivität nach BMP-2 Stimulation, was einen synergistischen Einfluss der BMPRII-RACK1 Interaktion auf die BMP Signalkaskade zeigt. Dieser Befund wird durch die Tatsache unterstüzt, dass die Depletion von RACK1 mittels small interfering RNA (siRNA) Technologie zu einer verstärkten Proliferation von glatten Gefässmuskelzellen der A. Pulmonalis führt, was für eine regulatorische Rolle von RACK1 auf das Zellwachstum spricht.

Mehrere BMPRII Varianten, welche aus dem internationalen PAH Patientenpool stammen, zeigten eine reduzierte Affinität für RACK1. Im Tiermodell der durch Monokrotalin induzierten pulmonalen Hypertonie wurde eine signifikant erniedrigte Expression von RACK1 auf RNA und Proteinebene gefunden.

Die vorliegende Arbeit beschreibt daher einen funktionell bedeutenden Einfluss der neu identifizierten Interaktion zwischen BMPRII und RACK1 auf die BMP Signaltransduktion. Die reduzierte Affinität von RACK1 für BMPRII Varianten und die erniedrigte RACK1 Expression im Tiermodell der pulmonalen Hypertonie sprechen für einen bedeutenden Einfluss von RACK1 und der RACK1-BMPRII Interaktion auf die Pathogenese der PAH.

1   Introduction

1.1   Pulmonary arterial hypertension

1.1.1   Characteristics of pulmonary arterial hypertension

Pulmonary arterial hypertension (PAH) is a progressive disease characterised by elevated pulmonary vascular resistance, which results in diminished right heart function due to increased right ventricular afterload. Clinically, PAH is defined as an elevation in the mean pulmonary arterial pressure of at least 25 mm Hg at rest, or greater than 30 mm Hg during exercise; while in healthy adults it does not exceed 12-16 mm Hg. Gradual clinical deterioration occurs when the mean pulmonary artery pressure plateaus at 60-70 mm Hg, and cardiac output progressively declines (Rich et al., 1987). The symptoms of PAH are largely non-specific, but may include shortness of breath, chest pain, syncope, fatigue, and peripheral oedema (Gaine and Rubin 1998; Strange et al., 2002).

This rare disorder with an estimated incidence of two to three cases per million (per year) worldwide, occurs most commonly in young and middle-aged women but is fatal, with a mean survival of two to three years after onset of symptoms (McLaughlin et al., 2002). The pathogenesis of IPAH remains poorly understood, although vasoconstriction is believed to be an early component in the development of the disease. Excessive vasoconstriction has been correlated with abnormal function or expression of potassium channels, as well as endothelial dysfunction, which subsequently leads to chronically impaired production of vasodilators such as nitric oxide and prostacyclin, along with overexpression of vasoconstrictors such as endothelin (ET)-1 (see Figure 1.1) (Humbert et al., 2004). Exposure to a variety of stimuli, including high-altitude hypoxia, appetite suppressants, monocrotaline extracts, inhaled solvents, cocaine, and infections (particularly with human immunodeficiency virus (HIV)) may also trigger an initial inflammatory response that may lead to PAH (Cheever 2005). Genetic predisposition may also direct the activity of pulmonary artery fibroblasts, smooth muscle cells (SMC), and endothelial cells, as well as platelets and leukocytes or their specific interactions with different extrinsic factors, that lead to the development of PAH (Humbert et al., 2004).
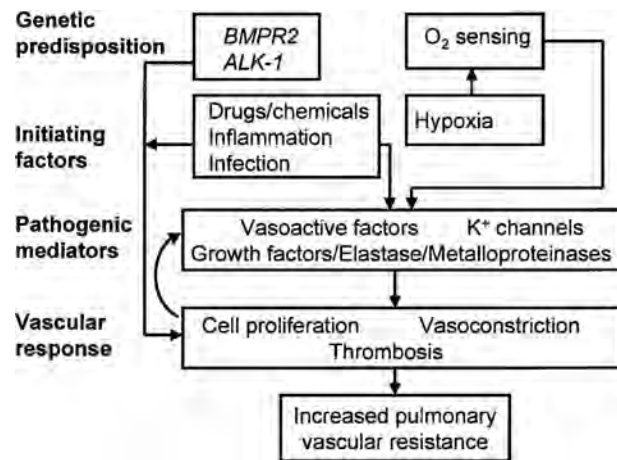
Figure 1.1   Interaction between genetic and extrinsic factors that lead to PAH (after Strange et al., 2002).

A recent classification of PAH is based on the aetiology of the various forms of this disease, and three principle categories of PAH have been identified: idiopathic pulmonary arterial hypertension (IPAH), familial pulmonary arterial hypertension (FPAH) and pulmonary arterial hypertension related to associated conditions (APAH). In the case of the latter, associated conditions include connective tissue disease, congenital heart defects, HIV infection and thromboembolic diseases (Simonneau et al., 2004).

1.1.2   Histopathology of pulmonary arterial hypertension

The different forms of PAH exhibit similar clinical presentation and functional derangement (Pietra 1994; Pietra et al., 2004). Histological changes, common to all forms of PAH, affect the pulmonary vasculature and the right ventricle. Pulmonary vascular remodelling associated with PAH involves all layers of the vessel wall, resulting in remarkable changes in the structure, numbers and function of all cells located in the vessel wall (endothelial cells, SMC, and fibroblasts) (see Figure 1.2). These changes include cellular hypertrophy, hyperplasia and an increased deposition of structural matrix proteins (e.g. collagen and elastin) in the vessel wall. During the development of PAH, a narrowing of the vessel lumen caused by intimal proliferation (proliferation of endothelial cells), medial thickening (through the hypertrophy and hyperplasia of SMC) and adventitial remodelling (via fibroblast proliferation and extracellular matrix deposition) is observed. In addition, a hallmark of PAH is the formation of a layer of myofibroblasts and extracellular matrix between the endothelium and the internal elastic lamina, termed the

neointima. Remodelling also involves the distal extension of SMC into small peripheral (normally nonmuscular) pulmonary arteries within the respiratory acinus as well as the formation of plexiform lesions. However, the precise composition of plexiform lesions is not known. It has been proposed that abnormal monoclonal endothelial cell proliferation, in a process of local angiogenesis, leads to occlusion of small arteries. Alternatively, plexiform lesions may be formed by transdifferentiation of endothelial cells into SMC (Tuder et al., 1994; Durmowicz and Stenmark 1999; Jeffery and Morrell 2002; Mandegar et al., 2004).

Donor **PAH**
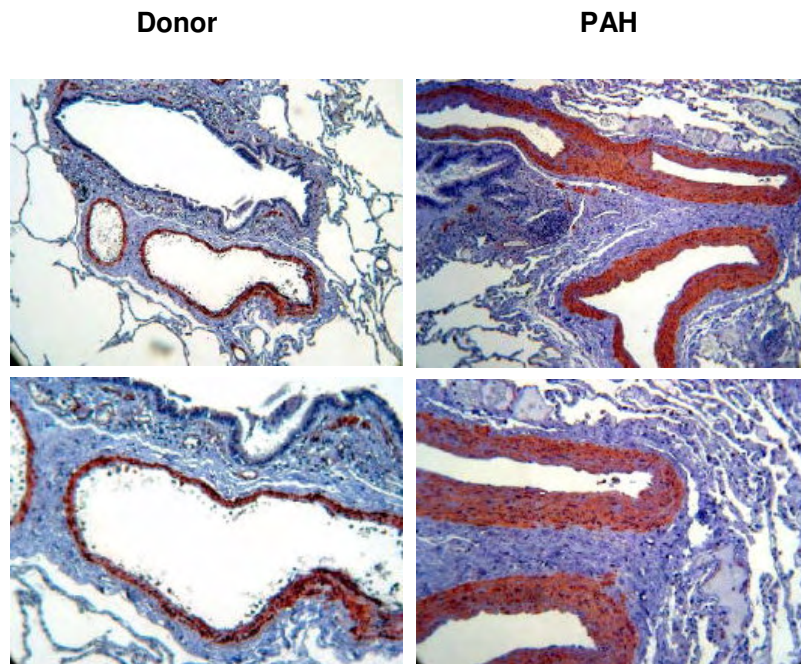
Figure 1.2   Histopathological changes observed in PAH.
Pulmonary arterioles in a normal patients (left) and in patients with PAH (right) with significantly hypertropic tunica medium (after Eickelberg and Seeger 2005).

1.1.3   Genetic basis of pulmonary arterial hypertension

In the National Institutes of Health (NIH) PAH registry, 6% of affected patients were identified as having a familial association with the disease (Rich et al., 1987). In an effort to understand the genetic basis of the disease, most studies have focused either on the imbalance between vasoconstriction and vasodilatation, or on specific growth factors, inflammatory mediators or ion channels (Geraci et al., 2001).

Mutations in two receptors of the transforming growth factor-beta (TGFβ) superfamily are present in majority of cases of FPAH (Lane et al., 2000). Mutations in

the exonic regions of the bone morphogenetic protein receptor type 2 *(BMPR2)* gene are found in about 50% of familial cases. Additionally, an activin like kinase type 1 (ALK1) gene mutation was found in patients with hereditary haemorrhagic telangiectasia (HHT) that was co-existant with PAH (Trembath 2001; Harrison et al., 2003). Furthermore, about 10% of patients with sporadic idiopathic IPAH have *BMPR2* mutations (Thomson et al., 2000).

The incidence of the *BMPR2* mutations in the general population is unknown, but is thought to be exceeding low. It is suggested that the 50% of familial cases lacking exonic mutations and apparently 90% sporadic cases have either intronic *BMPR2* or *ALK1* polymorphisms, or alterations in the promoter or 5´ UTR regions of these genes. It is also possible that genetic predispositions exist concerning normal variations in genes that influence the pulmonary circulation (Newman et al., 2004).

1.1.4   Animal models of pulmonary arterial hypertension

A number of animal models have been used to gain insight into pathogenesis of IPAH, most commonly employing hypoxia or monocrotaline. However none of these models reproduce the full spectrum of changes observed in IPAH patients. Nevertheless, they have been useful for hypothesis testing.

1.1.4.1   The monocrotaline rat model of pulmonary arterial hypertension

Monocrotaline (MCT) is a pyrrolizidine alkaloid, which after single administration in rats, causes pathologic alterations in the lung and heart comparable to what is observed in human PAH: induced neointimal formation, pulmonary arterial hypertension, pulmonary vasculitis, right ventricular failure and eventual death.

The initiating mechanism(s) by which this agent causes these pathological changes remain elusive. After administration, monocrotaline is first activated by the liver to the electrophile monocrotaline pyrole (MCTP), which has characteristics of a bifunctional cross-linking agent, and has a half-life of~3 s in aqueous environments at neutral pH. Stabilisation of MCTP by red blood cells facilitates its subsequent transport to the lung, where it induces endothelial injury by covalent reactions with cytosolic and cytoskeletal proteins.

An experiment with bovine pulmonary artery endothelial cells demonstrated that MCTP can cause a moderate decrease in endothelial permeability and inhibits cell

proliferation, due to cell cycle arrest in G_2/M phase. Apoptosis has also recently been shown to occur in rat pulmonary endothelial cells following the administration of MCT. Interestingly, MCT cannot be applied to all rodents, since MCT causes PAH in rats but not in mice (Lame et al., 2000; Nishimura et al., 2003).

1.1.4.2   The hypoxia-induced model of pulmonary arterial hypertension

Hypoxia also plays an important role in the pathology and physiology of the lung. During the early period of hypoxic exposure, pulmonary vascular resistance is increased due to hypoxic vasoconstriction. However, prolonged exposure to the hypoxic condition elevates vascular resistance by causing structural changes in the pulmonary vasculature (Kobs et al., 2005).

Mice exposed to 10% O_2 for three weeks develop medial wall hypertrophy within the small pulmonary arterioles, pulmonary hypertension, and finally *cor pulmonale*. Vascular remodelling results in increased pulmonary arterial pressure leading to the right heart hypertrophy.

1.1.4.3   Transgenic animals

A functional BMPRII is required for effective BMP signalling, consequently *BMPR2-/-* mice die early in development, before gastrulation; while *BMPR2+/-* mice develop normally and do not exhibit perturbations to pulmonary haemodynamics or histological changes indicative of a vascular remodelling event (Beppu et al., 2000).

To overcome the developmental lethality observed in traditional transgenic approaches, and to create a useful model to study the molecular and physiological abnormalities in PAH, a conditional, tissue-specific *BMPR2* transgenic mouse SM22-tet-*BMPR2*$^{delx4+}$ was created. This mouse conditionally expresses a cDNA encoded a dominant-negative BMPRII (West et al., 2004). This dominant-negative BMPRII arises from a mutation in the *BMPR2* gene that has been identified in patients with FPAH, where a T base is inserted at position 504 in the kinase domain of the protein, resulting in a premature stop after 18 amino acids into the kinase domain. A tetracycline-responsive element, and a transactivator gene driven by the smooth muscle-specific SM22 promoter in a FVB/N background control expression of this construct. Activation of the mutation led to mice recapitulating aspects of the pulmonary hypertensive phenotype, including an increase in pulmonary artery pressure, right ventricle-to-left ventricle plus septum ratio (RV/LV+S) and pulmonary arterial muscularisation. Intimal

(plexiform) lesions that are observed in PAH patients were absent in SM22-tet-*BMPR2*^{delx4+} mice but it is possible that loss of *BMPR2* signalling in endothelium would result in this pathology. Additional transgenic mice that utilise an endothelial-specific promoter have been constructed to address this possibility (West et al., 2004).

1.2   BMP signalling

1.2.1   Bone morphogenetic proteins

Bone morphogenetic proteins (BMP) are a group of secreted polypeptide growth factors originally identified as molecules that can induce ectopic bone and cartilage formation in rodents (Wozney et al., 1988). More than 20 BMP-related proteins have been identified to date, and are subdivided into several groups based on their structure and function (Kawabata et al., 1998). One subgroup consists of BMP2, BMP4, and the *Drosophila decapentaplegic* (*dpp*) gene product (BMP2/4 subgroup), while BMP5, BMP6, BMP7 (also termed osteogenic protein-1, OP1), BMP8 (OP2), and the *Drosophila gbb-60A* gene product, form another subgroup (the OP1 group). A third group consists of growth-differentiation factor-5 (GDF5), also termed cartilage-derived morphogenetic protein-1 (CDMP1), GDF6 (CDMP2 or BMP13), and GDF7 (BMP12). Members of the BMP family have distinct expression profiles and different biological activities (Table 1.1), but all with the exception of the metalloprotease BMP1, are members of the TGFβ superfamily. They are produced by, and act on, a wide variety of cell types including monocytes, epithelial, mesenchymal, neuronal, pulmonary smooth muscle, and endothelial cells, playing complex and multifunctional roles in a variety of tissues in addition to bone. Many of them have important functions in the regulation of a broad range of biological activities including proliferation, migration, differentiation, matrix production and apoptosis during embryogenesis, and throughout adult life (Kawabata et al., 1998; Massague and Chen 2000; Massague and Wotton 2000; Miyazono et al., 2001; Chen et al., 2004).

The BMPs are conserved broadly across the animal kingdom and like many proteins, are synthesised as precursor proteins that are composed of a signal peptide containing a prodomain, and a mature domain. The post-translational processing of BMPs is important for the secretion of biologically active molecules. After removal of the signal peptide, the proproteins undergo dimerisation. As processing proceeds, specific proteolytic enzymes cleave the dimerised proteins at a RXXR site, resulting in the generation of the biologically active dimeric mature protein. Monomeric proteins contain

seven conserved cysteine residues that are involved in folding of the molecules into a unique three-dimentional structure called a cysteine knot (Vitt et al., 2001). One-conserved cysteine residue, which is not involved in cysteine knot formation, builds a disulfide bridge between two subunits. This results in the formation of a covalently-linked dimer, which is critical for biological activity (Shimasaki et al., 2004). Interestingly, some of the BMP ligands can form homodimers but also heterodimers, particularly in the case of BMP2, 4, 5, and 7, which exhibit greater biological activity than their corresponding homodimers.

Table 1.1   Examples of BMP family members and their proposed functions (after Kawabata et al., 1998).

Ligand	Alternative name	Function
BMP2	BMP2A	Osteoinductive, osteoblast differentiation, apoptosis
BMP3	Osteogenin	Most abundant BMP in bone, inhibits osteogenesis
BMP3b	GDF10	
BMP4	BMP2	Osteoinductive, lung and eye development
BMP6	Vgr1	Osteoblast differentiation, chondrogenesis
BMP7	OP1	Osteoinductive, development kidney and eye
BMP8	OP2	Osteoinductive
BMP9	GDF2	Hepatogenesis, development of nervous system
BMP10		Cardiac development
BMP11	GDF8, myostatin	Patterning mesodermal and neuronal tissue
BMP12	GDF7	Induces tendom-iliac tissue formation
BMP13	GDF6	Induces tendon and ligament like tissue formation
BMP14	GDF5	Chondrogenesis, enhances tendon healing, bone formation
BMP15	GD9B	Modifies follicle-stimulating hormone activity

1.2.2   BMP receptors

The BMP family members initiate their cellular actions by binding to transmembrane receptors with intrinsic serine/threonine kinase activity. This receptor family consists of type I and type II receptors, which are structurally similar (ten Dijke et al., 1996; Yamashita and Miyazono 1999; Massague and Chen 2000; Wrana 2000). Both types of receptors contain a small cysteine-rich extracellular ligand binding domain, a single hydrophobic transmembrane domain, and an intracellular segment containing the kinase domain. Type II receptors differ from type I receptors in that they lack a so-called GS domain. The GS domain is a region located immediately upstream of the

kinase domain, and is rich in glycine and serine residues. It plays important roles in controlling type I receptor kinase function. Type II receptors have a constitutively active cytoplasmic kinase domain, but are unable to activate downstream signals in the absence of a type I receptor (Ventura et al., 1994; Wrana et al., 1994).

The BMPs interact with three type II receptors, namely the BMP type II receptor (BMPRII) and activin type II receptors (ActRII and ActRIIB), and in turn activate four distinct type I receptors: BMPRIA (ALK3), BMPRIB (ALK6), ALK2 and ALK1 (Yamashita et al., 1996; Miyazono et al., 2005).

The ligand-receptor relationship between various BMP ligands and their cognate receptors are not exclusive (see Table 1.2). Both ActRII and ActRIIB originally identified as activin receptors, can also act as receptors for BMP6, BMP7, and GDF5. In addition BMPRII can bind BMP2, BMP4, BMP6, BMP7, BMP15, GDF5, and GDF9.

Table 1.2   The relationship between ligands, receptors (R), and Smads in the BMP family (after Shimasaki et al., 2004).

Ligands	Type II-R	Type I-R	Smads	Refserences
BMP2 BMP4	BMPRII	ALK3 (BMPRIA) ALK6 (BMPRIB)	Smad1/5/8	(Liu et al., 1995) (Rosenzweig et al., 1995)
GDF5	BMPRII ActRII ActRIIB	ALK3 (BMPRIA) ALK6 (BMPRIB)	Smad1/5/8	(Nishitoh et al., 1996) (Aoki et al., 2001)
BMP6 BMP7	BMPRII ActRII ActRIIB	ALK2 (ActRIA) ALK6 (BMPRIB)	Smad1/5/8	(Liu et al., 1995) (Ebisawa et al., 1999)
BMP15	BMPRII	ALK6 (BMPRIB)	Smad1/5/8	(Moore et al., 2003)
GDF9	BMPRII	Not identified	Smad2	(Vitt et al., 2002)

After ligand binding, the constitutively active type II receptor forms a heterocomplex with the type I receptor and transphosphorylates the GS domain, which leads to the activation of the type I receptor-linked kinase. The activated type I receptor

transduces a signal by phosphorylation of downstream effector molecules. The assembly of the receptor complex is not only triggered by ligand binding, but is also stabilised by direct interaction between the cytoplasmic segments of the receptors. This model predicts that type II and type I receptors act in concert, which is supported by the findings that overexpression of the kinase-domain-truncated BMP type I receptors block the signal transduction induced by BMPs (Maeno et al., 1994; Suzuki et al., 1994; Namiki et al., 1997). In contrast, substitution mutations at the GS domain of BMP type I receptors activate downstream signalling in the absence of binding or phosphorylation by type II receptors (Wieser et al., 1995; Akiyama et al., 1997; Fujii et al., 1999). It remains unclear whether BMP ligands bind first to the type I, or to the type II receptor. The situation is complicated by the fact that BMPs bind with a low affinity to BMP type I or type II receptors individually, and with high affinity only when the two BMP receptor types are present together. With respect to ALK3, ALK6 and BMPRII, two models of receptor activation have been described. BMP binds with high affinity to ALK3 or ALK6 and then recruits BMPRII into a hetero-oligomeric complex (BMP-induced signalling complexes: BISC). This process leads to activation of the p38 mitogen activated protein kinase (MAPK) pathway. The other alternative is to bind simultaneously to preformed hetero-oligomeric complexes consisting of at least one type I, and one type II receptor. This complex then activates the Smad signalling pathway. The stoichiometry of these receptor complexes remain to be elucidated (Nohe et al., 2002; Hassel et al., 2003).

1.2.3   The BMP signalling pathways

It is well established that ligand binding activates the type I receptor by phosphorylation, leading to signalling by a Smad restricted pathway (Heldin et al., 1997; Wrana 2000). Additionally, recent studies have demonstrated an involvement of the MAPK pathway in BMP signalling, mediated by TGFβ activated kinase 1 (TAK1)/ TAK1 binding protein (TAB1) inducing the activation of p38. Several lines of evidence document the activation of the RAS pathway and extracellular signal-regulated kinase (ERK) pathway due to BMP stimulation, but little is known about this regulation at the molecular level (Figure 1.3) (Nohe et al., 2002).

1.2.3.1   Smad-dependent pathways

Smad proteins are known to function as key signal transducers downstream of the TGFβ superfamily type I receptors (Wrana and Attisano 2000). The activated BMP

type I receptor directly recruits and phosphorylates a set of cytoplasmic receptor-regulated Smads (R-Smads), including Smad1, Smad5 and Smad8 which are known to preferentially transduce BMP signals. The phosphorylation of R-Smads at a carboxy terminal SSXS motif triggers the release of Smads from the receptor, and formation of homo and hetero-oligomers with Smad4 (also known as the Co-Smad), which is "shared" between several TGFβ signal transduction pathways (Kawabata et al., 1998; Mehra et al., 2000). The phosphorylation and heterocomplex formation then results in nuclear translocation, and after binding to DNA together with other transcription factors, regulation of the transcription of target genes (Miyazono et al., 2000; Souchelnytskyi et al., 2001; ten Dijke and Hill 2004).
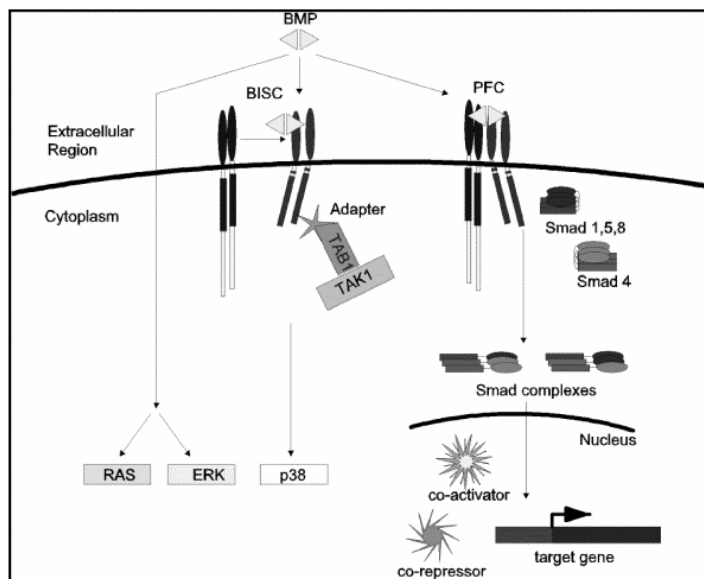
Figure 1.3   BMP receptor-signalling pathway.
BMP can bind to the preformed oligomeric receptor complexes **(PFC)**, which leads to the activation of the Smad signalling pathway. Binding of the ligand to the homo-oligomeric type I receptors recruitit of the type II receptor leads to the activation of the p38 pathway, possibly mediated by TGFβ activated kinase 1 **(TAK1)**/TAK1 binding protein **(TAB1)**. Studies also show the activation of RAS and extracellular signal-regulated kinase **(ERK)** due to BMP stimulation, but not much is known about the molecular mechanism. **BISC;** BMP-induced signalling complexes (after Nohe et al., 2002).

Structurally, R-Smads and Co-Smads are similar. They share two highly-conserved regions, an N-terminal MH1 (Mad Homology 1) domain and a C-terminal MH2 (Mad homology 2) domain, separated by a poorly-conserved linker region. However, the Co-Smad does not contain the C-terminal SSXS phosphorylation motif present in R-Smads, and is thus not phosphorylated by the receptor

(Macias-Silvia *et al.*1996; Zhan et al.1996). The MH1 domain of the Co-Smad and R-Smads can bind to specific DNA sequences, while the MH2 domain mediates protein-protein interaction with Smads, transcriptional coactivators like p300, CBP (histone acetylase), or co-repressors, resulting in the regulation of specific gene expression.

The BMP signalling pathway is also negatively regulated. The BMP and activin membrane bound inhibitor (BAMBI), Smad ubiquitination regulatory factor-1 (Smurf1), Smad6 and Smad7 are the best known intracellular factors which are induced by BMP signalling and inhibit the BMP-Smad dependent pathway at different levels, establishing a negative feed-back loop.

BAMBI. The BMP and activin membrane bound inhibitor (BAMBI) exhibits significant sequence similarity to TGFβ receptors, but lacks the intracellular kinase domain. It can function as a naturally occurring dominant-negative receptor which associates with other receptors and thus prevents formation of functional receptor complexes, and blocks BMP signalling (Onichtchouk et al., 1999; Sekiya et al., 2004).

Smurf1. Smad-ubiquitination regulatory factor 1 (Smurf1) displays E3 ubiquitin ligase activity, interacts with Smad1 and Smad5, and specifically targets them for ubiquitination, leading to proteosomal degradation and thus signal inhibition (Murakami et al., 2003).

Smad6 and Smad7. Unlike the other members of the Smad family, Smad6 and Smad7 are inhibitors of TGFβ superfamily signalling. Hence they are called inhibitory Smads (I-Smads). This inhibition occurs through their ability to complete with the R-Smads for binding to the activated type I receptors. Smad6 inhibits BMP signalling by forming a complex with Smad1, thereby competing with Smad4 binding (Hata et al., 1998; Miyazono et al., 2001).
The BMP signalling can also be inhibited extracellularly by secreted proteins such as Chordin, Noggin, Gremlin, Dragon, Cerberus and Tolloid/BMP1-related metalloproteases (Yoshida et al., 2000; Gerlach-Bank et al., 2002).

1.2.3.2 BMP-MAPK dependent pathway

In addition to the canonical BMP-Smad-dependent signalling pathway the MAPK pathway also mediates TGFβ signal transduction. Activated BMP receptors may interact

with X-linked inhibitor of apoptosis (XIAP), which in turns activates the mitogen activated protein kinase kinase kinase (MAPKKK) TAK1 by interacting with TAB1. The TAK1 can activate nemo-like kinase (NLK) and inhibits the DNA-binding activity of the β-catenin/T-cell-specific transcription factor (TCF) complex, which normally activates dorsally expressed target genes of the Wnt/β-catenin pathway (Iwasaki et al., 1999; Kimura et al., 2000).

1.3   BMP signalling in lung development and homeostasis

Different growth factors, including members of TGFβ superfamily such as BMPs, regulate diverse biological processes including migration, proliferation, and differentiation of pluripotent progenitor cells that are involved in the development of several organ systems during embryogenesis and in adult tissue repair. Regulation of these cellular functions is also critical for normal lung development and homeostasis (Kawabata et al., 1998; Sakou 1998).

The BMPs play an essential role in the establishment of the basic embryonic body plan. Several studies in embryos have revealed that BMP4 induces ventral mesoderm formation. Gene targeting studies have demonstrated that BMP signals are required for gastrulation of mouse embryos. While *BMP2* deletion-mutant embryos do form mesoderm cells, they fail to close the proamniotic canal, and also exhibit a defect in cardiac development. The majority of homozygous *BMP4* null embryos die at or around the time of gastrulation, without forming embryonic mesoderm (Beppu et al., 2000; Warburton et al., 2003).

Several BMPs, including BMP3, 4, 5 and 7, are expressed during embryonic lung development and exist in lung tissue throughout the adult life (Bellusci et al., 1996).The expression of BMP5 and BMP7 has been detected in the mesenchyme and the endoderm of the developing embryonic lung respectively, while BMP4 expression is restricted to the distal epithelial cells and the adjacent mesenchyme and plays an important role in regulating early branching morphogenesis. Addition of BMP4 to embryonic lung explant culture medium dramatically stimulates lung branching, whereas it inhibits the growth of isolated epithelial cells. Interestingly, *in vivo* overexpression of BMP4 (driven by the *SP-C* promoter in the distal endoderm of transgenic mice) causes abnormal lung morphogenesis, with cystic terminal sacs and inhibition of epithelial-cell proliferation.

The BMPs act not only as instructive signals during embryogenesis but also contribute to the maintenance and repair of adult tissues. For example BMP7 inhibits

serum-stimulated and growth factor-induced proliferation of human aortic SMC (Dorai et al., 2000), while BMP2 has been shown to inhibit injury induced intimal hyperplasia in the rat carotid artery balloon injury model (Nakaoka et al., 1997).

Most of the BMP signalling pathway components, such as BMP receptors (both type II and type I, ALK2, 3, and 6) and BMP-specific receptor-regulated Smads (R-Smads) are expressed in early embryonic mouse lung development. These findings suggest strong involvement of this pathway in lung development and homeostasis. The *SP-C* promoter-driven overexpression of either the BMP antagonist Xnoggin or a dominant-negative ALK6 BMP receptor block BMP signalling, resulting in severely reduced distal epithelial cell phenotypes and increased proximal cell phenotypes in lungs of transgenic mice. The critical role of BMPRII and the BMP pathway in vascular development is evident from studies in knock-down mice. Homozygosity for the null mutation in the *BMPR2* gene is lethal during early embryogenesis. Smooth muscle-specific expression of a dominant-negative BMPRII in mice with activated expression after birth, develop increase pulmonary artery pressure, RV/LV+S ratio, and pulmonary arterial muscularisation with no increase in systemic arterial pressure (West et al., 2004). Gene targeting analyses have revealed the critical functions of Smad4 and Smad5, which act downstream of BMP receptors, during embryonic development. *Smad4-/-* embryos die before 7.5 days postcoitum (E7.5) with gastrulation defects and abnormal visceral endoderm formation. *Smad5-/-* embryos die between E9.5 and E11.5 and exhibit multiple defects including a lack of normal vasculature, as they fail to recruit vascular smooth muscle to endothelial structures (Warburton et al., 2003).

Taken together, these findings suggest that disruption of BMP signalling pathways may result in a failure of the crucial antiproliferative/differentiation mechanisms in the pulmonary vasculature and may couse vascular remodelling characteristics for PAH patients. To date, the most extensively studied molecule from this pathway remains BMPRII. Several mutations found in this receptor might cause disruption of BMP signalling that contribute to the cellular proliferation and vascular oblitreation observed in this disease. This hypothesis is supported by the finding that pulmonary arterial SMC (paSMC) described in patients with PAH exhibit altered growth responses to the BMPRII ligands compared with cells isolated from normal (control) lungs (Morrell et al., 2001).

1.4   BMPRII and pulmonary arterial hypertension

1.4.1   Genomic structure and function of BMPRII

The genomic structure of the *BMPR2* gene, located on chromosome 2q33, covers approximately 190 kb, comprising 13 exons, which encode a 4 kb transcript that generates a polypeptide with 1038 amino acids in humans. The mature protein harbours four distinct functional domains, namely the extracellular ligand-binding domain encoded by exons 2 and 3, a single pass transmembrane domain generated by exon 4, and a serine/threonine kinase domain extending from exon 5 to exon 11. The sequence and structure of the receptor is highly conserved; for example, overall amino acid sequence identity between mouse and human BMPRII is 96.6% (Beppu et al., 1997). Unique to BMPRII among the members of TGFβ receptor superfamily is the large C-terminal cytoplasmic tail encoded by exons 12 and 13. The precise function of this domain remains unknown (Rosenzweig et al., 1995). To date, three molecules that interact with this region of BMPRII have been identified: LIM kinase 1 (LIMK1), Tctex1 and Src kinase. The LIMK1 regulates dynamics of the cytoskeletal protein actin by phosphorylation and inactivation of cofilin. The BMPRII inhibits the ability of LIMK1 to phosphorylate cofilin through interaction with its C-terminal tail, and this inhibition is alleviated by BMP4 (Foletta et al., 2004). The Tctex1 protein is the light chain of the motor complex dynein. The BMPRII induces phosphorylation of Tctex, resulting in the movement of Tctex along the microtubules and the efficient activation of downstream signal mediators (Machado et al., 2003). The interaction between BMPRII and c-Src tyrosine kinase inhibit c-Src tyrosine kinase activity in the presence of BMP ligand by reducing its phosphorylation at tyrosine-418 residue. The inhibition of c-Src activity by BMP signaling may inhibit downstream cell cycle regulators such as cyclins D and E and subsequently prevent smooth muscle cell proliferation (Wong et al., 2005). In addition, Hassel et al., 2000 performed a proteomics analysis of BMPRII interacting proteins and found that several proteins of the cytoskeletal components interact with the C-terminal tail as well as the kinase domain of BMPRII. Thus, the C-terminal tail is thought to posses important regulatory functions for cytoskeletal proteins. Interestingly, an isoform of BMPRII termed the BMPRII "short-form" is generated by alternative splicing of exon 12 and the exposure of a premature translation termination codon within exon 13, and thus lacking the long cytoplasmic domain, was recently identified. Overexpression of the short form of BMPRII indicates that it is capable of activating Smads, indicating that the

cytoplasmatic tail might not be required for the well-characterised BMP signalling pathway.

The BMPRII is widely expressed in different tissues, including heart, brain, skeletal muscle, kidney and lung. In normal lungs, BMPRII mRNA and protein are predominantly found in endothelial cells, macrophages, and to a lesser extent SMC (Atkinson et al., 2002).

1.4.2 *BMPR2* mutations in pulmonary arterial hypertension patients

Extensive analyses of the *BMPR2* coding region and intron-exon boundaries have been conducted in patients with FPAH and IPAH from a wide range of ethnic groups, including Americans, Europeans, Asians (Deng et al., 2000; Machado et al., 2001; Morrell et al., 2001; Newman et al., 2001; Thomson et al., 2001; Nishihara et al., 2002; Rudarakanchana et al., 2002; Uehara et al., 2002; Morisaki et al., 2004; Sugiyama et al., 2004). Germline mutations (therefore present in all cell types) were detected in 55% (40 to 73) of recognised familial cases. In IPAH, the mutation rate ranges from 11% to 40%. These findings indicate that this autosomal dominant disorder displays reduced penetrance.

Figure 1.4   Alignment of described *BMPR2* mutations.
The *BMPR2* gene structure is aligned with its corresponding cDNA, along with the mutations described thus far. BMPRII protein domains are designated by different intensities of grey color. **SP**; signalling peptide, **TM**; transmembrane domain (after Eickelberg and Seeger, 2005).

To date, more than 100 different mutations have been described in both familial and sporadic cases (see Table 5.1, Appendix). These span the entire open reading frame of the *BMPR2* gene. Among the known mutations, at least four different types of mutations have been identified (Machado et al., 2001). In the first group, nonsense or frame-shift mutations in the extracellular domain lead to a premature truncation of the proteins and absence of BMPRII protein on the plasma membrane. The second group is characterised by missense mutations in the extracellular domain, mostly involving highly conserved cysteine residues. The third group of mutations has either missense or frame-shift mutations in the kinase domain, while the fourth group has frame-shift or nonsense mutations within the cytoplasmic tail, resulting in cytoplasmic truncation of the receptor protein (see Figure 1.4).

1.4.3   Functional consequences of *BMPR2* mutations

The different types of mutations distributed throughout the entire coding region of the *BMPR2* gene suggest a high degree of heterogeneity concerning their contribution to the pathogenesis of PAH. The possible consequence of mutations occurring in conserved or functionally critical domains of the receptor may interfere with BMP signalling and might reduce or completely abolish the signal-transducing abilities of the receptor. The mechanism by which *BMPR2* mutations disrupt BMP/Smad signalling is heterogeneous and mutations can result in alterations to transcriptional activity, decreased ligand binding ability, or improper BMPRII trafficking to the membrane (Eddahibi et al., 2002; Rudarakanchana et al., 2002).

1.4.3.1   Loss of transcriptional activitiy

Experiments investigating disease associated with *BMPR2* mutations suggest a dominant-inhibitory effect of mutations in the extracellular or kinase domains on receptor function, with respect to Smad signalling. Receptors with mutations in these two domains are neither able to induced transcriptional activation of a BMP-specific promoter reporter construct nor are they able to phosphorylate BMP-specific Smads. Co-expression with wild-type BMPRII represses, in a dose-dependent manner, the transcriptional activity induced by this receptor. In contrast, mutations in the C-terminal tail of the receptor do not affect its biological activities. In agreement with these findings, these receptors are able to phosphorylate BMP-specific Smads, albeit less efficiently than the wild-type BMPRII (Rudarakanchana et al., 2002).

1.4.3.2 Decreased ligand binding ability

Different mutations were also tested for their ligand-binding ability. Structural changes to the extracellular domain of the receptor can abolish ligand-binding capacity, while BMPRII variants generated from a *BMPR2* gene carrying a mutation in the kinase, or C-terminal encoding domain in the presence of ALK3 bound BMP6 and BMP4 efficiently (Rudarakanchana et al., 2002).

1.4.3.3 Failure of BMPRII trafficking to the plasma membrane

In PAH patients, many of the missense mutations within the extracellular domain-encoding region of BMPRII have been found in cysteine codons (Machado *et al.,* 2001). It is known that extracellular cysteine residues of BMPRII are essential for the formation of the correct three-dimensional structure required for membrane targeting of many receptors (Zeng *et al.*, 1999). Overexpression of a mutated gene encoding BMPRII carrying cysteine substitutions in the ligand-binding domain or kinase domain, resulted in altered receptor trafficking to the cell surface, and most of the abnormal proteins were detected in the endoplasmic reticulum. In contrast, receptors carrying non-cysteine variants within the kinase domain do reach the cell surface but fail to activate a BMP Smad-responsive luciferase reporter gene. These results suggest that loss of signal-transducing abilities induced by the missense mutations in exons encoding the extracellular ligand binding region are not only due to loss of ligand-binding ability of the extracellular domain, but are also caused by subcellular miss-localisation (Rudarakanchana et al., 2002).

1.4.3.4 Activation of Smad-independent BMP signalling pathways

Overexpression of mutated *BMPR2* genes leads to ligand-independent activation of p38 MAPK and enhanced serum-induced proliferation of mouse epithelial cells. Based on the results of these studies, a reduced cell-surface expression of BMPRII might favor activation of p38 MAPK-dependent signalling pathway, while inhibiting Smad-dependent signalling in a mutation-specific manner. Ligand-induced and ligand-independent signalling may be an important mechanism contributing to the abnormal cell proliferation observed after transfection with expression constructs carrying mutations in the *BMPR2* gene (Rudarakanchana et al., 2002).

1.4.3.5 Increased of BMP signalling

Based on recent studies demonstrating that ablation of BMPRII in paSMC does not abolish BMP signalling but leads to diminished signalling by BMP2 and BMP4 and augmented signalling by BMP6 and BMP7, there are two novel hypotheses which might explain the pathological consequences of *BMPR2* mutations. It is possible that a truncated form of BMPRII lacking a transmembrane domain, kinase and C-terminal tail might increase BMP signalling by providing inactive targets for constitutively expressed inhibitors. Another explanation for these observations is that BMPRII might function not only by transducing BMP signals, but also by regulating the activity of alternative receptors such as ActRIIa. Disruption of BMPRII in paSMC force BMP signals to be transduced by an alternate receptor, ActRIIa, a function that appears to be suppressed by BMPR2 in wil-type cells (Yu et al., 2005).

1.4.3.6 Down-regulation of BMPRII expression

The expression of BMPRII protein in the lung is dramatically reduced in patients harboring an underlying *BMPR2* mutation that predicted to cause truncation of the protein. In addition, *BMPR2* expression is markedly reduced in subjects, where no BMPRII mutation was identified (Atkinson et al., 2002). These findings stress the importance of understanding how other environmental and genetic factors might regulate the expression of BMPRII in lung cells, and might provide important clues as to why the vascular abnormality is restricted to the lung, particularly since BMPRII is widely expressed in normal adult tissues.

1.4.3.7 Failure of antiproliferative effects on vascular cells

It is well documented that BMP2, 4 and 7 display a significant antiproliferative effect on normal paSMC. Interestingly, this growth-inhibitory effect is diminished in cells obtained from patients with IPAH or FPAH. This phenomenon was observed in all cases, irrespective of whether or not specific *BMPR2* mutations were identified, suggesting the defective BMP-mediated signalling may be a common factor in IPAH and FPAH (Robbins 2004).

1.5   Experimental design and aim of the project

Heterozygous mutations in the *BMPR2* gene, encoding the type II BMP receptor, which have been identified in PAH patients suggest that alterations to BMPRII function may be involved in the onset and/or progression of PAH. To further elucidate the function of BMPRII in this context, we sought to:

- Identifiy novel interacting partners of BMPRII by yeast two-hybrid analysis, using the kinase domain and total intracellular part of the receptor as a bait.

- Verify true positives - thus real interacting partners of BMPRII by further *in vitro* (GST pull down), and *in vivo* (co-immunoprecipitation, co-localisation in tissue and specific cell types) studies.

- Demonstrate the relevance of these interactions in lung homeostasis and their influence on the pathogenesis of PAH by functional analyses.

2 Materials and methods

2.1 Materials

2.1.1 Equipment

Cell Culture Incubator; Cytoperm2	Heraeus, Germany
Chroma SPIN-1000 DEPC-H_2O Columns	Biosciences, Clontech, USA
Developing machine; X Omat 2000	Kodak; USA
Electrophoresis chambers	Bio-Rad, USA
Fluorescence microscope; LEICA AS MDW	Leica, Germany
Freezer -20 ℃	Bosch, Germany
Freezer -40 ℃	Kryotec, Germany
Freezer -80 ℃	Heraeus, Germany
Fridge +4 ℃	Bosch, Germany
Mini spin centrifuge	Eppendorf, Germany
Multifuge centrifuge, 3 s-R	Heraeus, Germany
Light microscope; LEICA DMIL	Leica, Germany
PCR-thermocycler	MJ Research, USA
Pipetboy	Eppendorf, Germany
Pipetmans: P10, P20, P100, P200, P1000	Gilson, France
Power Supply; Power PAC 300	Bio-Rad, USA
Western Blot Chambers: Mini Trans-Blot	Bio-Rad, USA
Mini-Protean 3 Cell	Bio-Rad, USA
Vortex machine	Eppendorf, Germany
Film cassette	Sigma-Aldrich, Germany
Filter Tip FT: 10, 20, 100, 200, 1000	Greiner Bio-One, Germany
Filter units 0.22 µm syringe-driven	Millipore, USA
Glass bottles: 250, 500, 1000 ml	Fisher, Germany
Gel bloting paper 70 × 100 mm	Bioscience, Germany
Petri dish with vents	Greiner Bio-One, Germany
Pipette tip: 200, 1000 µl,	Sarstedt, Germany
Pipette tip 10 µl	Gilson, USA
Radiographic film X-Omat LS	Sigma-Aldrich, Germany
Serological pipette: 5, 10, 25, 50 ml	Falcon, USA

Test tubes: 15, 50 ml   Greiner Bio-One, Germany

Tissue culture chamber slides   BD Falcon, USA

Tissue culture dish 100 mm   Greiner Bio-One, Germany

Tissue culture flask 250 ml   Greiner Bio-One, Germany

Tissue culture plates: 6, 24, 48 well   Greiner Bio-One, Germany

Trans blot transfer medium (0.2 µm)   Bio-Rad, USA

2.1.2   Reagents

Acetic acid   Merck, Germany

Acrylamide solution, Rotiphorese Gel 30   Roth, Germany

Agarose   Invitrogen, UK

Ammonium persulfate (APS)   Promega, Germany

Ammonium sulfate   Sigma-Aldrich, Germany

Ampicillin sodium   Sigma-Aldrich, Germany

β-glycerophosphate   Sigma-Aldrich, Germany

β-mercaptoethanol   Sigma-Aldrich, Germany

Bromophenol blue   Sigma-Aldrich, Germany

Calcium chloride   Sigma-Aldrich, Germany

3-[3-chloramidopropyl) dimethylammonio]-

1-propanesulfonate (CHAPS)   Sigma-Aldrich, Germany

D-(+)-Glucose   Sigma-Aldrich, Germany

D-MEM medium   Gibco BRL, Germany

RPMI/640 medium   Gibco BRL, Germany

Difco yeast nitrogen base without amino acids   Biosciences, Clontech, USA

Dimethyl sulfoxide (DMSO)   Sigma-Aldrich, Germany

Ethylendinitrilo-*N, N, N´, N´,* -tetra-acetic acid (EDTA)   Promega, USA

Dublecco' s phosphate buffered saline 10 × (PBS)   Laboratories, Austria

Ethanol absolute   Riedel-de Haen, Germany

Foetal bovine serum (FBS)   Gibco BRL, Germany

Gel extraction kit   Qiagen, Germany

Glass beads   Sigma-Aldrich, Germany

Glycine   Roth, Germany

Glycerol   Merck, Germany

2-(-4-2-hydroxyethyl)-piperazinyl-1-ethansulfonate

(HEPES)   Sigma-Aldrich, Germany

Histostain-SP Kit	Zymed, USA
Igepal CA-630	Sigma-Aldrich, Germany
Lipofectamine	Invitrogene, UK
Lithium acetate	Sigma-Aldrich, Germany
Luria-Bertani Medium	Invitrogen, UK
MiniElute Gel Extraction Kit	Qiagen, Germany
Magnesium chloride	Sigma-Aldrich, Germany
Magnesium sulfate	Sigma-Aldrich, Germany
Methanol	Fluka, Germany
pGEM-T Easy Vector System Kit	Promega, Germany
Platinum Taq DNA polymerase	Invitrogen, Germany
Polyethylene glycol 6000	Merck, Germany
Potassium acetate	Sigma-Aldrich, Germany
Potassium chloride	Merck, Germany
Potassium phosphate	Sigma-Aldrich, Germany
Precision Plus Protein^{TM} Standards	Bio-Rad, USA
2-Propanol	Merck, Germany
Pure Yield Plasmid Midiprep System	Promega, Germany
Restriction endonucleases	Promega, Germany
RNase inhibitor	Promega, Germany
RNeasy Midi Kit	Qiagen, Germany
Rnase H^{-} reverse transcriptase	Promega, Germany
SD/-Ade supplenent	BD, Clontech, USA
SD/-His supplenent	BD, Clontech, USA
SD/-Leu/-Trp supplement	BD, Clontech, USA
SD/-Ade/-His/-Leu/-Trp supplement	BD, Clontech, USA
Select agar	Invitrogen, UK
Select peptone 140	Gibco BRL, Germany
Select yeast extract	Gibco BRL, Germany
Sodium acetate	Sigma-Aldrich, Germany
Sodium chloride	Merck, Germany
Sodium dodecyl sulfate (SDS)	Promega, USA
Sodium phosphate	Sigma-Aldrich, Germany
Sodium sulfate	Merck, Germany
Taq DNA polymerase	Invitrogen, Germany
T4 DNA ligase	Promega, Germany

Tween 20	Sigma-Aldrich, Germany
Tris	Roth, Germany
Triton X-100	Promega, USA
Trypsin/EDTA	Gibco BRL, Germany
QIAprep Spin Miniprep Kit	Qiagen, Germany
Yeast Plasmid Isloation Kit	Clontech, USA

2.1.3 Cell Lines

2.1.3.1 Mammalian cell lines

NIH/3T3 (Swiss mouse embryo), fibroblast	DSMZ, Germany
COS 7 (African green monkey kidney) fibroblast-like	DSMZ, Germany
A549 (human lung carcinoma), epithelial	DSMZ, Germany

2.1.3.2 Yeast cells

Sacharomyces cerevisiae AH109	Clontech, USA
Sacharomyces cerevisiae Y187	Clontech, USA

2.1.3.3 Prokaryotic cells

E. coli strains:

DH5α	Clontech, USA
BL21	Clontech, USA
KC8	Clontech, USA

2.1.4 Animals

2.1.4.1 A monocrotaline rat model of pulmonary arterial hypertension

Monocrotaline (MCT) was dissolved in 0.5 M HCl, and the pH was adjusted to 7.4 with 0.5 M NaOH. The solution was administered as a single intrajugular injection (60 mg/kg) to male Sprague-Dawley rats. Control rats received an equal volume of isotonic saline. Pathological changes were observed after one to five weeks after treatment. Right ventricular hypertrophy was used as a marker for PAH development. Right ventricular hypertrophy was quantified as a factor for PAH changes. The heart was

dissected, and the ratio of the right ventricle to left ventricle plus septum weight (RV/LV + S) was used as an index of right ventricular hypertrophy.

2.1.4.2 Hypoxia mouse model of pulmonary arterial hypertension

Male BALB/cAnNCrlBR mice (20 to 22 g; Charles River, Sulzfeld, Germany) were exposed to normobaric hypoxia [inspiratory O_2 fraction (FiO_2) 0.10] in a ventilated chamber. The level of hypoxia was held constant by an autoregulatory control unit supplying either nitrogen or oxygen. Excess humidity in the recirculating system was prevented by condensation in a cooling system. The CO_2 was continuously removed by soda lime. Mice exposed to normobaric normoxia were kept in a similar chamber at a FiO_2 of 0.21. After 1, 7 or 21 days, the animals were anesthetised by intraperitoreal administration of 180 mg of sodium pentabarbital/kg body weight. A cannula was inserted into the trachea by tracheostomy, a midline thoracotomy was performed, and the lungs were flushed via a catheter in the pulmonary artery with Krebs-Henseleit buffer (4.3 mM KCl, 1.1 mM KH_2PO_4, 2.4 mM $CaCl_2$ 1.3 mM $MgCl_2$, and 13.32 mM glucose) at pressure of 20 cm H_2O at room temperature. It was equilibrated with a gas mixture 1% O_2, 5.3% CO_2, balanced with N_2. The pH was adjusted with $NaHCO_3$ to 7.40. During perfusion of the lung, the buffer was allowed to drain freely from a catheter in the left ventricle. Once the effluent was clear of blood, lungs were dissected and immediately frozen in liquid nitrogen. Preparation of the hypoxic animals was continuously performed in the hypoxic environment. As a factor for PAH changes, the heart was dissected, and RV/LV + S ratio was calculated as an index of right ventricular hypertrophy.

2.2   Methods

2.2.1   RNA isolation

RNA isolation from lung tissue or cell lines was performed according to the manufacturer's instructions provided together with the reagents in the RNeasy Midi Kit.

2.2.2   Reverse Transcription

Reverse Transcription Polymerase Chain Reaction (RT-PCR) is an enzymatic reaction carried out by reverse transcriptase (RT), which synthesises cDNA using RNA as a template.

To perform RT reactions, 100 to 500 ng of total mouse or human RNA was mixed with 4 µl of oligo-(dT)$_{15}$ (100 µg/ml) primers in a PCR tube. Samples were heated at 70 °C for 5 min, chilled on ice, and the following RT reaction components were added.

2.2.2.1 RT - Mix

Components:	Volume:	Final concentration:
5 × RT buffer (MgCl$_2$ free)	4 µl	1 ×
25 mM MgCl$_2$	4.8 µl	6 mM
10 mM dNTP mix	1 µl	0.5 mM
RNAsin inhibitor (1 U/µl)	1 µl	1.0 U
Reverse Transcriptase (1 U/µl)	1 µl	1.0 U
RNAse free water	to 20 µl	not applicable

The RT amplification was performed as follows: 25 °C (5 min), 42 °C (1 h).

Newly generated cDNA was used for PCR amplification immediately, or stored at -20 °C.

2.2.3   The Polymerase Chain Reaction (PCR)

The Polymerase Chain Reaction (PCR) is a method, which allows million-fold amplification of DNA segments from selected regions of the genome. The newly synthesised DNA is produced in a reaction catalyzed *in vitro* by purified DNA polymerase.

The reaction consists of three steps: denaturation (generation of single strand DNA), annealing (binding of primers to the target sequence), and extension (amplification of a sequence of interest by polymerase enzyme).

2.2.3.1 PCR - Mix

The following components were combined in a 0.5 ml microcentrifuge tube, on ice:

Components:	Volume:	Final concentration:
10 × PCR buffer (MgCl$_2$ free)	5 µl	1 ×
10 mM dNTP mixture	1 µl	0.2 mM each
50 mM MgCl$_2$	1.5 µl	1.5 mM
10 µM forward primer	1 µl	0.2 µM

10 µM reverse primer	1 µl	0.2 µM
Template DNA	~1 µl	**
Platinum *Taq* DNA Polymerase (5 U/µl)	0.2 µl	1.0 U
Autoclaved, deionised water	to 50 µl	not applicable

**1 µg mammalian genomic DNA or 1.0 to 100.0 pg of plasmid DNA

All primers sequences used for PCR amplification are shown in Table 5.2, Appendix.

The components were mixed briefly. After denaturing at 94 °C for 5 min, the PCR amplification was performed.

2.2.3.2 PCR program

To perform effective DNA amplification 20-35 cycles of PCR reaction were required.

Time and temperature for particular steps were performed as follows:

<u>Denaturation</u>	30 s	94 °C
<u>Annealing</u>	30 s	55 °C (GC content <50%) or
		60 °C (GC content >50%)
<u>Extension</u>*	~60 s/kb product	72 °C

* The PCR was completed by incubation 10 min at 72 °C

New generated DNA of interest was immediately used for cloning or stored at -20 °C.

2.2.4   Site-directed mutagenesis

The QuikChange[TM] site-directed mutagenesis strategy was employed to introduce mutation into cDNAs. The QuikChange[TM] mutagenesis was performed using *Pfu* DNA polymerase, a proofreading thermostable DNA polymerase with high fidelity. In the reaction, double-stranded pGEX-4T1 plasmid containing cDNA insert endcoding the kinase domain of *BMPR2* served as a template, and a pair of synthesised complementary oligonucleotides as primers. The primers contained the desired mutation in the middle, flanked by 10-15 deoxynucleotides bases of 100% sequence at wild-types end. During thermocycling, the primers annealed to the complementary strands of the

template and were extended by *Pfu* DNA polymerase. On incorporation of the oligonucleotide primers, a mutated plasmid containing staggered nicks was generated.

2.2.4.1 The QuikChange™ PCR-Mix

Components:	Volume:	Final concentration:
10 × *Pfu* polymerase buffer	5 µl	1 ×
10 mM dNTP mixture	1 µl	0.2 mM each
10 µM forward primer	1 µl	0.2 µM
10 µM reverse primer	1 µl	0.2 µM
Template DNA	~1 µl	~ 50 ng
Pfu DNA Polymerase (6 U/µl)	0.5 µl	3.0 U
Autoclaved, deionised water	to 50 µl	not applicable

Between 30-35 temperature cycles were performed. The cycling parameters were identical to those used for normal PCR amplification (see 2.2.3.2), exept that the extension time was 2 min/kb of plasmid length. Primers sequences for this reaction are presented in Table 5.3, Appendix.

Following the QuikChange™ reaction, the product was treated with 20 U *Dpn*I for 1 h, at 37 °C. The *Dpn*I endonuclease is specific for methylated and hemimethylated DNA, and was therefore used to digest the parental DNA template and to select the mutated-daughter DNA strand. An aliquot of the nicked DNA plasmid incorporating the desired mutation was transformed into *E. coli* DH5α, where the nicks were repaired. The plasmid was expended, purified and fully sequenced to ensure presence of the expected mutations.

2.2.5   Gel electrophoresis

Gel electrophoresis is a method that allows separation of macromolecules, either nucleic acids or proteins, based on size, electric charge, pH and other physical properties.

2.2.5.1 Agarose gel electrophoresis

To analyse or separate nucleic acid fragments, agarose gel electrophoresis was performed according to a standard protocol (Sambrook *et al.*, 1989). Depending on the size of DNA fragments to be separated, 1-2% agarose gels containing 0.5 µg/ml ethidium bromide, a fluorescent intercalating dye, were prepared in 1 × Tris-acetate-EDTA (TAE) buffer. Different gels, varying in agarose content, were used to resolved DNA fragment of different sizes:

Agarose concentration (%):	DNA length (bp):
1.0	400-8000
1.2	300-7000
1.5	200-4000
2.0	100-3000

Before loading onto the gel, nucleic acid samples were mixed 1:5 with 6 × agarose gel-loading buffer. The electrophoresis was performed at 100 V/cm, in 1 × TAE buffer. For analytical gels, the electrophoresis result was illuminated with short wavelength ultraviolet light (λ = 254 nm), and photographed.

> 1 × TAE buffer:
> 40 mM Tris-acetate, pH 8.0
> 1 mM EDTA; pH 8.0

> 6 × agarose gel-loading buffer:
> 0.025% (w/v) bromophenol blue
> 40% (w/v) sucrose

2.2.5.2 SDS polyacrylamide gel electrophoresis (SDS-PAGE)

For the analytical separation of proteins under SDS-denaturating conditions, gels were composed of an 8-15% separating gel and a 6% stacking gel (~2 cm long). Before loading, proteins samples were mixed with an equal volume of 2 × SDS gel-loading buffer, and denatured by heating for 5 min at 95 °C. The electrophoresis was performed with a vertical gel chamber in 1 × SDS-running buffer.

Stacking gel:

5% acrylamide/bisacrylamide

125 mM Tris-HCl, pH 6.8

0.1% (w/v) SDS

0.1% (w/v) APS

0.1% (v/v) TEMED

Separating gel:

8-12% acrylamide/bisacrylamide

375 mM Tris-HCl, pH 8.8

0.1% (w/v) SDS

0.1% (w/v) APS

0.1% (v/v) TEMED

1 × SDS-running buffer:

25 mM Tris-HCl, pH 8.3

250 mM glycine

0.1% (w/v) SDS

2 × SDS gel-loading buffer:

125 mM Tris-HCl, pH 6.8

20% (v/v) glycerol

4% (w/v) SDS

10% (v/v) β-mercaptoethanol

0.025% (w/v) bromophenol blue

2.2.6 Recombinant DNA technology

Cloning involves the use of recombinant DNA technology to propagate DNA fragments inside a foreign host. The fragments are amplified in a PCR reaction or are isolated from chromosomes using restriction enzymes and then united with a carrier (a vector, a small, self-replicating circular molecule of DNA that is separate from the chromosomes). Following introduction into suitable host cells, the DNA fragments can then be reproduced along with the host cell DNA.

2.2.6.1 PCR product purification

To clone a gene of interest into an expression vector, the DNA of interest was first amplified by PCR (see 2.2.3), and separated on the agarose gel. Bands of the expected size were excised and gel-purified using a commercially available Gel Extraction Kit.

2.2.6.2 Ligation of PCR products into the pGEM-T Easy Vector

Purified PCR product was ligated into the pGEM-T Easy vector containing a complementary unpaired 3´-thymidine residue that was complementary to the single 3´-adenosine overhang generated by *Taq* DNA polymerase. The reaction was carried out with bacteriophage T4 DNA ligase overnight at 16 °C using the pGEM-T Easy Vector System Kit.

2.2.6.3 Ligation-Mix

Components:	Volume:
2 × rapid ligation buffer	5 µl
pGEM-T Easy Vector (50 ng)	1 µl
Purified PCR product	x µl[*]
T4 DNA ligase	1 µl
Autoclaved, deionised water	to 10 µl

*dependent on the DNA concentration

2.2.7 Subcloning into expression vectors

To clone DNA of interest into an expression vector, the DNA fragment containing the gene of interest was isolated from the pGEM-T Easy vector using restriction enzymes and then ligated into a plasmid that had been cut with the same restriction enzymes, to generate complementary ends ("sticky end"). Vectors and restriction sites used for cloning of particular genes are ilustrated in Table 5.5, Appendix.

2.2.7.1 DNA digestion using restriction endonucleases

The digestion reaction was carried out by appropriate restriction endonucleases, which recognise short DNA sequences and cut the DNA molecules at those specific sites. Digestion was performed at 37 °C for 1 h.

Restriction reaction mix contained:

Components:	Amount:
10 × restriction endonuclease buffers	2 µl
Restriction endonuclease	1 to 5 U/µg DNA
DNA sample in H_2O or Tris/EDTA (TE) buffer	0.1 to 4 µg
Autoclaved, deionised water	up to 20 µl

The following restriction endonucleases were employed in this study:

Enzymes:	Recognition and cleavage site:
AluI	AG↓CT
BamHI	G↓GATCC
EcoRI	G↓AATTC
EcoRV	GAT↓ATC
HindIII	A↓AGCTT
XhoI	C↓TCGAG

After digestion the insert and vector were separated by agarose gel electrophoresis, extracted and ligated over night, and the ligation mixture was transformed into competent *E. coli* DH5α cells. After minipreparation, to screen for the presence of an insert of the correct size plasmids were digested with appropriate restriction enzymes. In-frame cloning was verified by sequencing.

2.2.8   Immunological methods

2.2.8.1   Immunoblot (Western blot)

2.2.8.1.1   Protein extraction from mammalian cells

Confluent monolayers of mammalian cells were washed twice with ice-cold Dublecco's phosphate-buffered saline (PBS), after which lysis buffer was applied directly to cell monolayers (100 µl/100 mm^2), and cells were detached by scraping, transferred

into 1.5 ml microfuge tubes, incubated on ice for 30 min for complete lysis, and centrifuged for 15 min at 13 000 g. After centrifugation, the supernatant was mixed with 2 × SDS gel-loading buffer, boiled, and resolved by SDS-PAGE.

2.2.8.1.2 Protein extraction from yeast cells

Total protein extracts from a 50 ml liquid culture of *S. cerevisiae* AH109 transformed with bait constructs were prepared by boiling pellets of yeast cells grown to an OD_{600} of 0.6 in limiting synthetic medium lacking tryptophan in 50 µl of sample buffer.

Sample buffer:
60 mM Tris-HCl, pH 6.8
10% (v/v) glycerol
2% (w/v) SDS
5% (v/v) β-mercaptoethanol
0.025% (w/v) bromophenol blue.

2.2.8.1.3 Protein bloting

Proteins resolved by SDS-PAGE were transferred to a 0.25 µm pure nitrocellulose membrane. Transfer was performed at 120 V for 1 h.

2.2.8.1.4 Protein detection

For protein detection, membranes were blocked for 1 h in blocking buffer and then incubated overnight at 4 °C with the appropriate primary antibody in blocking buffer. After three washes for 10 min with Tris-buffered saline containing 0.1% (v/v) Tween 20 (TBST), the membranes were incubated for 1 h with horseradish-peroxidase-labelled secondary antibody, and washed again 5 × for 10 min with the same buffer. Detection of protein was performed using the enhanced chemiluminescent immunoblotting system and exposure to radiographic film. Antibodies are listed in Table 5.6, Appendix.

Transfer buffer, pH 7.4:
24 mM Tris base
193 mM glycine
10% (v/v) methanol

Blocking buffer:

5% (w/v) non-fat dry milk in PBS, containing 0.01% (v/v) Tween 20

TBS buffer:

20 mM Tris, pH7.4

15 mM NaCl

TBST buffer:

20 mM Tris, pH7.4

15 mM NaCl

0.05% (m/v) Tween 20

2.2.8.2 Co-immunoprecipitation

This method for identification of protein-protein interaction was used to verify whether two proteins of interest identified by yeast two-hybrid screen associated in mammalian cells.

Either NIH/3T3 or COS 7 cells were co-transfected with HA-BMPRII and Myc-RACK1 expression vectors using Lipofectamine™ 2000. After 48 h cells were washed twice with ice-cold PBS and lysed using buffer for immunoprecipitation (IP buffer) containing   0.5% (v/v) Triton X-100 or NP-40, 50 mM Tris-HCl, pH 7.4, 150 mM NaCl, 10 mM sodium pyrophosphate, 2 mM sodium orthovanadate, 100 mM NaF and a protease inhibitor cocktail. Proteins were solubilised on ice for 30 min. Cell lysates were clarified by centrifuging at 13 000 g for 15 min. To remove proteins that non-specifically bind to the protein A-Sepharose beads cell lysate were incubated for 30 min at 4 °C with 50 µl of protein A-Sepharose on a rotating shaker. Pre-cleared lysate was incubated with gentle shaking at 4 °C for 2 h with anti-HA monoclonal antibody cross-linked to protein A-Sepharose beads. Immunocomplexes were washed three times with IP buffer, dissociated by boiling in SDS gel-loading buffer and resolved by SDS-PAGE, transferred to nitrocellulose and immunobloted for Myc-RACK1 with an mouse monoclonal anti-Myc antibody as described in Section 2.2.8.1.

2.2.8.3 Glutathione S-transferase (GST) pull-down

This method for the identification of associated proteins was used to verify the interactions between a GST-fusion protein and a protein of interest in a mammalian cell lysate.

BMPRII fused to GST was overexpresed in *E. coli* BL21. Expression was induced by adding IPTG to a final concentration of 1 mM to a bacterial culture at OD_{600}~0.5. Bacteria were cultured for 4 h at 27 ℃ with shaking at 120 rpm, and centrifuged at 5 500 g for 20 min. The pellet was resuspended in Lysis Buffer B1 and sonicated. After complete lysis, the lysate was centrifuged at 15 000 g and the supernatant was applied to a gluthatione-Sepharose matrix and incubated for 2 h at 4 ℃ with rotation. To avoid non-specific binding, beads were extensively washed with Washing Buffer B2 containing 0.5% (v/v) Triton X-100. Cells overexpressing the protein of interest were lysed and the lysate was applied to beads containing purified GST-BMPRII or GST-tag alone as a negative control. After 1.5 h of incubation at 4 ℃ with rotation, beads were washed three times, and GST-tagged proteins together with bound partners were eluted in western blot loading buffer, boiled for 5 min and loaded onto a 12% SDS-PAGE gel.

Lysis Buffer B1:
20 mM Tris-HCl, pH 7.5
10 mM EDTA
5 mM EGTA
150 mM NaCl
0.1% (v/v) β-mercaptoethanol
1 mM PMSF

Washing Buffer B2:
20 mM Tris-HCl, pH 7.5
10 mM EDTA
150 mM NaCl
0.5% (v/v) Triton X-100
1 mM PMSF

2.2.8.4 Immunohistochemistry

Expression of particular proteins in human or mouse lung tissue was demonstrated using the standard avidin/biotin system according to the manufacturer's instructions (Histostain-SP Kit, Zymed).

Endogenous peroxidase activity in paraffin-embedded tissues was quenched using 1% (v/v) H_2O_2. After blocking with blocking solution for 10 min sections were incubated with primary antibody over-night, followed by a biotinylated secondary antibody. Antibody concentrations used for immunohistochemical studies are shown in Table 5.6, Appendix. Slides were developed for 5 min with diaminobenzidine (DAB) and counterstained with Mayers hematoxyllin.

2.2.8.5 Immunocytochemistry

Cells were plated in 8-well tissue culture chamber slides and incubated at 37 °C for approximately 16 h. Cells were transfected with appropriate expression vectors using Lipofectamine™ 2000 at 90% confluence. After 24 h of harvesting, cells were washed twice with ice-cold 1 × PBS, fixed with 100% methanol for 5 min at -20 °C. After two washes with 1 × PBS cells were incubated in blocking solution (5% (v/v) FCS in 1 × PBS) for at least 1 h at room temperature. The appropriate primary antibody was prepared in blocking solution (2.5% (v/v) FCS in 1 × PBS) at dilution 1:100, and approximately 300 µl was applied per well. Cells were incubated at room temperature for 1 h, washed three times with PBS (10 min each), and incubated with FITC-labelled secondary antibody at 1:300 dilution in the blocking buffer at room temperature for 1 h. After five washes with PBS, the plastic border of the chamber slide was removed, and slides were covered with mounting medium containing 4´,6´-diamidino-2-phenylindole (DAPI) (1:1000 dilution) for visualisation of nuclei, and samples were analysed by fluorescent microscopy.

2.3 Methodology of the yeast two-hybrid system

The yeast two-hybrid system is a procedure that facilitates the identification of novel protein-protein interaction partners, or mapping the domains of interaction between two known interacting molecules (Fields and Song 1989).

The yeast two-hybrid system emerged from studies on eukaryotic transcription factors (Figure 2.1), which usually contain separable DNA-binding domains (BD) and transcriptional activation domains (AD). The BD is capable of binding to a specific

promoter sequence, a region situated upstream from the gene, while the AD directs the RNA polymerase II complex to transcribe a downstream gene. Both of these domains are required for transcription, but they do not necessarily have to be located on the same protein. The BD can activate transcription when simply bound to another protein containing an AD (Figure 2.2). This principle forms the basis of the yeast two-hybrid technique.
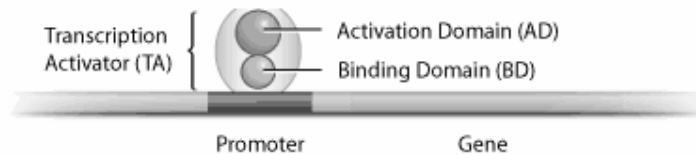
Figure 2.1   Principle of normal transcription.
Normal transcription requires both the DNA-binding domain (**BD**) and the activation domain (**AD**) of a transcriptional activator (**TA)** (after Solmaz Sobhanifar et al., 2004).

In a two-hybrid assay, two fusion proteins are created: the protein of interest (X), which contains a DNA binding domain attached to its N-terminus, and its potential binding partner (Y), which is fused to an activation domain. If protein X interacts with protein Y, the association of these two proteins will form an intact and functional transcriptional activator. This newly formed transcriptional activator will lead to transcription of a reporter gene; for which the gene product can be easily detected and measured (Figure 2.2).
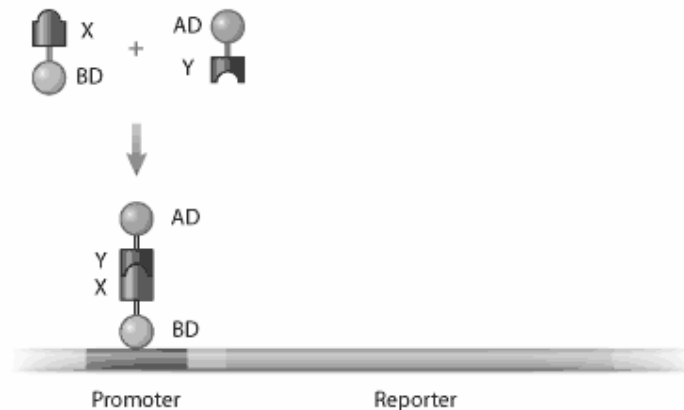
Figure 2.2   Principle of yeast two-hybrid transcription.
The yeast two-hybrid technique measures protein-protein interactions by measuring transcription of a reporter gene. If protein X and protein Y interact, then their DNA-binding domain and activation domain will combine to form a functional transcriptional activator (**TA**). The TA will then proceed to transcribe the reporter gene that is paired with its promoter (after Solmaz Sobhanifar et al., 2004).

In this study, the MATCHMAKER yeast two-hybrid system was employed. This system uses an enhanced GAL4 two-hybrid system to detect or confirm protein-protein interactions. The GAL4 acts as a transcriptional activator of their target genes by binding to upstream activating sequences (UAS) and thus directing RNA polymerase II to the corresponding promoters. In the MATCHMAKER system, the yeast strain that was used, *S. cerevisiae* AH109 includes four reporter genes: *ADE2, HIS3, lacZ,* and *MEL1* that are under control of distinct GAL4 UAS, while a TATA boxe, provides the binding site for the GAL4-DNA-BD. These promoters yield strong and specific responses to GAL4 and thus eliminate many false positives and maintain stringency of selection. The *MEL1* and *lacZ* genes encode α-galactosidase and β-galactosidase respectively. The α-galactosidase is a secreted enzyme and it can be assayed directly on X-α-GAL indicator during the screen process. This feature allows the identification of novel protein interactions while providing access to the genes encoding the interacting proteins.

In the two-hybrid screen, the GAL4-DNA-BD is expressed as a fusion product with the protein of interest. This is designated the "bait protein". At the same time, the GAL4-DNA-AD is expressed as fusion of product with proteins coded in a genomic or a cDNA library and is called the "prey". Therefore, when the bait and the prey interact, the interacting proteins activate transcription of the reporter genes as the GAL4-DNA-BD and the GAL4-DNA-AD are brought together (Figure 2.3).
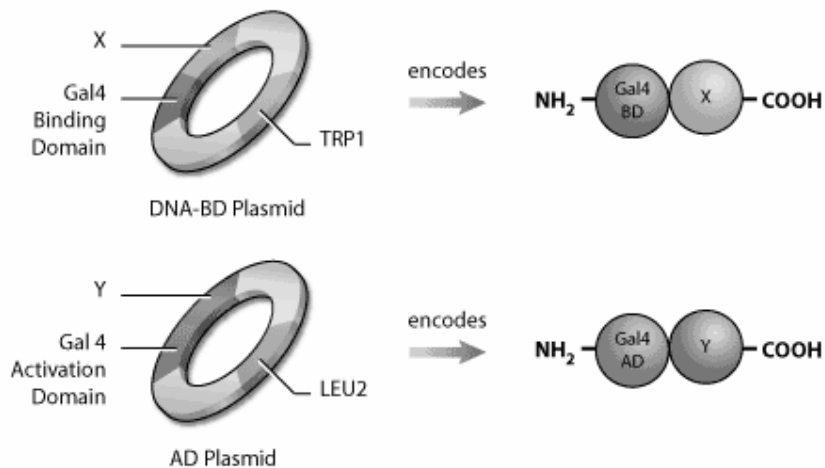
Figure 2.3   Scheme of bait and prey vectors and their protein products.
The yeast two-hybrid assay uses two plasmid constructs: the bait plasmid, which is the protein of interest fused to a GAL4 binding domain, and the hunter plasmid, which is the potential binding partner fused to a GAL4 activation domain (after Solmaz Sobhanifar et al., 2004).

The properties of plasmids used to express the bait and prey are very important. The vectors that are chosen for the two-hybrid screen often are designed to carry different antibiotic resistance marker such as ampicillin and kanamycin to allow for their counter selection. They also have a nutritional marker specific for a certain amino acids that allows the yeast carrying the plasmid to grow on limiting synthetic medium lacking that amino acids. Another important portion of the cloning vectors is the truncated ADH1 promoter. This promoter, truncated or full-length, is used to drive expression of the fusion protein in the cloning vector. The full-length ADH1 promoter leads to high-level expression of sequences under its control. However, transcription is repressed by the high amounts of ethanol that accumulate in the medium as a by-product of yeast metabolism. As a result, the vectors that were used in the study all contained some form of truncated ADH1 promoter.

2.3.1.1   Bait plasmids constructions

To generate bait constructs for BMPRII, particular regions of the *BMPR2* gene encoding the kinase domain, cytoplasmic tail and full intracellular region were cloned into the pGBKT7 vector, resulting in a fusion to the GAL4-DNA-BD at the 5' end. Total mouse RNA was used as a template in RT-PCR reactions (Section 2.2.2); to isolate particular regions of the *BMPR2* gene using primers containing restriction sites for *EcoRI* (forward) and *BamHI* (reverse). Primers sequences are displayed in Table 5.2, Appendix. The PCR reaction was carried out according to the protocol in Section 2.2.3. The PCR products were digested with *EcoRI* and *BamHI*, and separated on 1% agarose gel. Bands of 0.9 kb, 1.5 kb, 2.5 kb, were excised and gel-purified. The pGBKT7 vector was linearised with the same restriction endonucleases, resolved on a 1% agarose gel, and gel-purified in a similar manner. The PCR products from *EcoRI* and *BamHI* digestion were cloned into the linearised pGBKT7 (Figure 2.4). These ligation products were transformed into *E.coli* DH5α cells, and plated on LB/kanamycin plates. Resulting clones were screen with restriction endonucleases for the presence of an insert of the correct size. Clones with correct insert sizes after digestion were sequenced to confirm correct reading frame.
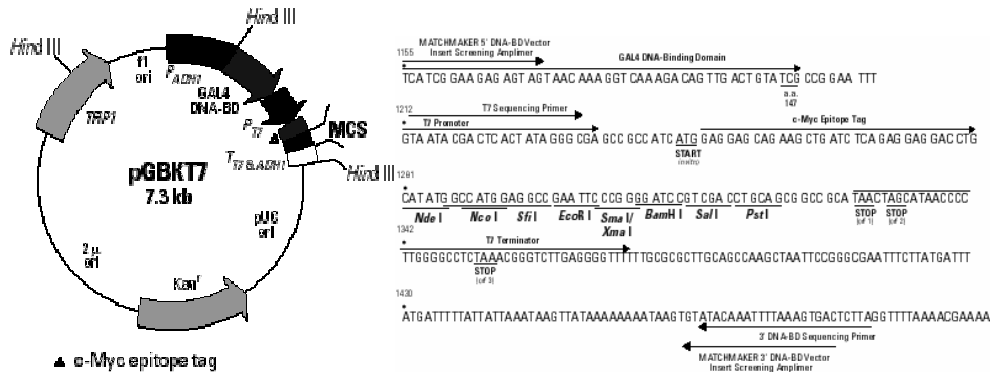
Figure 2.4   The pGBKT7 cloning vector (Clontech).
The vector generates hybrid proteins, which contain the GAL4-GAL4-DNA-BD at the N terminus of the bait. The fusion protein is expressed in the yast host cells from the constitutive truncated *ADH1* promoter; transcription is terminated at the *ADH1* transcription terminator signal. pGBKT7 also contains the T7 promoter, a c-Myc epitope tag, and a MCS. pGBKT7 replicates autonomously in both *E. coli* and S. *cerevisiae* from the pUC and 2 μ ori, respectively. The vector carries the kanamycin resistance gene for selection in *E. coli* and the *TRP1* nutritional marker for selection in yeast.

2.3.1.2   Verification of bait protein expression

2.3.1.2.1 Transformation of bait constructs into *S. cerevisiae* AH109 yeast strain

        Bait constructs (0.1 μg) were mixed in a 1.5 ml microcentrifuge tube with 100 μl of competent yeast, 0.1 mg herring testes carrier DNA and 600 μl sterile polyethylene glycol/lithium acetate (PEG/LiAc) solution. Cells were then incubated at 30 °C for 30 min with rotation and after treatment with 70 μl of DMSO, heat-shocked for 15 min in a water bath at 42 °C and then incubated on ice for 2 min, after which 100 μl of each transformation culture was plated on medium lacking tryptophan (SD/-Trp), and maintained at 30 °C for three days.

2.3.1.2.2 Extraction of yeast total protein

        Total protein extracts from *S. cerevisiae* AH109 transformed with bait constructs were prepared by boiling a pellet from 50 ml of yeast culture grown to an OD_{600}~0.6 in SD/-Trp.

Sample buffer:

60 mM Tris-HCl, pH 6.8

10% (v/v) glycerol

2% (w/v) SDS

5% (v/v) β-mercaptoethanol

0.025% (w/v) bromophenol blue.

2.3.1.2.3 Detection of bait protein expression

For immunoblot analysis, 15 µl aliquots of protein extract were resolved on a 10% SDS polyacrylamide gel under reducing conditions, followed by electrotransfer to a 0.25 µm nitrocellulose membrane. Immunoblotting was performed according to the standard protocol (Section 2.2.8.1).

2.3.1.3 Test of the GAL4-DNA-BD/ bait protein for transcriptional autoactivation

Prior to performing a two-hybrid screen, it is important to verify that the baits alone do not activate reporter genes. Therefore, the bait GAL4-DNA-BD fusion constructs were independently transformed into *S. cerevisiae* AH109 and plated on the SD/-Trp media containing X-α-Gal. This indicated whether there was autoactivation of the *lacZ* gene by the bait constructs alone.

The autoactivation of the bait plasmid might occur if the bait plasmid alone acts independently as a transcription factor. Autoactivation would have yielded blue colonies.

A second autoactivation test was performed after mating *S. cerevisiae* AH109 transformed with the bait construct and *S. cerevisiae* Y187 containing an empty prey vector. These diploid cells were plated on the SD/-Trp/-Leu media containing X-α-Gal. This revealed whether there was autoactivation of the other reporter genes via direct interaction of GAL4-DNA-AD domain with the bait protein. Autoactivation would result in growth of blue colonies.

2.3.1.4 Gal4-DNA-AD fusion cDNA library

The mouse 11-day embryo cDNA library was commercially available from Clontech. The library was prepared in pACT2 (Figure 2.5, Clontech), which facilitates expression of prey proteins as N-terminal fusions to the Gal4-DNA-AD.

The library titer was determined to be ≥ 5 x 10^7/ml and contains 3.5×10^6 independent clones with an average DNA insert size of 2 kb.

The library was prepared by randomly shearing the cDNA obtained by RT and using XhoI-(dT)$_{15}$ primer to attach polylinkers on the ends of each fragment that contains EcoRI sites. This permitted use of EcoRI and XhoI for the excision of the inserts from the pACT2 from positives colonies. The pACT2 library was amplified in *E. coli* strain BNN132, and the plasmid DNA was isolated and used to transform *S. cerevisiae* Y187.
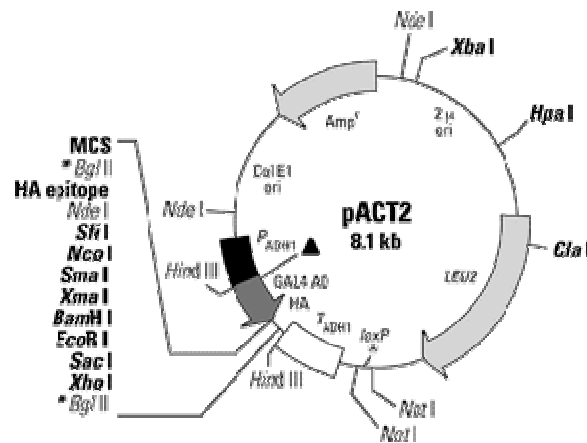
Figure 2.5   The pACT2 expression vector (Clontech).
The vector generates hybrid proteins that contain the sequences for the GAL4 activation domain. It carries the gene (for ampicillin resistance in *E.coli*) and the *LEU2* nutritional marker that allow yeast auxotrophs carring this vector to grow on limiting synthetic medium lacking leucine. The hybrid protein is expressed at high levels in yeast host cells from the constitutive *ADH1* promoter (P); transcription is terminated at the *ADH1* transcription termination signal (T).

2.3.2   Screening the pretransformed cDNA library

2.3.2.1   Yeast mating

Yeast from 500 ml overnight culture (OD$_{600}$ >0.8) of the bait strain (*S. cerevisiae* AH109 transformed with the bait construct) were harvested by centrifugation (5 000g, 20 min, 25°C), and the pellet of the entire culture was combined with the 1 ml 11-day embryo cDNA library in a two-litre sterile flask, after which 45 ml of 2 × YPDA medium was added, and the culture incubated at 30 °C for 24 h with gentle swirling.

After 24 h, the mating culture was transferred to a sterile centrifuge bottle and cells were harvested by centrifugation at 1 000 g for 10 min. The supernatant was decanted, and

the cell pellet was resuspended in 10 ml of 0.5 × YPDA. Cotransformants were plated on high-stringency plates (SD/-Trp/-Leu/-Ade/-His/+X-α-Gal) to eliminate backgroun

2.3.2.2 Identification of positives colonies

Positives colonies from the screen appeared as blue colonies on selective medium after 21 days. These colonies were picked, and the plasmids (a mixture of the GAL4-DNA-BD/bait and AD/library) were isolated according to the manufacturer's instructions using Chroma SPIN-1000 DEPC-H$_2$O columns.

The plasmids were transformed into *E. coli* DH5α, which were selected for GAL4-DNA-AD or GAL4-DNA-BD clones by resistance to ampicillin or kanamycin.

After transformation, bacteria were plated on LB/ampicillin plates. Due to the incompatibility of the plasmids, only the one type of plasmid was replicated in each bacterial cell. Colonies from ampicillin plates were selected; plasmids were isolated and digested with EcoRI and XhoI, and sequenced using the sequencing primer GAL4. Nucleotide sequences were translated into amino acids according to the open reading frame (ORF) fused to the GAL4 AD sequence, and analysed in GenBank using the BLAST algorithm.

2.4   Luciferase assay

Cells were plated in 48-well dishes (20 000 cells/ well) and after 12 h were transfected with 0.2 µg of a different luciferase reporter constructs containing the Id1 promoter or the BMP-Responsive Element (BRE). Approximately 0.2 µg of pGL3 luciferase construct was used as reference for transfection efficiency. Cells were stimulated for 24 h with BMP (20 ng/ml) or were not stimulated (in the case of control). Medium was removed, and cells were lysed using the lysis buffer provided in the Dual Luciferase System Kit. After 1 h, cell lysate (40 µl) was added to 50 µl luciferase assay reagent in a 96-well plate. Samples were analysed in a Packard Lumicount luminometer.

2.4.1   Microbiological methods

2.4.1.1 Cultivation of *E. coli*

For plating, *E. coli* cells were spread on LB-agar plates and incubated at 37 ℃ for 8-15 h. For liquid culture, *E. coli* cells were propagated by vigorous shaking at 37 ℃ in LB medium or LB medium containing the appropriate antibiotic.

LB Medium (Luria-Bertani Medium):

1% (m/v) bacto tryptone

0.5% (m/v) bacto yeast extract

1% (m/v) NaCl

1.5% (m/v) agar*

adjusted to pH 7.0 with NaOH; sterilised for 20 min at 121 °C, 15 psi

*only for plate preparation

Additives:

50 µg/ml ampicillin

30 µg/ml kanamycin

20 µg/ml X-gal

0.1 mM isopropyl β-thiogalactopyranoside (IPTG)

2.4.1.2 Preparation of competent *E. coli* cells for transformation

Using an inoculating loop, *E. coli* DH5α were streaked from frozen stock onto the surface of an SOB agar plate and incubated for 16 h at 37 °C. Five isolated colonies were transferred into 500 ml SOB containing 20 mM $MgSO_4$ and grown at 37 °C to an OD_{600} of~0.4. The cultures were transferred into ice-cold 50 ml polypropylene tubes and centrifuged at 2 700 g for 10 min; the pellet was resuspended in 20 ml of ice-cold FSB transformation buffer. After 10 min incubation on ice, the cells were recovered by a 10 min centrifugation at 2 700 g, decanted, and the pellet was resuspended in 4 ml ice-cold FSB. For frozen stock preparation, 140 µl of dimethyl sulfoxide (DMSO) was added twice into 4 ml of resuspended cells. Competent bacteria were stored at -80 °C until needed.

FSB transformation buffer:

10 mM potassium acetate, pH 7.5

45 mM $MnCl_2 \cdot 4H_2O$

10 mM $CaCl_2 \cdot 2H_2O$

10 mM KCl

100 mM hexamminecobalt chloride

10% (v/v) glycerol

SOB Medium:

1% (m/v) bacto tryptone

0.5% (m/v) bacto yeast extract

0.05% (m/v) NaCl

1.5% (m/v) agar*

2.5 mM KCl

10 mM $MgCl_2$ (after autoclaving)

adjusted to pH 7.0 with NaOH; sterilised for 20 min at 121 °C, 15 psi

*only for plate preparation

SOC Medium:

1% (m/v) bacto tryptone

0.5% (m/v) bacto yeast extract

0.05% (m/v) NaCl

1.5% (m/v) agar*

2.5 mM KCl

20 mM glucose (after autoclaving)

adjusted to pH 7.0 with NaOH; sterilised for 20 min at 121 °C, 15 psi

*only for plate preparation

2.4.1.3 Transformation of plasmid DNA into competent *E. coli* cells

An aliquot of competent *E. coli* cells was slowly thawed on ice and 100 µl of highly competent bacteria (1×10^8 cfu/µg DNA) was mixed with 3 µl of plasmid DNA. The mixture was incubated on ice for 30 min, followed by heat shock at 42 °C for 1 min, and then incubated on ice for 3 min. SOC medium (900 µl) was added, and the mixture was further incubated for 1.5 h at 37 °C with shaking. The transformed bacteria were plated, and incubated at 37 °C overnight.

2.4.1.4 Plasmid minipreparation

Individual colonies were picked from LB agar plates and innoculated into 5 ml of LB medium containing the appropriate antibiotic. After overnight incubation at 37 °C with shaking, the bacterial culture was pelleted by centrifugation at 5 500 g for 8 min and

plasmid purification was performed according to the manufacturer's instruction provided together with all reagents in QIAprep Spin Miniprep Kit.

2.4.1.5 Plasmid midipreparation

According to the protocol from PureYield Plasmid Midiprep System 5 ml of a 4 h culture was inoculated into 200 ml of LB medium, pelleted by centrifugation at 5 500 g for 15 min and plasmid purification was performed according to the manufacturer's instructions.

2.4.2 Cultivation of yeast

For plating, yeast cells were streaked on YPD or an appropriate synthetic drop-out (SD) medium plate and incubated at 27 °C for 12 h-18 days. For liquid culture, yeast cells were propagated by vigorous shaking at 27 °C in YPD or appropriate SD medium.

YPD (A)* medium:

2% (m/v) bacto tryptoneee

1% (m/v) bacto yeast extract

3% (m/v) agar (for plates only)

2% (m/v) glucose

adjusted to pH 6.5 with NaOH; sterilised for 20 min at 121 °C, 15 psi
*For YPDA medium extra 15 ml of 0.2% (m/v) adenine hemisulfate solution.

SD Medium:

0.067% (m/v) nitrogen base without amino acids

DO supplement*

3% (m/v) agar (for plates only)

2% (m/v) glucose

pH 5.8 adjusted with NaOH; sterilised for 20 min at 121 °C, 15 psi.
  *amount dependent on the type of DO supplement

2.4.2.1 Preparation of competent *S. cerevisiae* cells for transformation

S. cerevisiae AH109 or Y187 cells were cultured in YPDA medium to an OD_{600}~0.6, then treated with Tris-EDTA/lithium acetate (TE/LiAc) solution.

TE/LiAc buffer:
1 × TE buffer, pH 7.5
1 × LiAc

2.4.2.2 Transformation of bait constructs into AH109 yeast strain

Bait constructs (0.1 µg) were mixed in 1.5 ml microcentrifuge tube with 100 µl of competent yeast cells, 0.1 mg herring testes carrier DNA and 600 µl sterile PEG/LiAc solution. Then cells were incubated at 27 °C for 30 min with shaking and after treatment with 70 µl of DMSO, heat-shocked for 15 min in a water bath at exactly 42 °C and then incubated on ice for next 2 min. Aliquots (100 µl) of each transformation culture were plated on SD/-Trp medium and maintained at 27 °C for three days.

PEG/LiAc solution:
40% (m/v) PEG
1 × TE buffer, pH 7.5
1 × LiAc

2.4.3 Culture of mammalian cells and transfection technique

2.4.3.1 Cell culture conditions

Mammalian cells were grown in tissue culture plates in D-MEM medium (NIH/3T3, COS 7, A549) containing 10% (v/v) FBS at 37 °C, 5% CO_2 and 95-100 % humidity. Each cell line was passaged twice weekly. The cells were washed once with PBS, treated with 3 ml trypsin solution for maximum 3 min, resuspended in D-MEM medium, and split for further culture.

PBS (phosphate-buffered saline):
0.08% (m/v) NaCl
0.02% (m/v) KCl
0.115% (m/v) $Na_2HPO_4 \cdot 2H_2O$

0.02% (m/v) $KH_2PO_4 \cdot 2H_2O$

pH 7.4 adjusted with NaOH; sterilized for 20 min at 121 °C, 15 psi

Trypsin solution:

0.25% (m/v) trypsin

1.23 g/l EDTA

2.4.3.2 Transient transfection using Lipofectamine^{TM} 2000 reagent

Transient transfection is a method used to transfer DNA into eukaryotic cells; the transfected DNA does not become integrated into the host chromosomes.

Approximately 24 h prior to transfection, cells were plated at cell density 1-3 × 10^4/cm^2 in complete growth medium to obtain 90% confluence the following day. Transfection reagent (Lipofectamine^{TM} 2000) was mixed with Opti-MEM I Medium without serum and incubated for 5 min at room temperature. The DNA was added, gently mixed and the transfection solution was left for 20 min at room temperature to allow DNA-Lipofectamine complexes to form. The ratio of DNA to Lipofectamine in OptiMEM medium was 1:2.5.

The transfection mixture was added to plates containing cells in growth medium, mixed gently by rocking the plate back and forth. Cells were harvested at 37 °C in a CO_2 incubator for 18-48 h; 4 h after transfection additional, fresh medium was added.

2.4.3.3 Transient transfection of SMC using Nucleofector technology

Transfection of primary paSMC has been optimized using the Nucleofector technology from Amaxa Biosystems. This is a novel and proprietary transfection method designed for primary cells and difficult to transfect cell lines. The procedure relies on a non-viral method based on a unique (and undisclosed) combination of electrical parameters and cell-type specific solutions that transports the DNA directly into the nucleus. Using this technology, we routinely achieve 50% to 90% transfection efficiency in primary paSMC, which is not possible with several other techniques employed such as lipofection or electroporation. In addition, paSMC transfected with this method are viable and continue to retain the paSMC phenotype. The transfection was performed according to the protocol from Basic Nucleofector Kit; Amaxa.

2.4.3.4   Transfection with small interfering RNA (siRNA)

The paSMC were trypsinised and plated aproximately 24 h prior to transfection in complete growth medium to obtain 40-50% confluence the following day. To downregulate RACK1, four different siRNA (si#1, si#2, si#3, si#4) against RACK1 were tested. Mock (universal negative control siRNA, commercially available from Ambion) served as a non-specific siRNA to control possible non-specific siRNA effect. The siRNA sequences are available in Table 5.4, Appendix. Transfection reagent (X-tremeGENE siRNA) was mixed with Opti-MEM I Medium without serum and incubated for 5 min at room temperature, and then individual siRNAs were added (at 100 nM final concentration), gently mixed and incubated at room temperature for 20 min. The siRNA-transfection reagent complexes were added to the cells, and cells were harvested 24 h for RNA or 48 h for protein extraction or used for functional analysis.

2.4.3.5   Proliferation assay

To assess the effect of RACK1 depletion on cell proliferation, paSMC were plated in 96-well culture plates at a density of 7.5 x 10^3 cells/well. The following day, wells were treated with (siRNA) Cells were then harvested by trypsinisation, and cells were counted using a hemocytometer at the indicated time points.

In select experiments, cell counts were confirmed by monitoring DNA synthesis by [^{3}H]-thymidine incorporation assays. Cells were seeded into 96-well plates and treated as indicated. Cells were then pulsed with 0.6 μCi of [^{3}H]-thymidine (GE Healthcare, Little Chalfont, Buckinghamshire, UK) for 4 h. Plates were washed twice with cold PBS and incubated with ice-cold 10% trichloroacetic acid for 30 min at 4 °C. Subsequently, samples were solubilised in 0.5 M NaOH. The contents of each well were then transferred into scintillation fluid and incorporated radioactivity counted in a liquid scintillation counter.

3   Results

3.1   Identification of new proteins interacting with the intracellular region of BMPRII

3.1.1   Construction and expression of the BMPRII baits

To identify novel proteins that interact with the intracellular region of BMPRII, we conducted a GAL4-based yeast two-hybrid screen (Fields and Song, 1989) (see methods 2.3).

For our analyses, we used as baits the kinase domain of BMPRII (amino acid residues 205-530 encoded by nucleotides 615-1590), the C-terminal tail domain of BMPRII (amino acid residues 530-1038 encoded by nucleotides 1590-3114) and the complete intracellular segment of BMPRII containing the kinase and C-terminal tail domains (amino acid residues 173-1038 encoded by nucleotides 519-3114). The intracellular parts of the receptor were fused to the C-terminus of the GAL4-DNA-binding domain (GAL4-DNA-BD) and termed "kinase", "tail", and "total" baits, respectively.

To create these molecules, the appropriate region of the *BMPR2* gene was amplified with specific primers and cloned in-frame into the pGBKT7 expression vector (Figure 3.1, 3.2). Plasmid digestion and full-length sequencing were used to confirm that the clone would express the desired chimaeric protein (Figure 3.3).
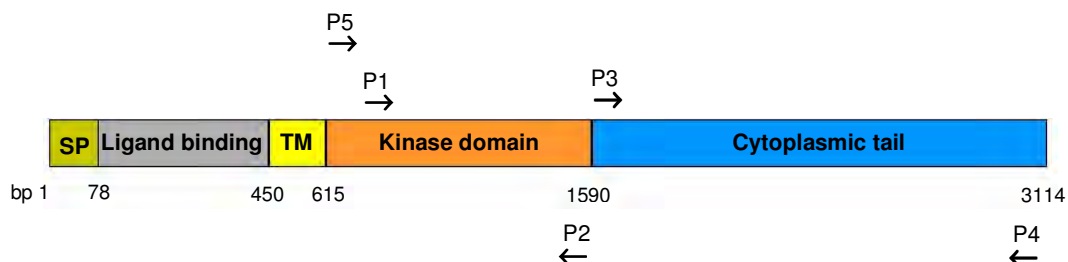
Figure 3.1   Graphic representation of the *BMPR2* open reading frame (ORF), and placement of primers selectively amplifying distinct regions of the gene for yeast two-hybrid bait construction.
Amplification of the kinase domain was performed with primers P1 and P2; to obtain cytoplasmic tail region primers P3 and P4 were used; the whole cytoplasmic segment of the receptor was amplified with primers P5 and P4. Full sequences of those primers are available in Table 5.2, Appendix. **bp**; base pair, **SP**; signal peptide, **TM**; transmembrane
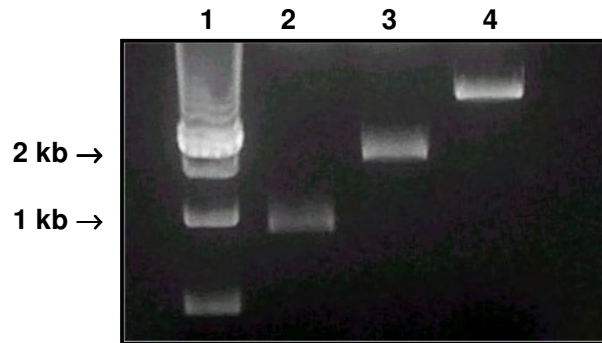
Figure 3.2   Amplification of distinct regions of mouse *BMPR2*.
Lane 1: Molecular mass markers, **lane 2**: PCR product encoding the kinase domain of BMPRII, **lane 3**: cytoplasmic tail, **lane 4**: total intracellular domain. PCR products were resolved on a 1% (m/v) agarose gel.
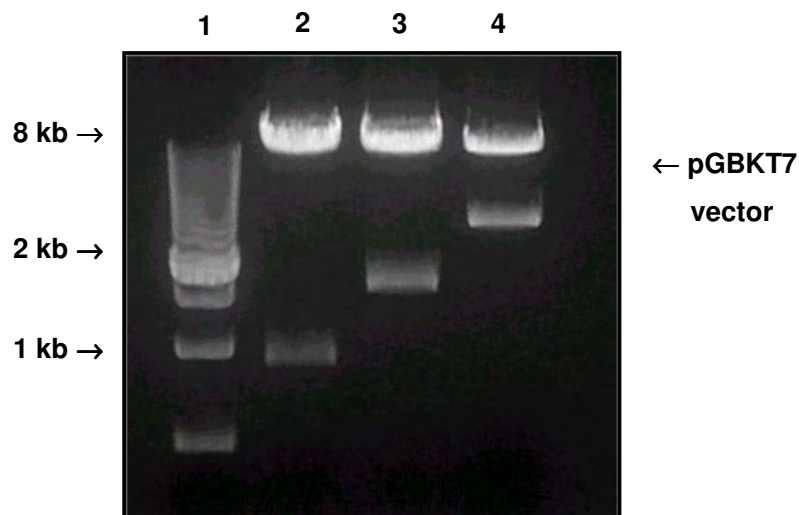
Figure 3.3   Confirmation of insert ligation.
Baits constructs were digested with *EcoRI* and *BamHI* restriction endonucleases to screen for the presence of an insert of the correct size. Digestion of the bait plasmids gave the expected fragment sizes **Lane 1**: molecular mass markers, **lane 2**: kinase bait (0.9 kb), **lane 3**: tail bait (1.5 kb), and **lane 4**: total bait (2.5 kb).

Three bait constructs were transformed separately into *S. cerevisiae* AH109, and transformants were selected for on SD/-Trp media. The proper expression of bait constructs was verified by immunoblotting with an anti-Myc tag antibody (Figure 3.4).

A)
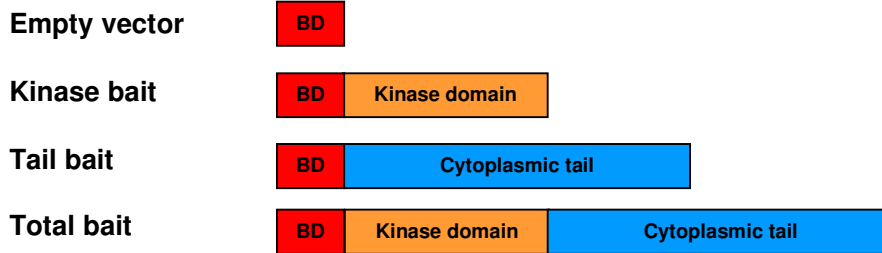
B)
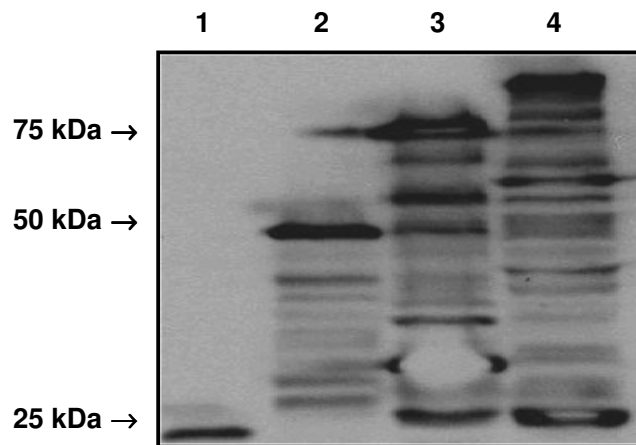
Figure 3.4   Test for expression of bait proteins.
A) Schematic representation of bait constructs. **B)** Immunoblot of protein extracts from *S. cerevisiae* AH109 carrying bait constructs with anti-Myc antibody. **Lane 1**: extracts of *S. cerevisiae* AH109 carrying an empty vector (pGBKT7) served as a negative control (the 25 kDa band corresponds to the size of binding domain (BD)), **lane 2**: extracts of *S. cerevisiae* AH109 carrying kinase bait (50 kDa), **lane 3**: tail bait (75 kDa), **lane 4**: total bait (100 kDa). Lower molecular mass bands represent degradation products attributable to the high proteolytic activity of yeast extracts. **BD**; binding domain.

3.1.2   Test for autonomous reporter gene activation

Prior to performing a two-hybrid screen, we verified that the baits alone do not activate the reporter genes (Figure 3.5). Empty BD vector, and BD vectors containing the apropriate region of *BMPR2* were independently cotransformed together with the empty AD vector into *S. cerevisiae* AH109, and plated on SD/-Leu/-Trp media containing X-α-Gal. Colonies containing the kinase and total baits appeared as white colonies, whereas yeast-containing the tail bait grew as blue colonies, as did those transformed with the positive control. We concluded that kinase and total baits did not autoactivate

the *lacZ* reporter gene, whereas the tail bait, due to its autoactivation capacity, was excluded from further investigation.
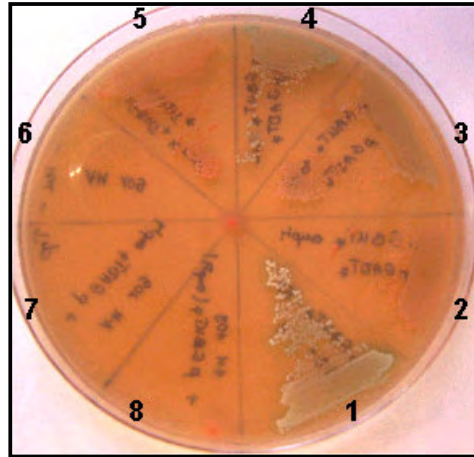
Figure 3.5   Test for bait protein autoactivation.
S. cerevisiae AH109 transfected separately with the three baits constructs were plated on SD/-Leu/-Trp media containing X-α-Gal. **Section 1**: *S. cerevisiae* AH109 transfected with a positive control vector, **section 2**: with empty BD and AD vector together, **section 3**: with total bait and empty AD vectors together, **section 4**: with tail bait and empty AD vector, **section 5**: with kinase bait and empty AD vector, **section 6**: untransfected *S. cerevisiae* AH109, **section 7**: transfected with empty AD vector, **section 8**: with empty BD vector alone.

3.1.3   A yeast two-hybrid screen using kinase and total baits

In order to find novel interacting partners for BMPRII, a mouse 11-day embryonic cDNA library was screened using baits expressing the kinase and the total intracellular domains of BMPRII. We chose to use this library, as there was no commercially available lung cDNA library, and we had observed that BMPRII was highly expressed throughout all embryonic stages of mouse development (data not shown). It is also well known that BMP signalling is involved in lung development (see Section 1.3).

S. cerevisiae AH109 either containing kinase or total bait constructs were mated with *S. cerevisiae* Y187 pretransformed with the cDNA library, and were then plated on high-stringency medium (SD/-Ade/-His/-Leu/-Trp/ + X-α-Gal) for screening. From the 3.5×10^6 independent clones screened, 187 blue colonies indicating putative positive interactions, were obtained from the kinase screen, and 168 were obtained from the total screen. The clones were individually picked, grown in liquid culture for plasmid isolation and sequenced. Insert sequences were translated in the same frame that they would have been translated as fusion products with the GAL4-DNA-AD. The translated products were subjected to a standard protein-protein blast search against all protein

sequences in the NCBI Protein Database. Translated products demonstrating greater than 85% homology to known proteins were consider putative true-positive interactions (Table 3.1). Other translated products were rejected as false-positives.

Table 3.1 **Deduced amino acid sequences obtained from inserts from positive clones.**
The "**Ki**" clones represent insert sequences obtained from the kinase bait screen, whereas "**To**" clones represent insert sequences obtained from total bait screen.

Clone	Deduce insert sequense	Homology with	Accession Number
Ki 19	GRVDELHSQEMQKRKEMQLRQEEERRRREEEMMIRQREMEEQMRRQREESYSRMGYMDPRERDMRMGGGGTMNMGDPY GSSGGQKFPPLGGGGGIGYEANPGVPPATMSGSMMGSDMRTERFGQGGAGPVGGQGLEEWGLELQQDMVEGEKSMKGQIKN PDFRYLGFHSSLVLSFLV	**Splicing factor proline/glutamine rich (98%)**	NP_076092.
Ki 21	GRVDRGFPVIPCPSHIIPIRVGNAALNSKICDLLLSKHSIYVQAINYPTVPRGEELLRLAPSPHHSPQMMENFVEKLLLAWTEVGLPL QDVSVAACNFCHRPVHFELMEWERSYFGNMGPQYVTTYA	**Alas2 protein**	AAH24575
Ki 23	AERLDFNPDRYLQDNPASGEKFAYVPFGAGRHRCVGENFAYVQIKTIWSTMLRLYEFDLINGYFPTVNYTTMIHTPENPVIRYKRRS K.EEEQEASVERGPQAAAGRE	**Cytochrome P450, family 51**	NP_064394
Ki 37	IHRGGGQIIPTARRCLYASVLTAQPRLMEPIYLVEIQCPEQVVGGIYGVLNRKRGHVFEESQVAGTPMFVVKAYLPVNESFGFTADL RSNTGGQAFPQCVFDHWQILPGDPFDNSSRPSQVVAETRKRKGLKEGIPALDNFLDK	**Eukaryotic translation elongation factor 2**	
Ki 41	GRVDVDAAARRHRASSFSLPEGRLACPVCRPPAKLESTDFSATMLPASLLRHPGLRRLMLQARTYAEAAAAPAPAAGPGQMSFT FASPTQVFFDSANVKQVDVPTLTGAFGILASHVPTLQVLRPGLVVVHTEDGTTTKYFGSPGQPGEGAVRTVRCGGRGSTG	**ATP synthase, H+ transporting, mitochondrial F1 complex, delta subunit**	AAH08273.
Ki 42	NEVGVTSQSTLWYAIVGLISGQLPHDDVISSDGQFALSGSWDGTLRLWDLTTGTTTRRFVGHTKDVLSVAFSSDNRQIVSGSRD KTIKLVWNTLGVCKYTVQDESHSEWVSCVRFSPNSSNPIIVSCGWDKLVKVWNLANCKLKTNHIGHTGYLNTVTVSPDGSLCASGG KDGQAMLWDLN	**Guanine nucleotide binding protein (G protein), beta polypeptide 2 like 1**	NM_008143
Ki 45	AEYGAEALERMFASFPTTKTYFPHFDVSHGSAQVKGHGKKVADALANAAGHLDDLPAALSALSDLHAHKLRVDPDNFKLLSHCLLV TLASHHPADFTPAVHASLDKFLASVSTVLTSKYR.AAFCGACLLAMPFFSPLHLYLLVFE	**Alpha globin 2**	AAL32372
Ki 46	GRVDVALVFQNTALFSRAVCSSSSPRIMATAVVVNIGKKLYEGKTKEVYELLDTPGRVLLQSKDQITAGNAARKNHLEGKAISNKITS CIFQLLQEAGIKTAFTKKCGETAFIAPQCEMIPIEWVCRRIATGSFLKRNPGVQEGYKFYPPKVEMFFKDDANNDPQWSEEQLIAA KFCFAGLVIGQTEVDIMSHATQAIFEILEKSWLP	**Phosphoribosylaminoimidazole carboxylase**	NP_080215.
Ki 56	LGPRGLTAKQLEAETGCKIMVRGKGSMRDKKKEEQNRGKPNWEHLNEDLHVLITVEDAQNRAEIKLKRAVEEVKKLLVPAAEGE DSLLKKMQLMELAILNGTYRDANIKSPTAQAAPRIITGPAPVLPPAALRTPTPAGPTIMPLIRQIQTAVMPNGTPHPTAAIVPPGPEAGLI VTRVE	**QKI isoform 7B**	AAM21010.
Ki 57	SPSPSLCNVFHIPLPSFQASNSQIPGPSGRAESACSWVGSYQGKSGTPPRGPPASHTASPAQASESCNQGPTHNILHETQ	**Slc25a23 protein**	AAH17139
Ki 58	LGVCKYTVQDESHSEWVSCVRFSPNSSNPIIVSCGWDKLVKVWNLANCKLKTNHIGHTGYLNTVTVSPDGSLCASGGKDGQAML WDLNEGKHLYTLDGGDIINALCFSPNRYWLCAATGPSIKIWDLEGKIIVDELKQEVISTSSKAEPPQCTSLAWSADGQTLFAGYTD NLVRVWQVTIGTR	**Guanine nucleotide binding protein (G protein), beta polypeptide 2 like 1**	NM_008143
Ki 80	CIDARFYGNVSRFINHHCEPNLVPVRVFMSHQDLRFPRIAFFSTRLIQAGEQLGFDYGERFWDVKGKLFSCRCGSSKCRHSSAAL AQRQASAAQEPQENGLPDTSSAAAADPL	**Euchromatic histone methyltransferase 1 isoform 2**	NP_766133
Ki 82	LQLTIQSLRIILGCKVPVQQKWWVTHLFTSSQEEVRSYSYDPPLKFMSVQRPGPYDRPGTARRYIGIVKQAGLDRMRSGAYSAGY GGYEEYSGLSDGYGFTTDLFGRDLSYCLSGMYDHRYGDSEFTVQSTTGHCVHMRGLPYKATENDIYNFFSPLNPVRVHIEIGPDG F RVTGEADVEFATHEEAVAAM	**Heterogeneous nuclear ribonucleoprotein F**	NP_598595
KI 83	VDAAMKLISPRDFVDLVLVKKYEDGTISSNATHVEHPLCCPPKPGFVRGFNHPCGCFCEPLPGDPNKTNLVTFFQTDLGYLPQSVV DSFFPRSMAEFYPNL	**StAR-related lipid transfer protein 5**	NP_075866
Ki 87	SGSHDESVRLWDVKSKQCLRTVTLKGPVTNAAIILAPPMLNPEFRPSLPLPHFNKHLLGAEHGDEAQGGGLRLQLGLHLQGKEPS YLERLEQLQAVLSSYLEKNMLGSQMLPARVFDLEDEVRSLRKINRDLFDFSTRIITRPSK	**Wdr18 protein**	AAH95984
Ki 93	NSLKYVRPGGGFEPNFTLFEKCEVNGEKAHPLFTFLRNALPTPSDDPTALMTDPKYIIWSPVCRNDIAWNFEKFLVGDGVPVRRY SRRFRTIDIEPDIETLLSQQSGNS	**Glutathione peroxidase 1**	NP_032186
Ki 97	FSPNSSNPIIVSCGWDKLVKVWNLANCKLKTNHIGHTGYLNTVTVSPDGSLCASGGKDGQAMLWDLNEGKHLYTLDGGDIINALCF SPNRYWLCAATGPSIKIWDLEGKIIVDELKQEVISTSSKAEPPQCTSLAWSADGQTLFAGYTDNLVRVWQVTIGTR	**Guanine nucleotide binding protein (G protein), beta polypeptide 2 like 1**	NM_008143
Ki 100	TVPVGRVETGVLKPGMVVTFAPVNVTTEVKSVEMHHEALSEALPGDNVGFNVKNVSVKDVRRGNVAGDSKNDPPEAAGFTAQVIIL NHPGQISAGYAPVLDCHTAHIACKFAELKEKIDRRSGKKLEDGPKFLKSGDAAIVDMVPGKPMCVESFSDYPPLGRFAVRDMRQT VAVGVIKAVDKKAAGA	**EEF1A1 protein**	AAH71619
Ki 101	LASTYPLSSTAPVWGAQGLAVPRLPFPLFPPLRSTGFLEVADEATGALASAVSGYVQALASAGVVAVLALGAPAPQGCAVAVASDR CSIHLQLQGLVDPARELGKLQAKRSEAQRQAQRLQERRAASSYSAKVPLEVQEADEAKLQQTEAELRKVDEAIALFQKML	**Valyl-tRNA synthetase 2**	NP_035820
Ki 103	ARSHDGKLLVSADDFGKVHLFSYPCCQPRALSHKYGGHSSHVTNVAFLWDDSMALTTGGKDTSVLQWRVA	**Eml2 protein**	AAH55476
Ki 107	VDQSQAVKFALDMARGMAFLHTLEPLIPRHALNSRSVMIDEDMTARISMADVKFSFQCPGRMYAPAWVAPKPCRRSLKTQTDAQ QTCGVSRCFCGNW	**Integrin linked kinase**	NP_034692
Ki 110	PSSTATWPTWGPSACACWTRGPTTCTWMHFVPNITFGHPVVESLRKQLGQDPFFDMHMMVSRPEQWVKPMAVAGAN	**unnamed protein product**	BAC26287.
Ki 122	LKSVNGQIESLISPDGSRKNPARNCRDLKFCHPELKSGYWVES	**Procollagen, type III, alpha 1**	AAH58724
Ki 126	KMWTSKQGEGMVKLLDELSPATAPHKYYIGFRYVHPLTEEAIEEMERDGLERAIAFTQYPQYSCSTTGSSLNAIYRYYNEVGQKPT MKWSTIDRVPTHPLLIQCFADHILKELNHFPEEKRSEVVILFSAHSLPMSVVNRGDPYPQEVGATVHKVMEKLGYPNPYRLVWQS KVGPVPWLGPQTDEAIKGLCERGRKNILLVPIAFTSDHFENSTNWILNTLKCWLKSVELKTSEERSLLMESLGLQALADLVPPT	**Ferrochelatase**	NP_032024
Ki 135	GAQQFVAKEPQGDDDLKLCSHTMMLPTRGQLEGRMIVTAYEHGLDNVTEEAVSAVVYAVENHLKDILTSVVSRRKAYRVRDGHFK YAFGSNVTPQPYLKNSVVAYNNLVEGPPAFSAPCANQSPASQPHPDDAEQQAAFLLACSGDTLPASLPPVNMYDLFEALQVHRE VIPTHTVYALNIERIIMKLWHPNHEELQQDKVHRQRLAAKEGLLLC	**SPT3-associated factor 42**	NP_084521
Ki 137	RIGRTGRVGNLGLATSFFNERNINITKDLLDLLVEAKQEVPSWLENMAFEHHYKGSSRGRSKSSRFSGGFGARDYRQSSGASSS SFSSSRASSSRSGGGGHGGSRGFGGGGYGGFYNSDGYGGNYNSQGVDWWGN	**PL10 protein**	NP_149068
Ki 140	RAQSSLRYLQVLWQQDVEPRDELRCKIPAGRLRRAARPHRRLGPTGKEVHALKRLRDSANANDVETVQQLLEDGADPCAADD KGRTALHFASCNGNDQIVQLLLDHGADPNQQDGLGNTPLHLAACTNHVPVITTLLRGGARVDALDRAGRTPLHLAKSKLNILQEGH SQCLEAVRLEVKQVSDSSVWWAPGLADSLSLLGLPV	**Hypothetical protein LOC223690**	NP_149068.
Ki 143	QKRECAWPRLGFLADGRDPTPRGEMLRSKTFLKKTRAGGVVKIVREHYLRDDIGCGAPACSACGGAHAGPALELQPRDQASSL CPWPHYLLPDTNVLLHQIISAWKPGTWASVASRLRPPGSLLMSSNTRPSEMSLCYKQ	**RIKEN cDNA 2810028N01**	NP_082591.
Ki 153	RGRVDLTDYLMKILTERGYSFVTTAEREIVRDIKEKLCYVALDFENEMATAASSSSLEKSYELPDGQVITIGNERFRCPETLFQPSFI GMESAGIHETTYNSIMKCDIDIRKDLYANNVLSGGTTMYPGIADRMQKEITALAPSTMKIKIIAPPERKYSVWIGGSILASLSTFQQMVVI SKQEYDEAGPSIVHRKCF	**Actin, alpha 2, smooth muscle, aorta**	NP_031418

Ki 160	GREVAVPLLPPHLCFLSFLGGQDLREECIKLKKRVFDLERQNQVLSALLQQKLQLTANSLPQIPLTPLQPPSERPTSPAPNVSEG PATSLPSGLCAGQREVRRSRHVWCVLLARGSTAGS	Hypothetical protein LOC380969	NP_001001884
Ki 161	GIEKTDPFYHSPGGLELYGEPRHTMYRSRFDLDYPRSLLPLQNRYPGTPGDLNSISMASSQLHQYNPDKSLTDYVTRLEALRRRL GAIQSGSTTQFHFGMRR	A kinase (PRKA) anchor protein	NP_919444.
Ki 167	EKYDNSLKIVSNASCTTNCLAPLAKVIHDNFGIVEGLMTTVHAITATQKTVDGPSGKLWRDGRGAAQNIIPASTGAAKAVGKVIPELN GKLTGMAFRVPTPNVSVVDLTCRLEKPAKYDDIKKVVKQASEGPLKGILGYTEDQVVSCDFNSNSHSSTFDAGAWHCSQ	Similar to glyceraldehyde-3-phosphate dehydrogenase	NP_032110
Ki 185	LIPQPALELKQTFQDALQAVDASETQQQQLQGMVPIVLMAKLRPQVIAATTRASPQLPPEEPELRSTHPLDFLLLDAPLGGSLGLN TLLEGDPAMALKHEERKCPYCPDRFHNGIGLANHVRGHLNRV	Unnamed protein product	BAE38766
To 1	GRVDNSSKSFSGPGGPSKPKKPKPGEEPQQEPEPPVDRDPVVYHPDLEDLLQPWPAEVPDEFFEVTVDDVRRRLAQLKSER KRLEEAPLVTKAFREAQMKEKLERYPKVALRVLFPDRYILQGFFRPSETVGDLRDFVRSHLGNPELSFYLFIAPPKMVLDDHTLTL FQANLFPAALVHFGAEEPTGE	Unnamed protein product	BAB23341.1
To 6	AITVDPIRGNLYWTDWNREAPKIETSSLDGENRRILINKDIGLPNGLTFDPFSKLLCWADAGTKKLECTLPDGTGRRVIQ NHLNYPFSIVSYADHFYHTDWRRDGVISVNKDSGQFTDEFLPEQRSHLYGITAVPYCPTGRK	nidogen-2	CAD21572
To 16	GRVDVTTAGGVEEDLIKCLAPTYLGEFSLRGKELRENGINRIGNLLVPNDNYCKFEDVLMPILDQMVLEQNTEGVKWTPSKMISRL GKEINNPDSVYYWAHKNHIPVLSPALTDGSLGDMIFFHSYKNPGLVLDIVEDLRLINTQAIFAKRSGMIILGGGVVKHHIANANLMLSRP SSASYPAFYSF	Dhps protein	AAH39963
To 18	GRVDAAELVEAKNMVMSFRVSDLQMLLGFVGRSKSGLKHELVTRALQLVQFDCSPELFKKIKELYETRYAKKSAEPGPQAPRPL DPLALHSMPRTPLSGPTVDYPVLYGKYLNGLGRLPTKTLKPEVRLVKLPFFNMLDELLKPTELGEWWVSPSRSPKQAQHCAP	Protein inhibitor of activated STAT, 4	AAH25159
To 66	GRVDLTLADCNLLPKLHIVQVVCKKYRGFTIPEAFRGVHRYLSNAYAREEFASTCPDDEEIELAYEQVARALK	Chloride intracellular channel 1	AAH04658
To 67	GRVDLQQQQQQQQPGQGTAEPSQPSGPTVASLEPPVKLKELHFSNMKTVDCVERKGKYMYFTVVMTEGKEIDFRCPQDQGW NAEITLQMVQYKNRQAILAVKSTRQKQQHLVQQQPPQTQQIQPQPQPQIQPQPQPQIQPQPQPQPQPQPQPQPQPQPQQLH SYPHPHPHPYSHPHQHPHPHPHPHPHPH	Pleckstrin homology-like domain, family A, member 1	AAH10295
To 70	GRVDIIIALPSLRILYIIDEINNPVLTVKTIGHQ.Y.SYEYTDYEDLCFDSYIIPTNDLKPGELRLLEVDNRVVLPIELPIRILISSEDVLHS AV PSLGLKTDAIPGRLNQATVTSNRPGLFYGQCSEICGSNHSFMPIVLEMVPLKYF	Unnamed protein product	CAA24083
To 87	GRVDADCGLSHLISPVPALRPRPAAMRFSCLALLPGVALLLASARLAAASDVLELTDENFESRVSDTGSAGLMLVEFFAPWCGHC KRLAPEYEAAATRLKGIVPLAKVDCTANTNTCNKYGVSGYPTLKIFRDGEEAGAYDGPRTADGIVSHLKKQAGPASVPLRTEEEFK KFISDKDASVVGFFRDLFSDAEGRDKLSDCVLPSVMSL	Protein disulfide isomerase associated 3	AAH33439
To 88	GRVDLNLSSGSKTKSPSLPPKGKKPKGLEISAPQLLLSGTDIGSIALNSPALPSGSLTPAFFTAQTPSGLFLASSPLLPSIHFWSSL SPVAPLSPARLQGPNTLFQFPTLLNGHMPVPLPSLDRAPSPVLLSPSSQKS	ELK3	AAH55735
To 94	GRVDLSPSRSESRRCCNQNHYTTCLRNLLQGEAERTDGVNILKEQTHSTHPPLRIHLHGQLCLTRETTTHIILEPSLYPGMTSSSP SCLFLLPPFL	H19	AAH25150
To 96	GRVDEVPISNGSGFVVASDGLIVTNAHVVADRRRVRVRLPSGDTYEAMVTAVDPVADIATLRIQTKEPLPTLPLGRSADV RQGEFVVAMGSPFALQNTITSGIVSSAQRPARDLGLPQNNVEYIQTDAAIDFGNSGGPLVNLVSVRVLLRIHAPG	Serine protease	AAF89534
To 137	GRVDPNPSDILENLDDSVFSKRHAKLELDEKRRKRWDIQRIREQRILQRLQLRMYKKKGIQESEPEVTSFFPEPDDVESLLITPFL PVVAFGRPLPKLAPQNFELPWLDERSRCRLEIQKKHTPHRTCRK	RIKEN cDNA 4121402D02	AAH58629
To 139	GRVDLPNSPGVAKAKMFKLDAGKMPVVYLEPCAVTKSTVKISELPDNMLSTSRKDKSMLAELEYLPAYIENSDGTDFCLSKDSEN SLRKHSPDLRIVQKYTLLKEPNWKYPDILDNSSTERIHDSSKGSTAESFSGKEDLGKKRTTMLKMAIPSKTVTASHSASPNTPGKR GRPRKLRLSKAGRPPKNTGKSLTAA	mKIAA4252 protein	BAD32240
To 146	GRVDESLPTAVFSLQKLRCLDVSYNNISTIPIEIGLLQNLQHLHITGNKVDILPKQLFKCVKLRTLNLGQNCIASLPEKISQLTQLTQLE LKGNCLDRLPAQLGQCRMLKKSGLVVEDQLFDTLPLEVKEALNQDVNVPFANGI	Unnamed protein product	BAE23361
To 159	GRVDVDTPSGTNSGAGKKRFEVKKVWNAVALWAWDIVVDNCAICRNHIMDLCIECQANQASATSEECTVAWGVCNHAFHFHCISR WLKTRHGVSVGQQRVGVPEVWALGKTFPQGVPICYSSSDFLLII	Ring-box 1	AAH51473

3.1.3.1   Identification of RACK1 as novel interacting partner of BMPRII.

We observed that the translated sequences of three clones, Ki 42, Ki 56, Ki 97, exhibited more than 97% identity with the guanine nucleotide binding protein (G protein), β polypeptide 2-like 1 binding protein (Gnb2l1, RACK1). RACK1 is a member of a superfamily of proteins containing WD40 domains that are found in a number of eukaryotic proteins with a wide variety of functions, including adaptor regulatory molecules in signal transduction, pre-mRNA processing and cytoskeleton assembly (Figure 3.6). Further sequence analyses revealed that all three clones encode overlapping regions of the C-terminal portions of RACK1 from WD4-WD7, suggesting these four WD repeats are sufficient for the binding to the kinase domain of BMPRII (Figure 3.7).
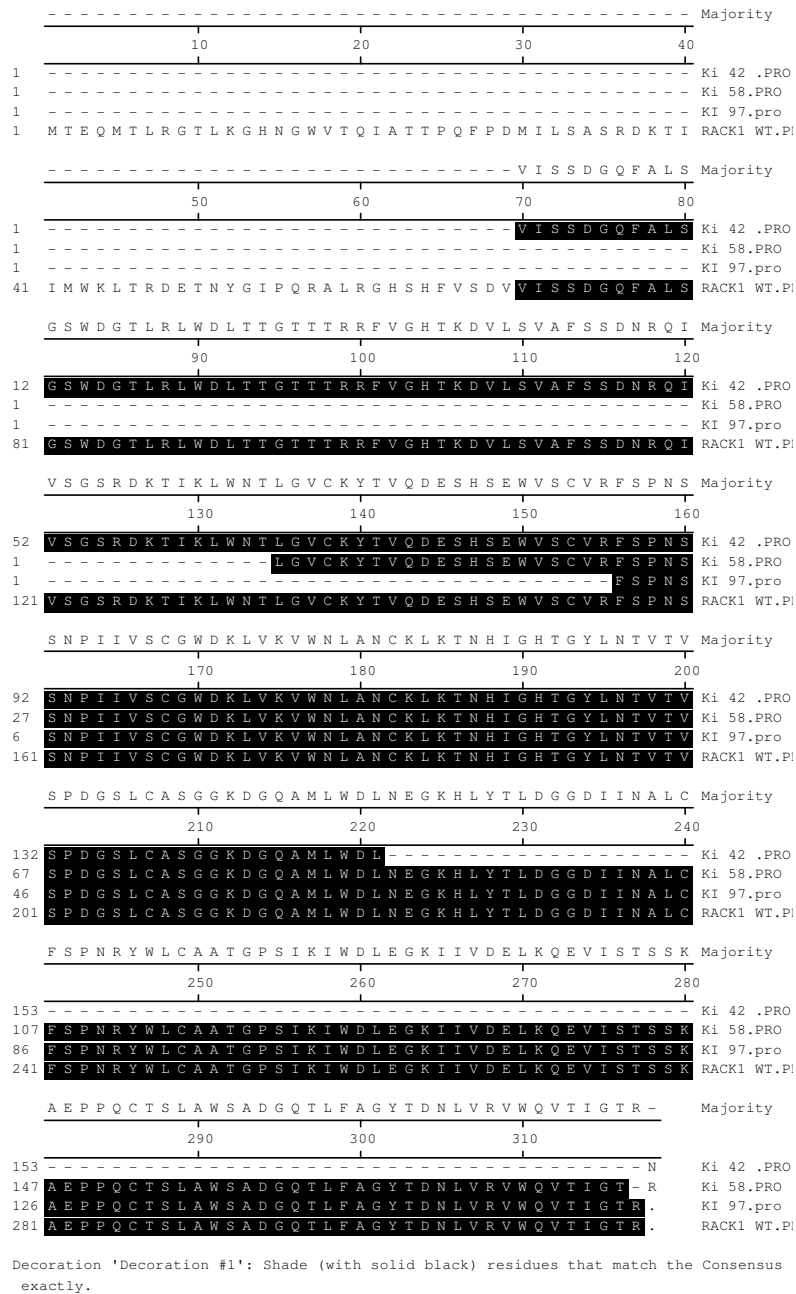
Figure 3.6   Sequence alignment of RACK1 from *Mus musculus* (GenBank^{TM} Accession Number NP 032169) and homologous clones from a yeast two-hybrid screen.
The region of homology with the translated protein sequences of clones Ki 42, Ki 58, and Ki 97 are shaded.
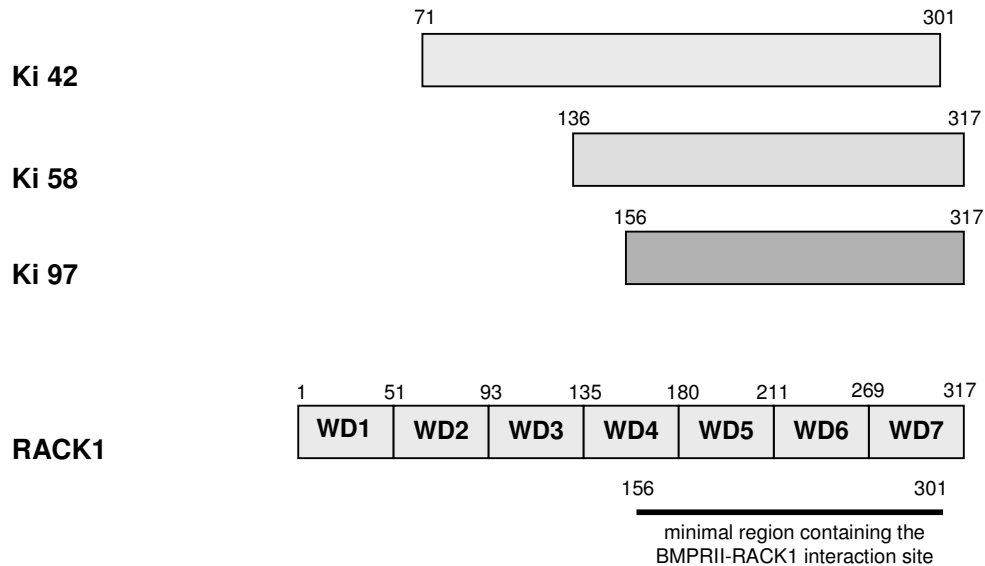
Figure 3.7   Schematic representation of the library clones isolated from the yeast-two hybrid screen and full-length RACK1.
The library clones were identified by direct sequencing and consisted of partial sequence of the full-length RACK1. Numbers of amino acids residues are indicated. **WD**; WD domain.

3.1.4   Confirmation of the BMPRII interaction with full-length RACK1 using the yeast two-hybrid system

To verify the interaction of RACK1 with BMPRII, we cloned the full-length RACK1 cDNA into the pACT2 expression vector and verified the interaction with the kinase and intracellular domains of BMPRII. To guard against false-positive results, the library-derived plasmids (Ki 42, Ki 58, Ki 97) were also re-transformed together with the bait plasmids. The interactions between BMPRII and the truncated RACK1 variants encoded by Ki 42, Ki 58, Ki 97 and full-length RACK1 were specific, since the growth of the colonies on high-stringency selective plates that lacked the nutritional markers adenine (Ade) and histidine (His), and contained X-α-Gal was apparent only in the presence of both BD-BMPRII and the AD-prey. Yeast transformed with bait plasmid and empty prey plasmid, or yeast transformed with library clones and empty bait plasmids were not able to grow on high-stringency selective plates (Figure 3.8, middle and right panel). Transformation did not alter the growth of the yeast host because all transformants were capable of growing on rich, non-selective yeast peptone dextrose (YPD) medium (Figure 3.8, left panel).
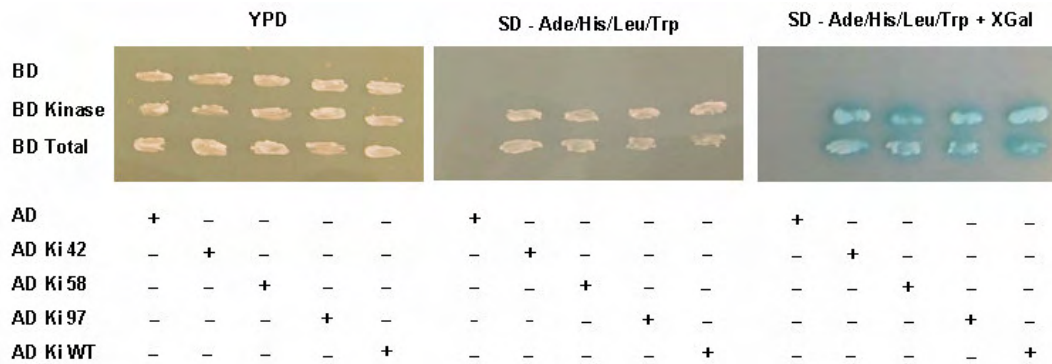
Figure 3.8   Interaction between cytosolic domains of BMPRII and full length RACK1 in a yeast two-hybrid system.
Growth of yeast transformants on YPD (complete) medium (left panel), high stringency selection plates (middle panel), and high stringency selection plates containing X-α-Gal (right panel). **AD**; activation domain, **BD**; binding domain, **WT**; wild type.

3.1.5   Confirmation of the interaction between the BMPRII kinase domain and the full-length RACK1 by GST pull-down

3.1.5.1   Overexpression of GST-tagged kinase domain of BMPRII.

To determine whether the BMPRII, which normally localises to the cell membrane as part of a BMPR complex, associates with RACK1, a full-length Myc-tagged RACK1 was overexpressed in NIH/3T3 cells. Either GST or GST-BMPRII kinase were overexpressed in *E. coli* BL21.

A bacterial expression system was chosen for overexpression of the BMPRII kinase domain fused to the C-terminal end of GST-tag because this system facilitates expression and harvesting of a large amount of recombinant protein. Overexpression was performed in 27 °C; *E. coli* BL21 were grown in medium containing 1 mM IPTG. The level of protein expression was evaluated at different time points after IPTG induction. After 4 h the level of expression reached a plateau. This condition was therefore chosen for further experiments (Figures 3.9, 3.10).

time after IPTG induction (h)
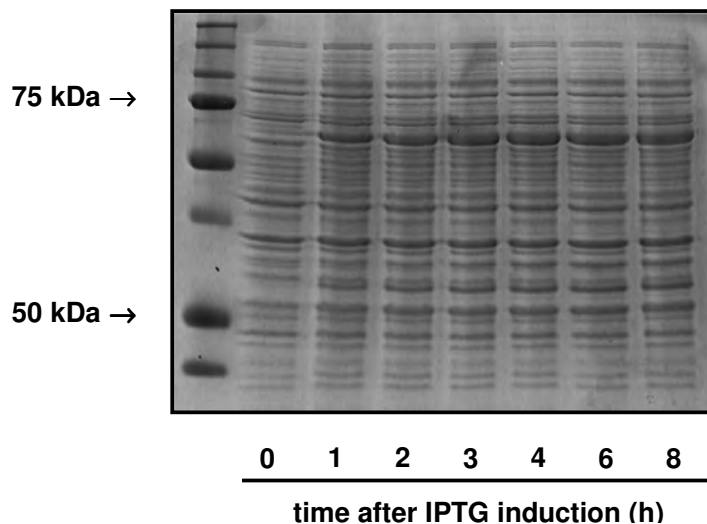
Figure 3.9   Standardisation of the overexpression condition for the GST-tagged kinase domain of BMPRII.
The *E. coli* BL21 cell lysates harvested at different time points after IPTG induction were resolved on a 12% SDS-PAGE gel, and stained with Coomassie Blue. **IPTG**; isopropyl β-thiogalactopyranoside.
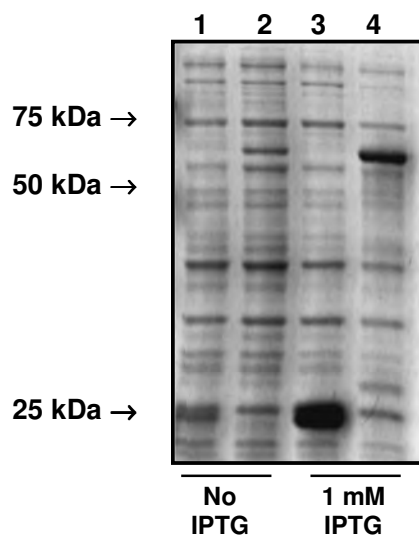
Figure 3.10   Overexpression of the GST-tagged kinase domain of BMPRII in *E. coli* BL21.
Cell lysates from *E. coli* BL21 transformed either with the empty pGEX-4T1 vector **(lane 1)** or pGEX-4T1 containing the BMPRII kinase domain (**lane 2**). **Lanes 3 and 4** represent the same set of cell lysates like in lane 1 and 2 respectively but 4 h after IPTG treatment. Proteins were visualised by Coomassie staining. GST cells transfected with empty pGEX-4T1, GST-SF cells transfected with pGEX-4T1 containing kinase domain of BMPRII. **IPTG**; isopropyl β-thiogalactopyranoside.

3.1.5.2 GST pull-down assay

Bacterial cell lysates containing overexpressed proteins were incubated with gluthathione-Sepharose beads. The proteins bound to the beads were incubated with lysates from NIH/3T3 cells. The RACK1 was bound to GST-BMPRII kinase (Figure 3.11, lane 1) but not to GST alone (Figure 3.11, lane 2), demonstrating that BMPRII interacts with RACK1 in a GST pull-down.
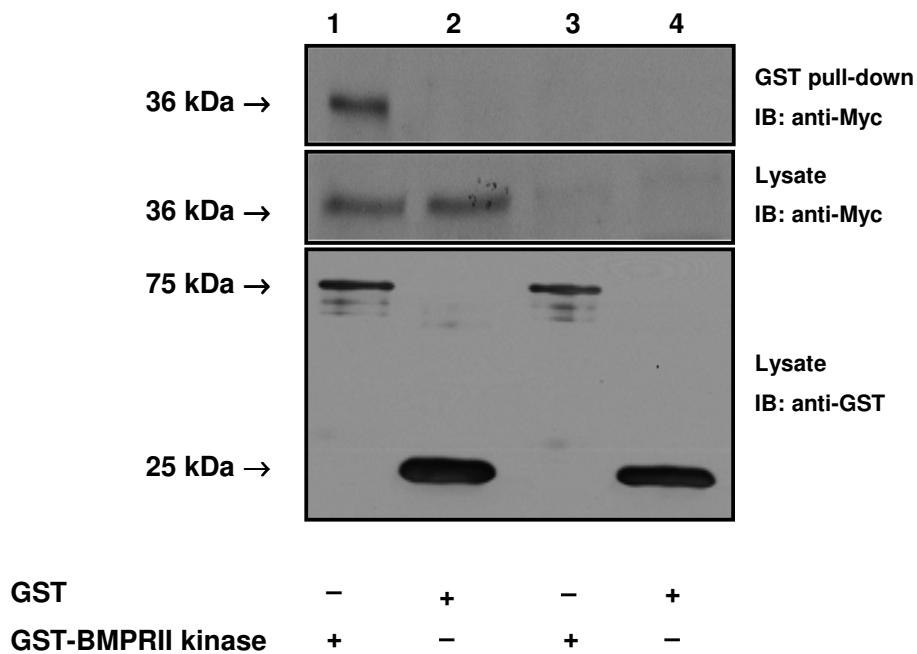
Figure 3.11   Verification of the BMPRII kinase domain interaction with RACK1 by GST pull-down assay.
Lane 1 represents the Myc-tagged RACK1 molecule, which interacts with the BMPRII kinase fused to the GST. **Lane 2** shows no interaction with the GST tag alone (negative control). **Lanes 3 and 4** lack interacting partners due to no overexpression of RACK1-Myc. Expression of RACK1 and GST and GST-BMPRII kinase is shown on the middle and lower blots. **IB**; immunoblot.

3.1.6   Co-immunoprecipitation of BMPRII with RACK1 in a BMP2 ligand-independent manner

To further support our contention that an interaction between BMPRII and RACK1 occurs *in vivo,* co-immunoprecipitation of the BMPRII-RACK1 complex was performed. The wild-type BMPRII was tagged at the C-terminus with an HA tag, and RACK1 was similarly tagged with Myc. The expression constructs encoding these

proteins were transfected into NIH/3T3 cells. RACK1 in the lysates of the transfected cells was immunoprecipitated with an anti-Myc antibody, and the presence of BMPRII was detected with an anti-HA antibody. When the RACK1 was expressed alone and immunoprecipitated with anti-Myc antibody, no BMPRII was detected with anti-HA antibody by immunoblot (Figure 3.12, lane 2). However, when RACK1 was expressed together with BMPRII, both proteins were co-immunoprecipitated by an anti-Myc antibody. Stimulation with BMP2 did not influence this interaction. This finding was in agreement with the results from the yeast two-hybrid experiments and the GST pull-down assay, and demonstrates a specific interaction between BMPRII and RACK1 when overexpressed in mammalian system. Our data further indicated that this interaction was independent of BMP2 stimulation.
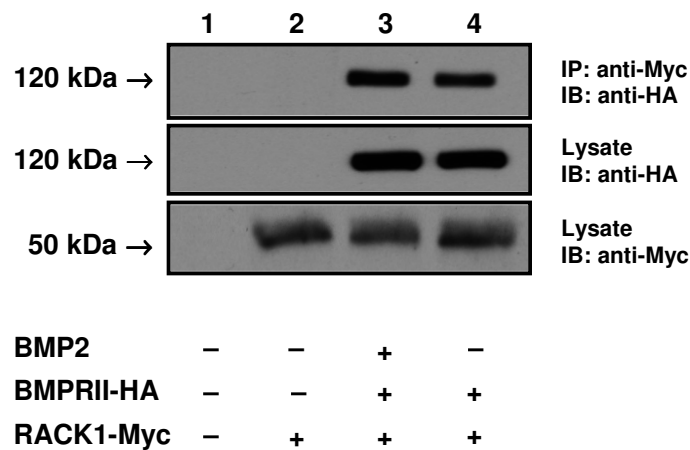
Figure 3.12   Immunoprecipitation analyses of overexpressed Myc-tagged RACK1 and its interaction with HA-tagged BMPRII proteins in NIH/3T3 cells.
The NIH/3T3 cells were transiently transfected with a plasmid encoding BMPRII-HA (**lane 3, 4**) and RACK1-Myc (**lane 2, 3, and 4**). The cell lysate was immunoprecipitated with anti-Myc antibody and bloted with anti-HA antibody to detect BMPRII. Proper and equal expression is illustrated on the blot. **Lane 1** containing lysate from untransfected NIH/3T3 cells served as negative control. **IB**; immunoblot, **IP**; immunoprecipitation.

3.2   Mapping the region of BMPRII required for RACK1 binding

3.2.1   Construction and overexpression of truncated variants of the GST-tagged kinase domain of BMPRII

After confirmation of an interaction between BMPRII and RACK1 we sought to determine which region of the cytoplasmic domain of BMPRII was responsible for this interaction.

The GST-BMPRII kinase domain construct was subjected to site-directed mutagenesis to reproduce four truncating mutations identified in patients with FPAH. The first mutation, Q495X, causes truncation by the replacement of the native glutamine residue with a premature stop codon at position 495, a second truncation W466X, was created by replacement of tryptophan at position 466 with stop codon. The third mutation at position 450, Q450X was obtained via exchange of glutamine with stop codon and the fourth mutation, R332X, replaced arginine at position 332 with a premature stop codon (Figure 3.13).
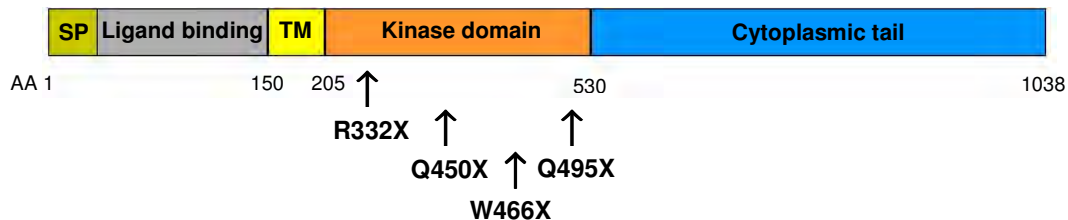
Figure 3.13   Schematic representation of BMPRII indicating point mutations that result in premature stop codons.
Sites of stop mutations in the kinase domain are indicated with arrows. **AA**; amino acid, **SP**; signal peptide, **TM**; transmembrane domain.

The site-mutated constructs were transformed into *E. coli* BL21 and protein expression was induced at 27 °C in LB medium containing 1 mM IPTG. The GST-tagged wild-type kinase domain of BMPRII domain was used as positive control for the overexpression (Figure 3.14).

1   2   3   4   5   6   7   8   9   10

75 kDa →

25 kDa →

no induction   **1 mM IPTG**
                          induction
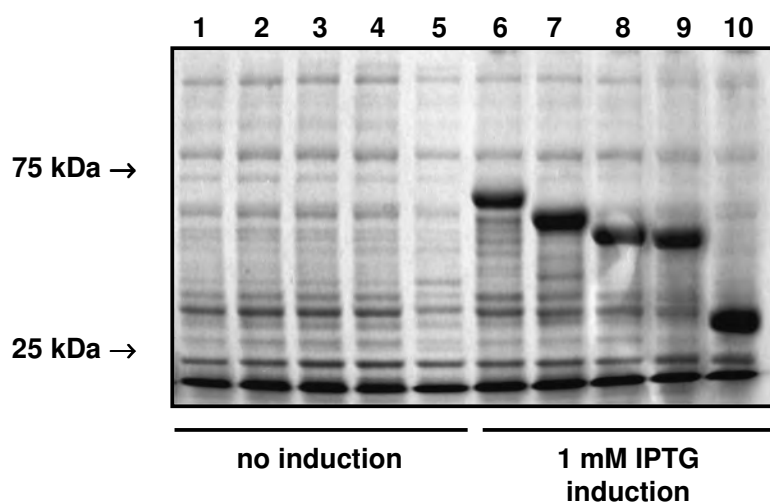
Figure 3.14   Overexpression of truncated GST-tagged BMPRII kinase domains.
Cell lysates from *E. coli* BL21 bacteria transformed with GST-BMPRII kinase wild-type (**lane 1, 6**),
or GST-BMPRII kinase variants prematurely truncated at position 495 (**lane 2,7**), 466 (**lane 3,8**),
450 (**lane 4,9**), 332 (**lane 5,10**). **Lane 1-5** cell lysates from bacteria that were not induced with
IPTG, **lanes 6-10** stimulated with 1 mM IPTG. Proteins were visualised by Coomassie Blue
staining. **IPTG**; isopropyl β-thiogalactopyranoside.

3.2.2   Effect of *BMPR2* mutations on the interaction with RACK1

The ability of these mutated variants to bind RACK1 was assessed by GST pull-
down assay. The GST tagged wild-type kinase domain of BMPRII was used as positive
control for interaction. Interestingly, none of the truncations abolished the interaction with
the RACK1 molecule, although all variants exhibited a reduction in binding capacity in
comparison with GST-tagged wild-type kinase domain of BMPRII (Figure 3.15).

1   2   3   4   5

36 kDa →   **GST pull-down**
                                    IB: anti-Myc

36 kDa →   **Lysate**
                                    IB: anti-Myc

75 kDa →

                                    Coomassie
                                    staining

25 kDa →
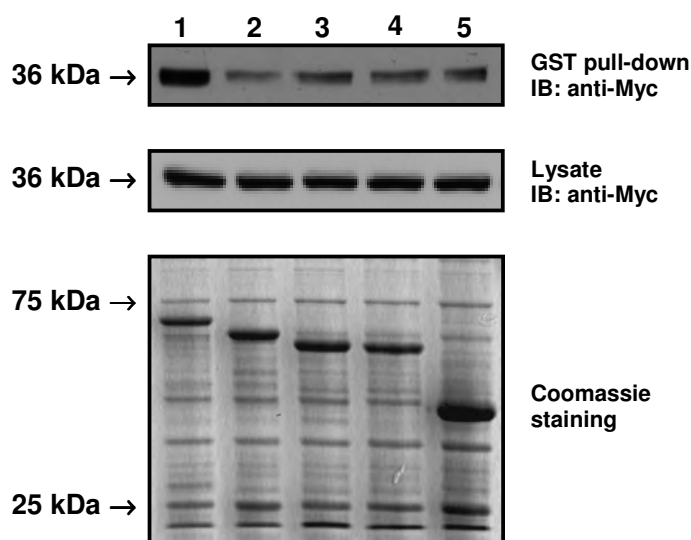
Figure 3.15   Mapping the BMPRII region required for RACK1 interaction.
Immunoprecipitation and immunoblot analyses of variants of the GST-tagged kinase domain of
BMPRII and Myc-tagged RACK1. **IB**; immunoblot.

3.3   RACK1 expression in different mouse tissues

To investigate a possible function of RACK1 in the lung, we investigated the expression of RACK1 in lung tissue (Figure 3.16). For this purpose, we isolated proteins from different mouse tissues including the lung and evaluated RACK1 expression by immunoblot. It was observed that RACK1 was abundantly expressed in lung tissue as well as in other tissues investigated, suggesting an important role of this molecule in many cellular processes.
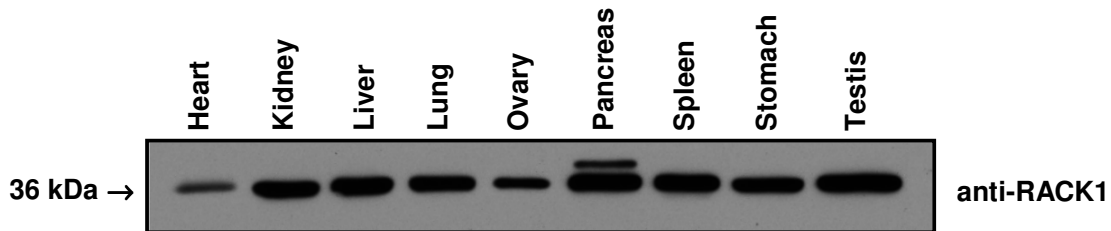
Figure 3.16   RACK1 expression in different mouse tissues.
Protein extracts obtained from different mouse tissues were probed on an immunoblot for expression of RACK1 with an anti-RACK1 antibody.

3.4   Expression of RACK1 in a rat model of monocrotaline-induced pulmonary hypertension

To assess a potential influence of RACK1 on the pathogenesis of pulmonary hypertension, we selected the monocrotaline (MCT) model for further investigations. Expression of RACK1 was analysed in rats treated with MCT. The mRNA levels of *RACK1* in control animals, as well as in animals treated with MCT and sacrificed two and four weeks after MCT administration was determined by semi-quantitative RT-PCR (Figure 3.17 A) and the results were verified by quantitative PCR (Figure 3.17 B). With these two methods we detected a significant down-regulation of *RACK1* mRNA four weeks after MCT treatment.

A)

B)
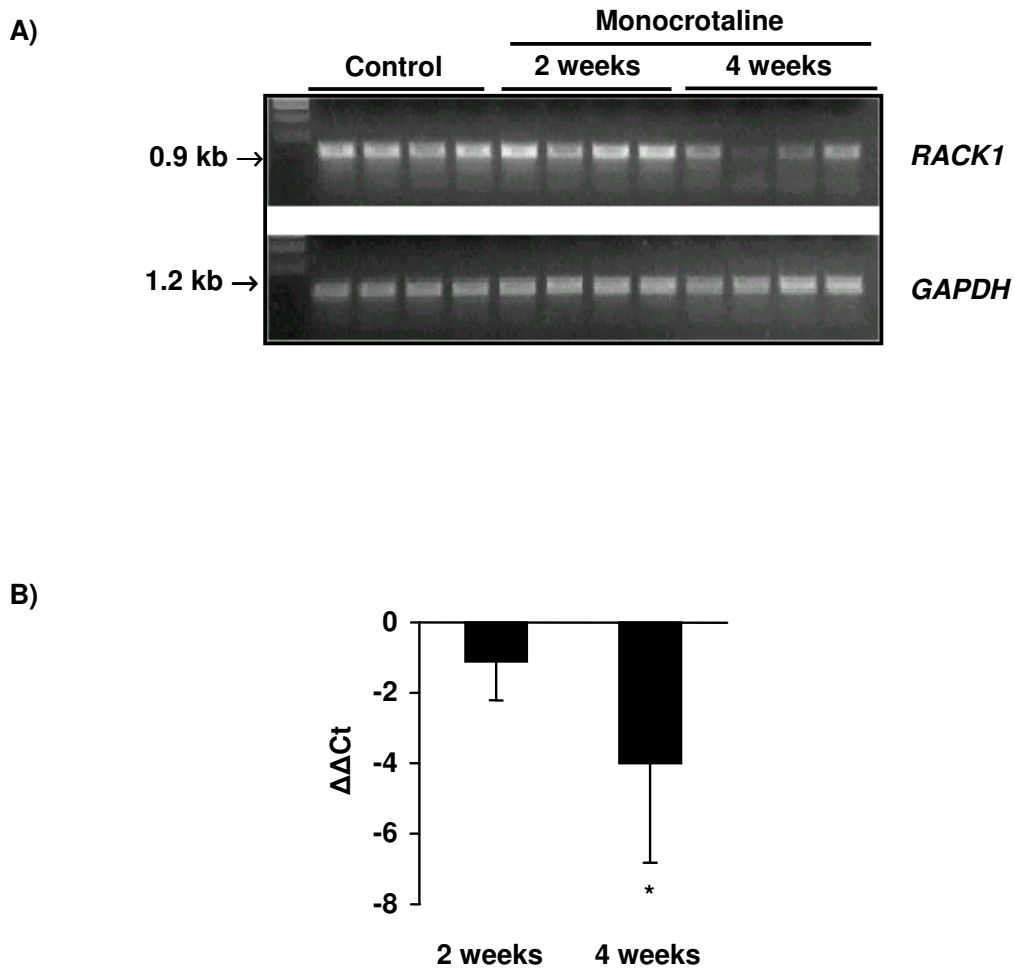
Figure 3.17 *RACK1* **mRNA expression in lungs from monocrotaline treated rats.**
(A) Changes in expression level of mRNA from four control rats and four monocrotaline-treated rats for two and four weeks after monocrotaline administration were assessed by semi-quantitative PCR. *GAPDH* served as a control gene. **(B)** Changes in expression levels of mRNA from control and monocrotaline-treated rats were assessed by quantitative PCR. Porphobilinogen deaminase (*PBGD*) served as a reference (house-keeping) gene control. Fold difference in mRNA expression from control and monocrotaline treated animals was presented as $\Delta\Delta$Ct (n=4, *p<0.05)

Expression of RACK1 was further evaluated at the protein level, and in agreement with the observations on mRNA expression levels, RACK1 expression was significantly downregulated four weeks after MCT treatment (Figure 3.18).

A)
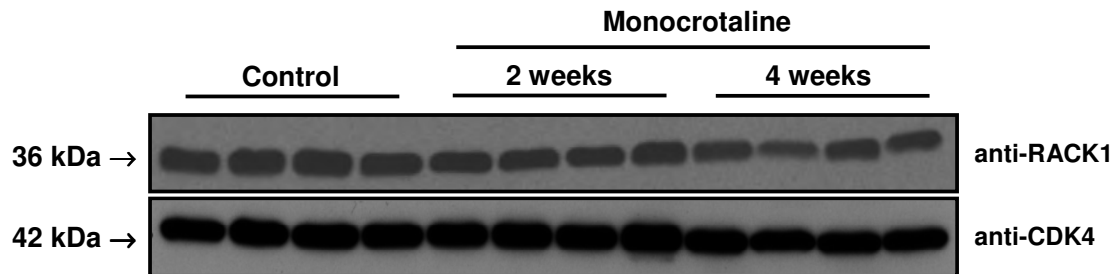
B)
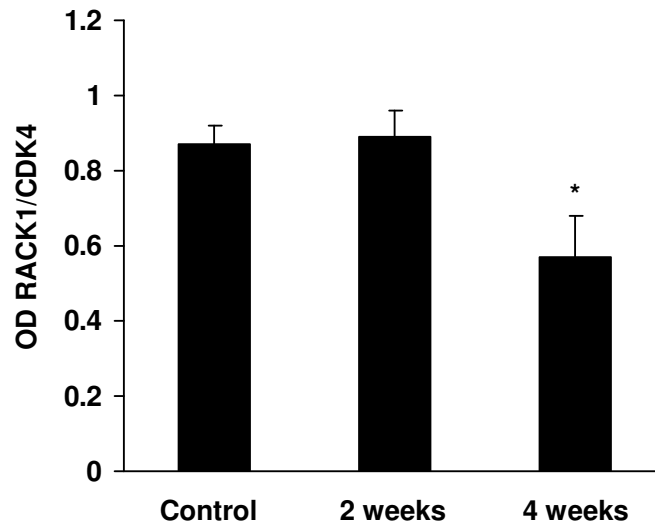
Figure 3.18   RACK1 protein expression in MCT-treated rats.
(A) Lung proteins extracts from four control and four MCT-treated rats were resolved on a 15% SDS-PAGE gel and blot with an anti-RACK1 antibody. The CDK4 protein served as loading control. **(B)** The intensity of the RACK1 signal detected by immunoblot was quantified by densitometric analysis (n=4, * $p < 0.05$). **OD**; optical density.

3.5   Expression of RACK1 in human lungs

Since RACK1 was downregulated in MCT-treated rat lung tissues, we sought to determine if the expression levels differ under pathological conditions in humans. For this purpose, we assessed RACK1 mRNA expression in human PAH and donor lungs by quantitative RT-PCR. Expression of *RACK1* in PAH patients was increased at the mRNA level, compared with donor samples (Figure 3.19).
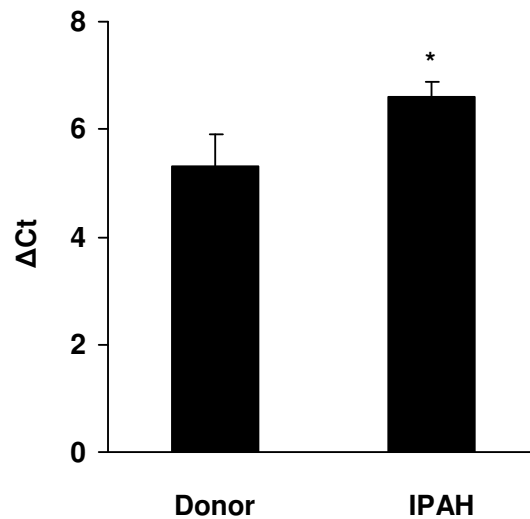
Figure 3.19   ***RACK1* mRNA expression in lungs of IPAH patients in comparison to donors.**
The mRNA from nine donors and twelve PAH patients was assessed by quantitative RT-PCR. The porphobilinogen deaminase (*PBGD)* gene served as a reference (house-keeping) control gene. The amount of mRNA is presented by the Δ Ct (n=4, * p< 0.001).

The same samples were also tested for RACK1 expression at the protein level by the immunoblot. Lung tissue from donors and PAH patients was homogenised and proteins were extracted and resolved by SDS-PAGE. The RACK1 was detected with an anti-RACK1 antibody. The CDK4 protein served as a control to demonstrate equal protein loading. Protein expression levels of RACK1 in the lung did not exhibit significant differences between PAH patients and healthy donors (Figure 3.20).
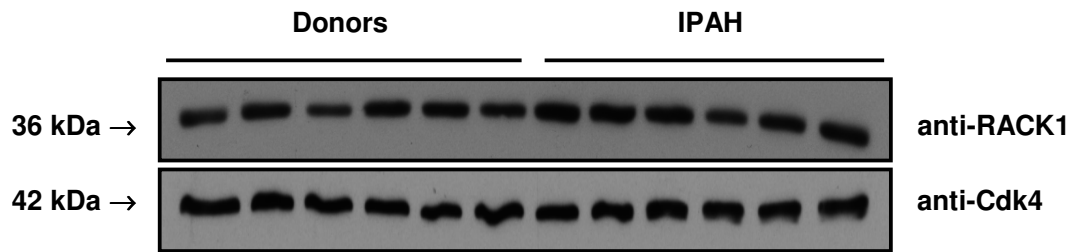
Figure 3.20   Protein expression of RACK1 in lungs of IPAH patients and healthy donors.
Lung protein extracts from six donors and six IPAH patients were resolved on a 15% SDS-PAGE
gel and blotted to a nitrocellulose membrane and probed with an anti-RACK1 antibody. CDK4
served as a loading control.

3.6   Immunolocalisation of BMPRII and RACK1 in the human lung sections

To determine the expression patterns of BMPRII and RACK1 in human lung
tissues, immunostaining was performed on healthy (donor) and IPAH (patient) lung
sections.

The BMPRII staining was detected in endothelial cells and paSMC, similar what
has been reported previously (Atkinson et al., 2002). The RACK1 was localised to SMC
with a similar distribution pattern to that seen for BMPRII. Furthermore, we observed a
clear co-localisation of BMPRII and RACK1 in the concentric leasions of PAH lungs
(Figure 3.21). The SMA staining served as a marker for SMC localisation.
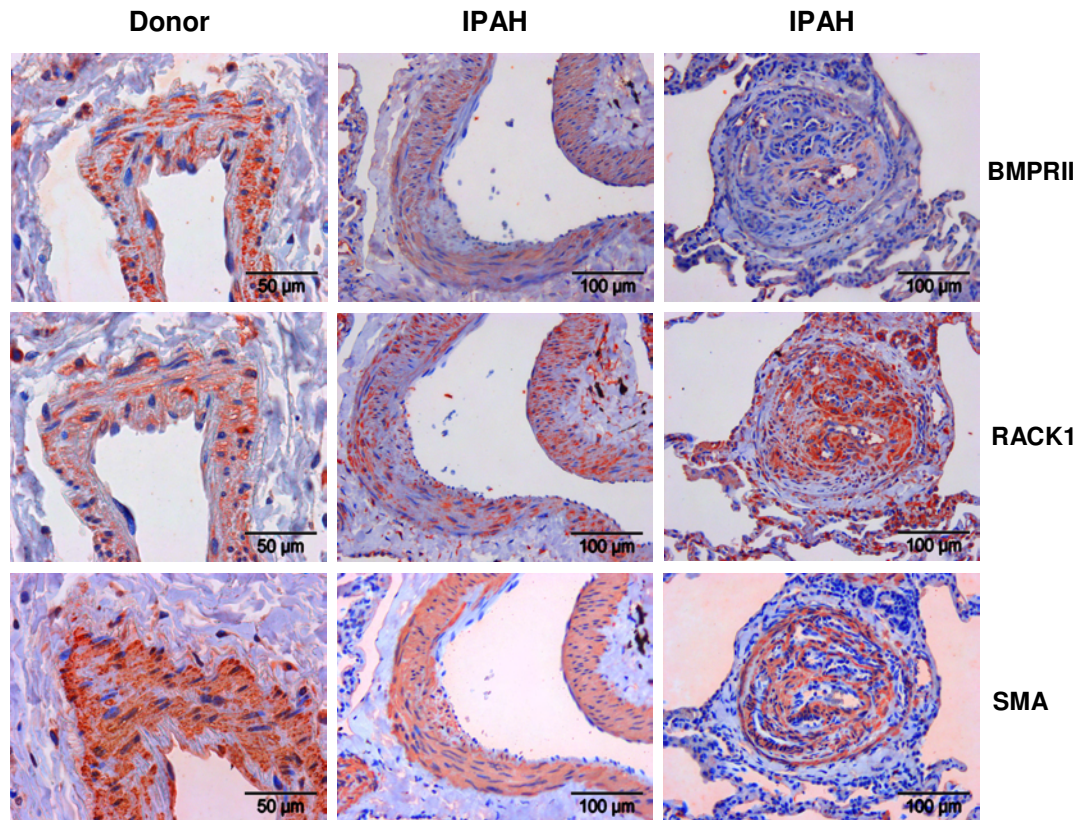
Figure 3.21   Immunohistochemical localisation of BMPRII and RACK1 in human lung section.
Paraffin-embedded specimens from healthy donors (left panel) and patients with IPAH (middle and right panel) were stained for BMPRII, RACK1, and smooth muscle actin (SMA).

3.7   Co-localisation of endogenous BMPRII and RACK1 in human paSMC

To support the observations made in lung tissue sections immunocytochemical staining in human paSMC was also performed. The purity of this cell population was verified by SMA staining (Figure 3.22). Staining for BMPRII and RACK1 was performed by indirect immunofluorescense using rabbit anti-BMPRII and mouse anti-RACK1 antibodies (Figure 3.23). The RACK1 exhibited diffuse staining throughout the cytoplasm, whereas BMPRII exhibited more membrane and perinuclear localisation. Co-localisation of these two molecules can be observed as yellow colour.
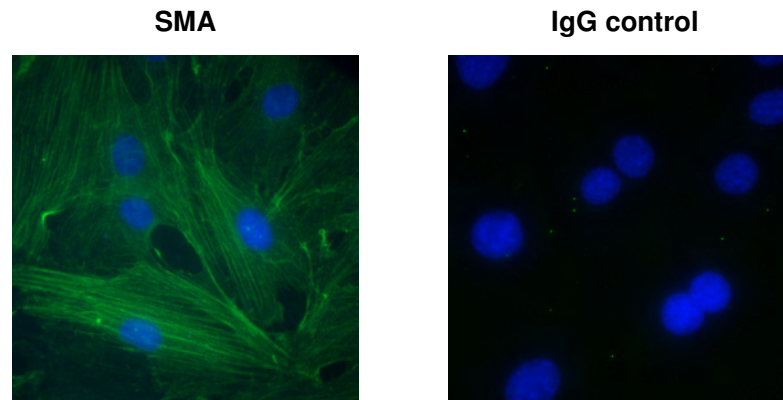
Figure 3.22   Verification of the paSMC phenotype.
Isolated cells were stained with FITC-labelled (green) for smooth muscle actin (SMA), to verified phenotype. DAPI staining (blue) visualised nuclear compartment of the cells. IgG isotype staining served as a negative control.
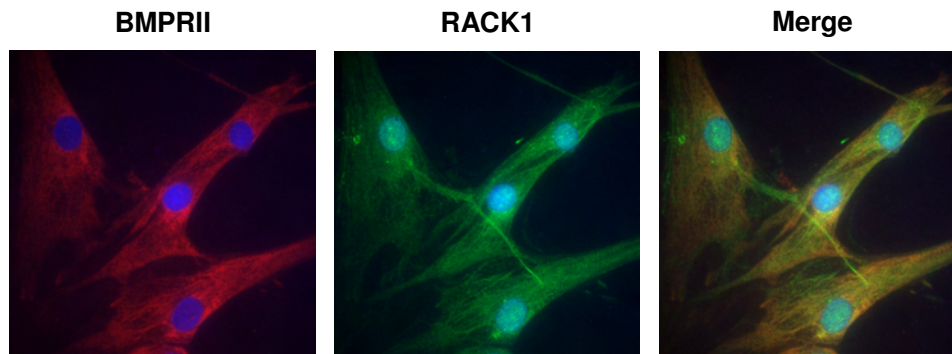
Figure 3.23   Co-localisation of BMPRII and RACK1 in human paSMC.
BMPRII was visualised with an secondary Alexa 549-labelled antibody (red), RACK1 was stained with FITC-labelled antibody. Co-localisation results in a yellow colour staining. Cell nuclei were visualised with DAPI (blue).

3.8   Effects of RACK1 on paSMC proliferation

As paSMC proliferation is a key event in the development of PAH, and since RACK1 expression was significantly altered in animal model of PAH, we continued by investigating the effect of RACK1 knockdown and overexpression on paSMC proliferation. Expression of RACK1 was downregulated using small interfering (si) RNA directed against *RACK1* (siRACK1). First, it was confirmed that siRACK1 was able to reduce *RACK1* mRNA levels. Four different siRNA sequences directed against *RACK1*

were tested. Using quantitative RT-PCR we assesed *RACK1* mRNA expression levels after treatment of paSMC with different siRNA (si#1, si#2, si#3, si#4). Full sequences of those oligonucleotides are available in Table 5.4, Appendix. Non-specific siRNA was used as a negative control. After transfection with siRNA (si#1, si#2, si#4) we observed a significant reduction of mRNA expression in comparison to the mock-treated cells. The si#3 sequence directed against *RACK1* failed to significantly decrease mRNA *RACK1* levels (Figure 3.24). In agreement with the observation on mRNA levels, the protein levels of RACK1 were also potently reduced after treatment with si#1, si#2, and si#4 (Figure 3.25).
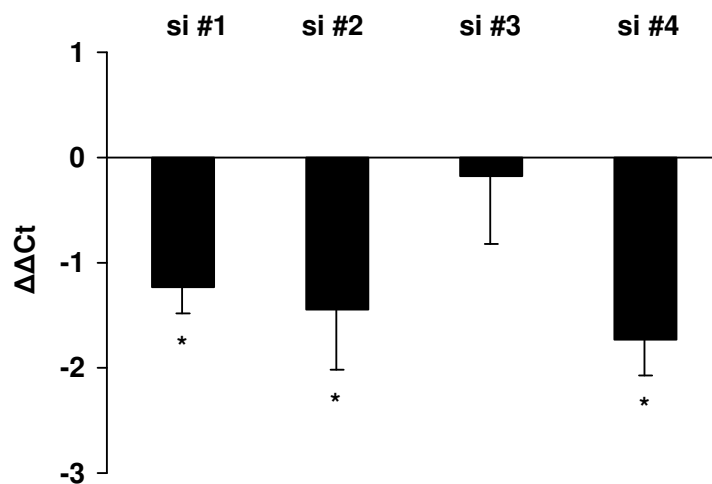
Figure 3.24   *RACK1* mRNA expression level after down-regulation with siRNA.
The mRNA levels of *RACK1* in paSMC transfected with different siRNA, assessed by quantitative RT-PCR. (n=3 * p< 0.01).
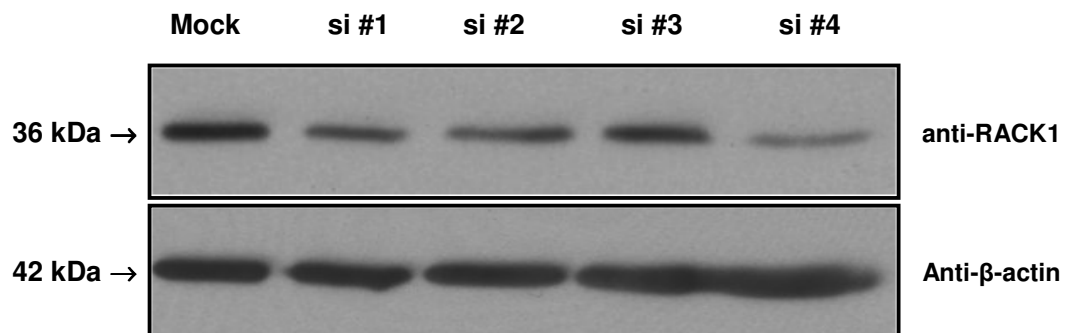
Figure 3.25   RACK1 proteins expression after down-regulation with siRNA.
Immunoblot of paSMC protein lysates obtained from paSMC after siRNA treatment. β-actin served as a loading control.

To analyse whether alteration in RACK1 expression would affect paSMC proliferation, [^{3}H]-thymidine incorporation, using paSMC transfected with siRNA directed against *RACK1*, was performed. As depicted in Figure 3.26, the [^{3}H]-thymidine incorporation assay demonstrated that knock-down of *RACK1* by siRNA results in a significant increase in proliferation of paSMC compared to mock-treated cells. These data further support a role of RACK1 in the regulation of paSMC proliferation, and suggest that perturbations of RACK1 expression and/or function may lead to enhanced paSMC cell growth in PAH.
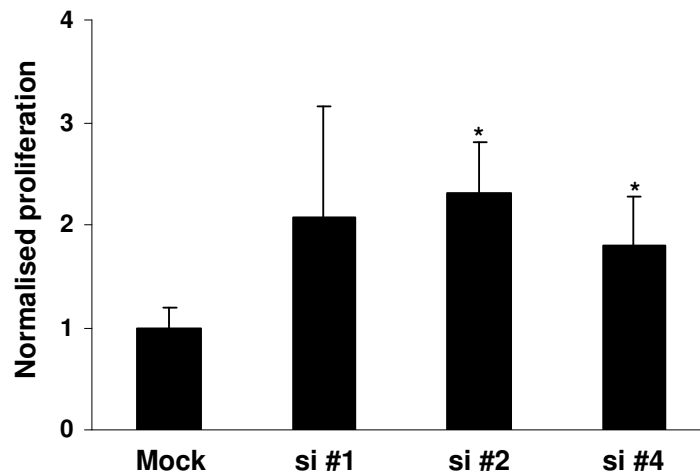
Figure 3.26   Increased proliferation of paSMC after RACK1 down-regulation using siRNA treatment.
The paSMC proliferation was assessed by direct [^{3}H]-thymidine incorporation analysis (n=3, * p< 0.05).

The functional outcome of RACK1 overexpression on paSMC proliferation was also investigated. The paSMC were transfected by electroporation using RACK1 cloned into pcDNA mammalian expression vector. The efficiency of transfection was evaluated by flow cytometric analyses using empty or green fluorescent protein (GFP) expression vector (Figure 3.27). The effect of RACK1 overexpression on paSMC proliferation was assessed by [^{3}H]-thymidine incorporation (Figure 3.28). To further confirm the antiproliferative effect of RACK1 overexpression on paSMC, the cell cycle distribution of paSMC using flow cytometric analysis was further investigated (Figure 3.29). In agreement with previous findings RACK1 overexpression resulted in decreased percentage of paSMC in S phase in comparison with cells transfected with empty vector.

This observation may explain the anti-proliferative effect of RACK1 overexpression due to the blockade of the G1/S cell cycle progression.
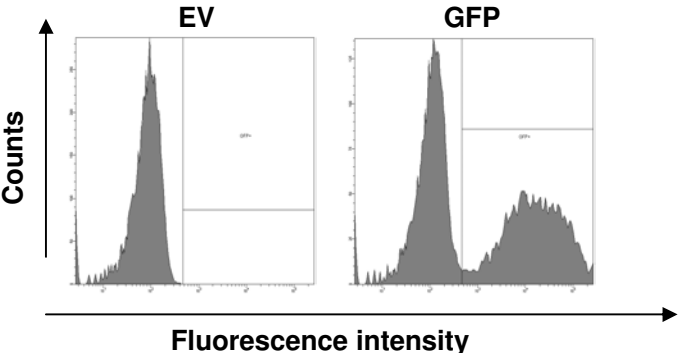
Figure 3.27   Transfection   efficiency   of   primary   paSMC   using   the   nucleofector technology.
Empty expression vector (EV) or GFP expression vector were transfected into primary paSMC and cultured for 24 h. Cells were then trypsinised and analysed for GFP expression by FACS. Panels demonstrate a 50% transfection efficiency of primary paSMC.
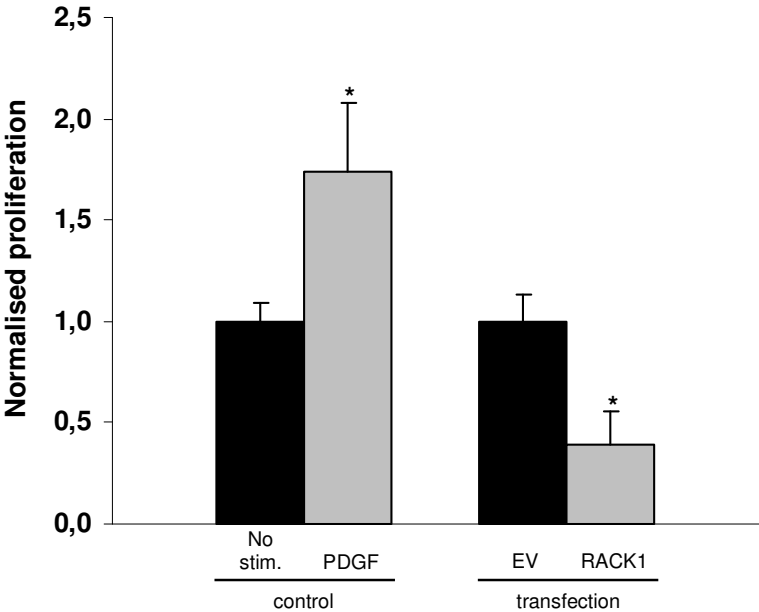
Figure 3.28   Decreased proliferation of paSMC after RACK1 overexpression.
The paSMC proliferation was assessed by direct [^{3}H]-thymidine incorporation analysis (n=3, * p< 0.001). **EV**; empty vector, **No stim**; no stimulation. Stimulation with PDGF was used as a positive control for the assay.
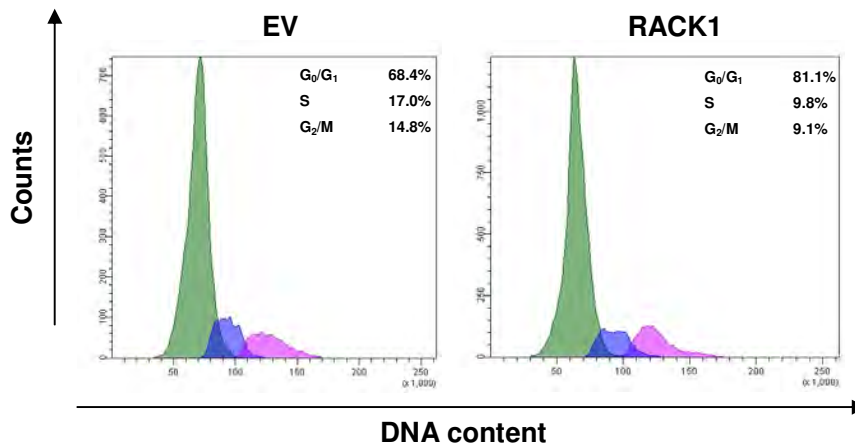
Figure 3.29   Decreased   percentage   of   the   paSMC   in   S   phase   after   RACK1 overexpression.
After transfection with EV or RACK1, synchronised paSMC were harvested after 24 h, fixed, stained, and analysed for DNA content by flow cytometry. The percentage of cells in G_0/G_1 phase (green), S phase (pink) and G_2/M phase (blue) are indicated.

3.9   Functional effect of RACK1 on BMP signalling

Using NIH/3T3 cells the functional role of RACK1 on BMP signalling was also investigated. The RACK1 was overexpressed in NIH/3T3 cells off the pcDNA mammalian expression vector, in a luciferase-based assay that evaluated BMP2 stimulation. The RACK1 overexpression led to a two-fold increase in luciferase expression after BMP2 stimulation, in comparison to the cells transfected with empty pcDNA vector (Figure 3.30). RACK1 in involved in regulation of BMP signalling, function as a positive regulator for the system.
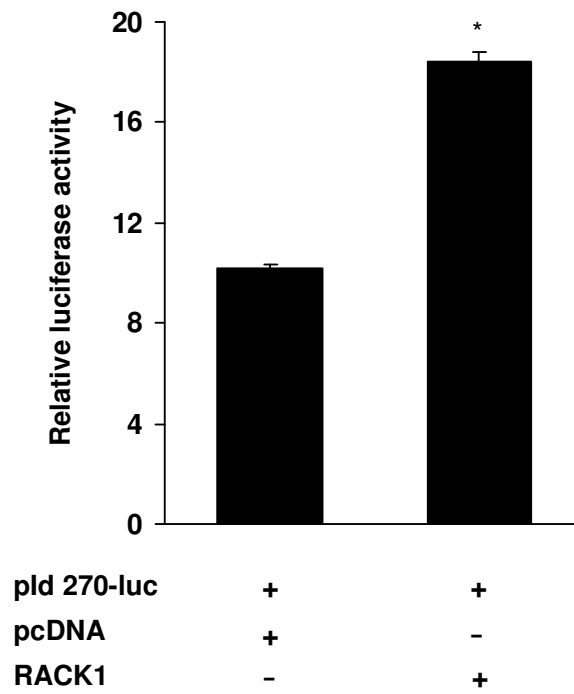
Figure 3.30   Increased luciferase activity after RACK1 overexpression.
Luciferase activation is expressed as a fold-induction between cells treated with BMP2 (20 ng/ml) and unstimulated control cells. (n=3, * p< 0.01).

4   Discussion

4.1   The yeast two-hybrid system as a powerful but limited tool in our study

In this study, RACK1 was identified as a novel interaction partner for BMPRII. The identification of RACK1 as a binding partner for BMPRII was facilitated using a yeast two-hybrid approach. The yeast two-hybrid methodology is widely employed for the detection of interacting proteins and to gain insight into protein function and signalling pathways. This assay permits the analysis of protein complexes in an intracellular setting, and can be used to screen for large numbers of possible interactions. As with any technology, the yeast two-hybrid assay has advantages and disadvantages compared to the other approaches. The assay tests protein interactions in living cells, does not require isolated proteins, and because of the signal amplification afforded using enzymes as reporters, the system is also very sensitive and can detect very transient protein-protein interactions. However, it remains an artificial system in which the proteins under investigation are chimaeric, having been fused to one of two transcription factor domains, and are also directed to the nucleus. Additionally, the yeast cell environment may not fully mimic that of mammalian cells, due to the lack of some post-translational modifications and different subcellular compartments. Some proteins have intrinsic transcriptional activation or are inherently "sticky", false-positives are common, and the rationale for eliminating these false-positives is complicated and very important. This powerful method requires confirmation with one or more independent methods (Fields and Song 1989). However, despite its limitations, the yeast two-hybrid assay has been one of the most fruitful tools for discovering and dissecting the function of protein interaction. It is estimated that over half of the protein interaction discoveries reported in literature originate from yeast two-hybrid investigations (Xenarios and Eisenberg 2001).

In the past three years, BMPRII has been intensively studied, and using this yeast two-hybrid assay, three new interacting partners have already been reported. The first molecule was identified during a search for LIM domain kinase 1 (LIMK1)-interacting proteins and yielded clones encoding the cytosolic tail region of BMPRII. Further analyses revealed that the interaction between LIMK1 and BMPRII inhibited the ability of LIMK1 to phosphorylate cofilin, which could then be overcome by the addition of BMP4. These interactions alter the dynamics of the actin cytoskeleton (Foletta et al., 2003). A second interacting molecule was identified as Tctex1, the light chain of dynein. This

molecule binds to, and it is phosphorylated by BMPRII, and is proposed to move along the microtubules and interact with downstream mediators of BMPRII, for example Smads (Machado et al., 2003). The third interacting partner discovered to date is Src kinase. The interaction between BMPRII and Src kinase inhibits Src kinase activity in the presence of BMP ligand by preventing its phosphorylation at Tyr418, and further inhibits downstream cell cycle regulators, which might influence cell proliferation (Wong et al., 2005). These discoveries have helped identify novel molecular pathways connecting BMPRII and the PAH phenotype. These findings also suggested that BMPRII might have important and diverse roles in cellular functions.

Considering that the major drawback of the yeast two-hybrid system technology is the inability to screen libraries with baits containing a transmembrane domain, novel BMPRII-interacting proteins were identified in the present study using defined intracellular BMPRII domains. These domains included the kinase, C-terminal tail and total intracellular domains of BMPRII. Prior to performing the yeast screen, bait constructs were examined for proper protein expression and autoactivation. On the grounds of autoactivation, the tail bait was eliminated from further investigations. This significantly reduced the number of false positive colonies obtained in this study. Positive clones were re-transformed into yeast and rechecked for positive interactions with the appropriate baits.

4.2   Possible candidates from yeast two-hybrid screen

To identify novel proteins interacting with BMPRII, we performed a yeast two-hybrid screen of a mouse embryonic cDNA library using the kinase domain and total intracellular segment of the BMPRII as bait. Surprisingly, this screen did not identify any of the previously described BMPRII-interacting proteins, including LIMK1, Tctex1, and Src. One possible explanation is that a different cDNA library was selected. Furthermore, the bait construct containing the C-terminal tail of the BMPRII employed in all previous investigations was excluded on grounds of autoactivation, and was replaced with the full intracellular region of the receptor. The screen did, however, identify several previously unknown interacting partners for BMPRII, and included cytosolic molecules with diverse enzymatic activity (eg. glutathione peroxidase factor 1, phosphoribosylaminoimidazole carboxylase), nuclear transcription factors (eg. eukaryotic translation elongation factor), transmembrane receptors, ion channels (eg. chloride intracellular channel 1). We selected for further investigation proteins that we considered most likely relevant to the pathogenesis of PAH.

4.2.1   PIASy

Protein inhibitor of activated STAT4 (PIASy), which belongs to a family of proteins implicated in the inhibition of cytokine signalling by STAT proteins was identified as a putative BMPRII-interacting protein (Sturm et al., 2000). This molecule is also known to function as a transcriptional cofactor for nuclear receptors, and small-ubiquitin-related modifier (SUMO) (Chun et al., 2003; Imoto et al., 2003; Galleguillos et al., 2004) . It is known that SUMO is involved in BMP signalling, where it supresses BMP2-induced signals. We hypothesised that BMPRII might be modified by sumoylation via interaction with PIASy. This BMPRII sumoylation could regulate receptor stability and/or proper membrane localisation. Analysing the BMPRII amino acids sequence, several possible sumoylation sites were identified (Figure 4.1).

However, the interaction between BMPRII and PIASy could not be confirmed by an independent method, and therefore, this aspect of the study was halted.


```
    1 MTSSLHRPFR VPWLLWAVLL VSTTAASQNQ ERLCAFKDPY QQDLGIGESR
   51 ISHENGTILC SKGSTCYGLW EKSKGDINLV KQGCWSHIGD PQECHYEECV
  101 VTTTPPSIQN GTYRFCCCST DLCNVNFTEN FPPPDTTPLS PPHSFNRDET
  151 IIIALASVSV LAVLIVALCF GYRMLTGDRK QGLHSMNMME AAAAEPSLDL
  201 DNLKLLELIG RGRYGAVYKG SLDERPVAVK VFSFANRQNF INEKNIYRVP
  251 LMEHDNIARF IVGDERLTAD GRMEYLLVME YYPNGSLCKY LSLHTSDWVS
  301 SCRLAHSVTR GLAYLHTELP RGDHYKPAIS HRDLNSRNVL VKNDGACVIS
  351 DFGLSMRLTG NRLVRPGEED NAAISEVGTI RYMAPEVLEG AVNLRDCESA
  401 LKQVDMYALG LIYWEVFMRC TDLFPGESVP DYQMAFQTEV GNHPTFEDMQ
  451 VLVSREKQRP KFPEAWKENS LAVRSLKETI EDCWDQDAEA RLTAQCAEER
  501 MAELMMIWER NKSVSPTVNP MSTAMQNERN LSHNRRVPKI GPYPDYSSSS
  551 YIEDSIHHTD SIVKNISSEH SMSSTPLTIG EKNRNSINYE RQQAQARIPS
  601 PETSVTSLST NTTTTNTTGL TPSTGMTTIS EMPYPDETHL HATNVAQSIG
  651 PTPVCLQLTE EDLETNKLDP KEVDKNLKES SDENLMEHSL KQFSGPDPLS
  701 STSSSLLYPL IKLAVEVTGQ QDFTQAANGQ ACLIPDVPPA QIYPLPKQQN
  751 LPKRPTSLPL NTKNSTKEPR LKFGNKHKSN LKQVETGVAK MNTINAAEPH
  801 VVTVTMNGVA GRSHNVNSHA ATTQYANGAV PAGQAANIVA HRSQEMLQNQ
  851 FIGEDTRLNI NSSPDEHEPL LRREQQAGHD EGVLDRLVDR RERPLEGGRT
  901 NSNNNNSNPC SEQDILTQGV TSTAADPGPS KPRRAQRPNS LDLSATNILD
  951 GSSIQIGEST QDGKSGSGEK IKRRVKTPYS LKRWRPSTWV ISTEPLDCEV
 1001 NNNGSDRAVH SKSSTAVYLA EGGTATTTVS KDIGMNCL
```

■ Motifs with high probability

■ Motifs with low probability

■ Overlapping Motifs

No.	Pos.	Group	Score	No.	Pos.	Group	Score
1	K342	SRNVL **VKND** GACVI	0.93	7	K691	LMEHS **LKQF** SGPDP	0.56
2	K976	KIKRR **VKTP** YSLKR	0.82	8	K461	REKQR **PKFP** EAWKE	0.50
3	K81	GDINL **VKQG** CWSHI	0.76	9	K964	ESTQD **GKSG** SGEKI	0.50
4	K37	ERLCA **FKDP** YQQDL	0.74	10	K753	KQQNL **PKRP** TSLPL	0.50
5	K772	TKEPR **LKFG** NKHKS	0.73	11	K539	HNRRV **PKIG** PYPDY	0.43
6	K230	ERPVA **VKVF** SFANR	0.58	12	K180	MLTGD **RKQG** LHSMN	0.27

Figure 4.1   Possible sumoylation sites in BMPRII.
Amino acids sequence of BMPRII with possible sumoylation sites indicates motifs with high and low probability of sumoylation indicated with different colour.

4.2.2   RACK1 as BMPRII-interacting protein

The most frequently observed protein interacting with BMPRII in the kinase screen was identified as RACK1. This interaction was confirmed by two independent methods: *in vitro* GST pull-down and *in vivo* co-immunoprecipitation.

The RACK1 protein is a very promising candidate in the context of BMPRII interaction partners. It is a 36 kDa cytosolic protein, composed of seven internal WD40 motifs, which are predicted to form a seven-bladed β-propeller structure with each blade made up of a β-sheet, predicted by crystallographic studies (Ron et al., 1994). Originally, RACK1 was identified based on its ability to bind to the activated form of protein PKC, stabilising the active form of PKC and permitting its translocation to different sites within the cell (Ron et al., 1994; Mochly-Rosen et al., 1995). Interestingly, RACK1 can also bind and inhibit Src family kinases (Chang et al., 1998). Through its interaction with PKC and Src kinases, RACK1 may function as a critical adaptor protein, mediating cross-talk between serine/threonine and tyrosine kinase signalling pathways. Indeed, RACK1 has many other binding partners, including integrins (Liliental and Chang 1998), the common β chain of the IL-5/IL-3/GM-CSF receptor (Geijsen et al., 1999), phospholipase C-γ and RasGAP (Chang et al., 2001), β-spectrin, dynamin (Rodriguez et al., 1999), the protein tyrosine phosphates PTPµ (Mourton et al., 2001) and a phosphodiesterase (Yarwood et al., 1999). Many reports suggest that RACK1 may act as a scaffolding protein, recruiting proteins to various transmembrane receptors and providing the platform for protein-protein interactions. Proteins that interact with RACK1 fall into two broad categories: constitutive, as with the cyclic AMP-specific phosphodiesterase PDE4D5 (Yarwood et al., 1999), and stimulus-dependent, such as PKC. The observations presented in this study describing a BMPRII and RACK1 interaction represents the constitutive category of interaction, and indeed, co-immunoprecipitation studies indicated no influence of BMP2 stimulation on this interaction. However, additional BMP ligands should also be tested.

The full range of domains that allow protein partners to interact with RACK1 have yet to be determined, however, Src homology (SH2) domains and plekstrin homology (PH) domains have already been identified as possible candidates (McCahill et al., 2002). The present study suggests that the interaction of BMPRII and RACK1 apparently involved direct binding of those molecules, but the site of interaction is not yet known. None of the identified RACK1-interaction motifs exist in BMPRII, but the fact that diverse proteins can physically interact with RACK1 suggested that RACK1 has multiple docking sites facilitating interaction with different consesus sequences not yet fully mapped. In

addition, the individual blades of the RACK1 β-propeller may be able to direct association with specific protein classes. The observation that PH domains and activated PKC can bind simultaneously to RACK1 indicates that RACK1 does indeed have multiple, independent protein binding sites (Figure 4.2).

The WD repeats of RACK1 are highly conserved across species, including plants, genetically malleable insects such as *Drosophila melanogaster*, higher mammals and humans (Vani et al., 1997). Taking this into consideration, and additional data which demonstrate that RACK1 is ubiquitously expressed in many tissues of higher mammals and humans, including brain, heart, kidney, liver, pancreas, spleen, and lung (Figure 3.15), it is likely that RACK1 plays an important functional role in many different cell types and integration signalling pathways with different physiological functions.
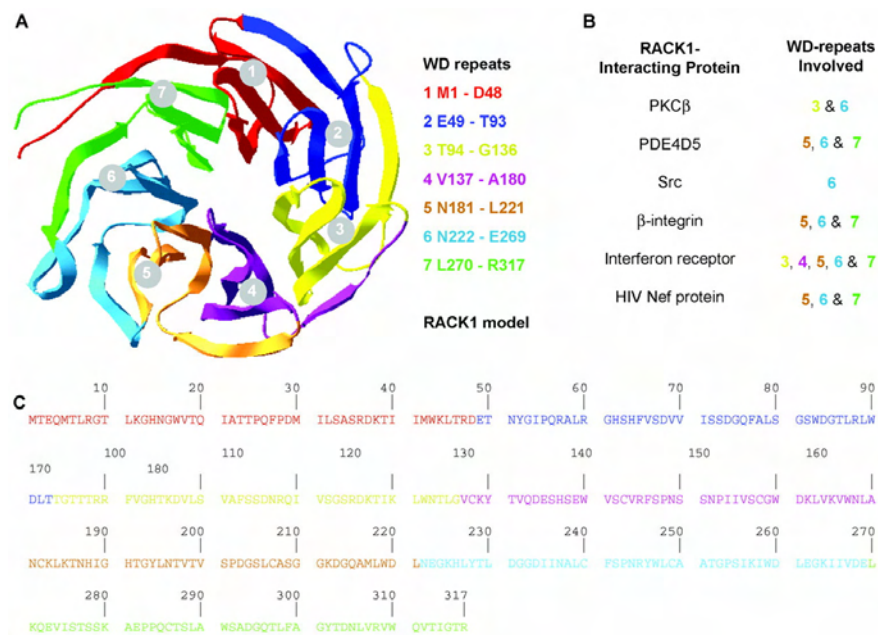
Figure 4.2   Propeller blade and WD repeats in a RACK1 structural model.
(**A**) The 7-fold β-propeller structure of RACK1; with propeller blades numbered from the N terminus and color-coding and residue numbering according to WD repeat sequences. (**B**) Proteins whose interaction with RACK1 has been mapped to particular WD repeats within RACK1, indicated by numbering and color-coding. (**C**) Linear amino acid sequence of human RACK1 including residue numbers and WD-repeat color-coding corresponding with those used in A (after Ron et al.; 1994).

4.3   Implications of RACK1-BMPRII interactions in human pathophysiology

Little is known concerning a functional role for RACK1 in physiology and pathophysiology, however*, in vivo* studies have indicated that RACK1 is up-regulated in human carcinomas and during tissue regeneration after ischaemic renal injury (Padanilam and Hammerman 1997; Berns et al., 2000).

The involvement of RACK1 in the control of cellular proliferation and growth implicated RACK1 in cancer and in angiogenesis. In agreement with these findings, RACK1 is up-regulated during all these proceses *in vitro* and *in vivo*, and in tissue associated with angiogenesis (Berns et al., 2000).

Thus, the lungs of PAH patients and donors were examined for expression of RACK1. Interestingly, expression levels of RACK1 did not exhibit significant differences between those two groups at the protein level, although mRNA expression appeared to be up-regulated in PAH patients. Similar studies were performed in the lungs of MCT-treated rats, in which RACK1 expression, both at the mRNA and at the protein levels, was significantly reduced when compared with healthy vehicle-treated rats. Two possibilities exist to explain these apparently conflicting data. Either the pathomechanism of IPAH and MCT-induced PAH are different, or that RACK1 is down-regulated during early development of the disease (for example, two and four weeks after monocrotaline treatment) while in late-stage chronic disease, compensatory mechanisms cause up-regulation of RACK1 expression.

Although RACK1 levels were not changed under pathological conditions, it has already been reported that BMPRII expression in SMC of PAH patients may be significantly decreased. Thus, it may well be that loss of the functional BMPRII-RACK1 interaction occurs not only as a result of BMPRII mutations, but also due to decreased levels of BMPRII expression independent on RACK1 expression (Atkinson et al., 2002).

4.3.1   RACK1 function: possible implications for development of pulmonary arterial hypertension

Pulmonary arterial hypertension is characterised by progressive narrowing and obstruction of small pulmonary arteries, leading to sustained elevation of pulmonary arterial pressure, progressive right heart hypertrophy and eventually, heart failure. Pulmonary vascular remodelling is the key pathological hallmark of PAH. Unlike large vessel atheromata in the systemic circulation, remodelling of the pulmonary vasculature

occurs primarily in small vessels (<500 µm diameter). Reduction in the lumenal area is caused by both a reduction in vessel number and by vessel-wall thickening. Remodelling, which occurs in all layers of the vessel-wall, includes hypertrophy (cell growth) and hyperplasia (proliferation) of vascular cells such as endothelial cells, fibroblasts and smooth muscle cells. In addition, remodelling stimulates the deposition of connective tissue matrix components such as collagen, elastin and fibronectin. There are some differences among animal models and human diseases concerning the degree of endothelial cell injury, inflammatory reactions and patterns of vascular smooth muscle hypertrophy. However, the process of remodelling is strikingly similar regardless of the initiating stimulus, suggesting a stereotypical response to the vascular injury.

Pulmonary vascular SMC undergo both hypertrophy and hyperplasia. The pattern of medial thickening is particularly characteristic of PAH associated with hypoxaemia. Smooth muscle hyperplasia results in the extension of proximal smooth muscle into distal, normally non-muscularised vessels. An important role of vascular smooth muscle in the synthesis of matrix material, such as elastin, which also contributes to the thickening of pulmonary vascular media. In precapillary segments, differentiation of pericytes and intermediate cells into myofibroblast causes extension of smooth muscle cells into partially or non-muscularised small vessels. These cells undergo phenotypic shifts towards SMC with characteristic changes in contractile and synthetic properties (Tuder et al., 1994; Durmowicz and Stenmark 1999; Jeffery and Morrell 2002; Mandegar et al., 2004).

The mechanisms of pulmonary vascular remodelling are currently the subject of intense research. Possible causal factors include physical causes, such as mechanical stretch and shear stress, and biological/physiological stimuli such as hypoxia, viral infection, vasoactive mediators and growth factors. Remodelling may also result from a lack of apoptosis (programmed cell death) of vascular cells or the lack of anti-proliferative factors.

The BMPRII plays a major role in mediating vascular smooth muscle and endothelial cell proliferation. Abnormalities in BMPRII structure due to mutations found in PAH patients might be expected to cause abnormal vascular cell proliferation. The RACK1 protein, selected by us as a new candidate for interaction with BMPRII, functions at the hub of a large array of signal transduction cascades that influence all cellular processes (proliferation, migration and cell growth), and loss of this interaction may therefore contribute to the pathogenesis of PAH.

4.3.1.1   Regulation of G_1/S cell progression and cellular growth

It has been demonstrated that RACK1 can prolong the G_0/G_1 phase of the cell cycle by inhibiting the activity of Src, and thereby the downstream cell cycle regulators including Myc, Stat3, Rho GTPases, and Vav2. Thus, overexpression of RACK1 causes suppression of cyclin D1, CDK4, and CDK2, activation of p27 and retinoblastoma, E2F1 is sequestered, and G_1/S progression is delayed. Conversely, siRNA inhibition of RACK1 expression activates Src-mediated signalling and accelerates G_1/S transition (Mamidipudi et al., 2004). Consequently, cells overexpressing RACK1 exhibited decreased growth rates by 40-50% compared with control cells transfected with empty vector (Mamidipudi et al., 2004).

4.3.1.2   Regulation of integrin-mediated adhesion and chemotactic cell migration

The RACK1 is also an important regulator of focal adhesion organisation, cell spreading, and migration. The effects of RACK1 on cell migration are at least in part mediated through the Src binding site of RACK1. Expression of RACK1 Y246F, a variant that does not bind to Src, induced a loss of central cellular adhesions, and inhibited chemotaxic cell migration. Interestingly, the Src binding site was critical for RACK1-mediated effects on protrusion and chemotactic cell migration, but not on random or haptotactic motility. This indicates that the Src binding site of RACK1 is not necessary for basal cell motility but is required specifically for directional motility during chemotaxis. This points to the interesting possibility that RACK1 may mediate cross-talk between growth factor receptors and integrins to promote directional migration towards chemotaxic gradients (Cox et al., 2003).

4.3.1.3   Regulation of protein kinase C and integrin-dependent cell migration

Cells stably or transiently overexpressing RACK1 have decreased migration compared to mock-transfected cells. The RACK1 transfectants also demonstrate an increased number of actin stress fibers and focal contacts. This effect on motility and cytoskeletal organisation did not result from RACK1 inhibition of Src. An active form did not reverse the migratory deficiency induced by RACK1 overexpression whereas overexpression of a variant with alanine substitutions in the putative PKC binding site in the third WD binding region exhibited no altered migration (Buensuceso et al., 2001).

4.3.1.4 Regulation of cell proliferation

The interaction between BMPRII and Src tyrosine kinase may inhibit Src tyrosine kinase activity in the presence of BMP ligand by reducing its phosphorylation at Tyr418. Inhibition of Src may consequently inhibit downstream cell cycle regulators such as cyclins D and E and subsequently prevent SMC proliferation. The inhibitory effect of BMP signalling on Src phosphorylation may oppose the growth signals of such mediators as 5-HT and PDGF, by down-regulation of cell cycle regulators.

Taking in to consideration all these data combined with our findings we can speculate that RACK1 might play important role in regulation of paSMC proliferation. Lost of these control might result in uncontrolled paSMC proliferation, vessels occlusion and finally development of PAH.

4.3.2   The paSMC and RACK1

Immunohistochemical studies performed in lung sections from normal and PAH patients demonstrate that BMPRII and RACK1 are expressed in the SMC of pulmonary arteries and arterioles. Co-localisation of these two molecules in the key site of pathogenic vascular remodelling observed in PAH adds weight to the potential importance of this protein in combination with BMPRII in maintaining the normal pulmonary vascular state. This finding was also confirmed by immunocytochemistry on freshly isolated paSMC, where the presence of these two molecules in the same SMC was observed.

To further determine whether PAH-associated mutations in *BMPR2* affect the interaction with RACK1, several truncated forms of the receptor containing nonsense mutations in the kinase domain of the BMPRII were tested for their ability to interact with RACK1. Surprisingly, all mutated forms of the receptor were still able to interact with RACK1, but the strength of the interaction was weaker. Every mutation in the kinase domain that generated a truncated form of BMPRII caused loss of efficiency in the binding of BMPRII to RACK1. The region between amino acids 495-530 of the kinase domain appeared to contain an important element required for stabilisation of this interaction. Alternatively, this region is important for folding of the receptor allowing for efficient interaction with RACK1. Although the expression levels of RACK1 are not altered in PAH, the possible loss of interaction with a truncated BMPRII might result in decreased BMPRII signalling.

Taken together, it appears that mutations in *BMPR2* do not completely abolish the interaction between BMPRII and RACK1, but rather change the intensity of this

interaction, which consequently effects downstream signalling, and ultimately contributes to the pathogenesis of PAH. Furthermore, in agreement with the observation in the previous study that RACK1 requires the full-length kinase domain for efficient interaction, while the tail does not seem to influence this binding.

Interestingly, abrogation of RACK1 expression by siRNA treatment resulted in significantly increased paSMC proliferation, whereas overexpression of RACK1 decreased paSMC proliferation. Taken together, these functional data derived from paSMC clearly point towards a key regulatory role of RACK1 in paSMC growth. A decrease in RACK1 expression, or a decreased RACK1/BMPRII interaction (in case of BMPRII mutations) can lead to increased smooth muscle cell proliferation, a key finding in the pathophysiology of PAH. While we do not propose that this is a dominant mechanism in all PAH patients, our data suggests that this may contribute to PAH pathogenesis in those patients with BMPRII mutations that lead to a truncation and/or loss of the BMPRII kinase domain.

4.4   Possible models for the involvement of RACK1 in the development of pulmonary arterial hypertension

Taking into consideration the model of interaction between BMPRII and c-Src proposed by Wong (Wong et al., 2005), together with the findings presented in the present study, it seems possible that RACK1 is an adaptor protein that is responsible for cross-talk between serine threonine kinases, which brings Src kinase and BMPRII together. The interaction between BMPRII and c-Src tyrosine kinase may inhibit c-Src tyrosine kinase activity in the presence of BMP ligand by reducing its phosphorylation at Tyr418 residue. The inhibition of c-Src activity by BMP signalling may inhibit downstream cell cycle regulators such as cyclins D and E and subsequently prevent SMC proliferation. Under pathological conditions, when RACK1 or BMPRII expression levels are decreased, or due to *BMPR2* mutations where RACK1 binds less efficiently to the receptor, which would alter Src activation, and may result in uncontrolled cell proliferation.

To determine the functional role of the interaction between BMPRII and RACK1, alternative functions of RACK1 in BMP signaling can be proposed. Although, the BMPRII-RACK1 interaction was ligand-independent, when RACK1 was overexpressed in a luciferase reporter assay using a BMP-responsive promoter (pId 270). RACK1 overexpression led to a two-fold increase in luciferase expression after BMP2

stimulation. These findings suggest that RACK1 is functionally significant in BMP signal transduction, for example, as a molecule required for receptor heterocomplex formation. These data suggest a potential role for RACK1 in the pathogenesis of PAH, which requires additional experimental demonstration.

4.4.1   BMP signalling and pulmonary arterial hypertension

The majority of cardiovascular abnormalities including PAH are associated with molecular, cellular, and histological alterations to the vasculature, a system ultimately defined by a single cell layer of endothelium, surrounded by vascular smooth muscle cells (VSMC), and adventitial tissue. Physiologically, vessel architecture and function is tightly controlled by a network of soluble mediators, cell-cell, and cell-matrix interactions. Many of the processes regulated by soluble factors act in a paracrine fashion on vascular wall-resident cells (Owens et al., 2004; Clark et al., 2005). Amongst these factors, members of the TGFβ superfamily, including TGFβs and BMPs are the most pleiotropic mediators and, due to the ubiquitous expression of their receptors, exhibit a series of effects on cells within the vascular system. In recent years, our knowledge about the signal transduction mechanisms of TGFβ superfamily members, and the diseases associated with perturbations to it has expanded considerably (Massague and Wotton 2000; Massague 2003; Massague et al., 2005). The TGFβ/BMP ligands are among the key factors controlling vessel physiology and pathology through multiple effects on differentiated and precursor endothelial cells, VSMC, myofibroblasts, and interstitial fibroblasts. The TGFβ and BMP isoforms essentially control endothelial and VSMC proliferation, as well as extracellular matrix (ECM) secretion and deposition by these cells (Seay et al., 2005). Knock-down animals for most members of the TGFβ superfamily are embryonically or perinatally lethal, and most of these animals exhibit severe defects in vasculogenesis [i.e. the TGFβ, TβRI (ALK5), ALK1, and Smad5 knock-downs]. In addition to its importance for normal embryogenesis, organogenesis, and development, perturbations to the TGFβ system have been associated with multiple cardiovascular diseases, such as atherosclerosis, myocardial fibrosis and pulmonary hypertension (Eickelberg et al., 2003).

The important roles for the TGFβ superfamily in endothelial and SMC growth, differentiation and matrix production reinforced the potential role of BMPRII in the vascular lesion of PAH. Disruption of TGFβ superfamily signalling as a consequence of *BMPR2* mutations and down-regulation of BMPRII expression observed under pathological conditions and down-regulation of BMP signalling in hypoxia-induced PAH

in rats and in the cell lines transiently transfected with mutant *BMPR2* might contribute to the cellular proliferation and vascular obliteration seen in these condition (Takahashi et al., 2006). In the context of these findings, transient overexpression of RACK1, which has been identified in the present study as a novel interacting partner for BMPRII, led to two-fold increase in the activity of a luciferase reporter construct containing a BMP-responsive Id promoter. From these findings, it appears that the presence of RACK1 is required for optimal BMP signalling, and lack of RACK1, or loss of, or decresaed intensity of the BMPRII-RACK1 interaction may lead to the reduction in BMP signalling commonly observed in PAH condition.

4.4.2   BMP signalling and vascular remodelling

Precise control of apoptosis and proliferation of paSMC plays a critical role in maintaining normal pulmonary vascular structure and function. In patients with PAH, hypertrophy of the pulmonary vascular wall and obliteration of small pulmonary arteries are the major causes of the elevated pulmonary vascular resistance and pulmonary arterial preassure (PAP). The pulmonary vascular remodelling is characterised by medial hypertrophy due to smooth muscle growth and is one of the most important factors contributing to the narrowing of the vascular lumen and increased the pulmonary vascular resistance.

Many vasoactive agonists, growth factors, and cytokines including BMPs regulate paSMC proliferation. Because mutations in the *BMPR2* gene have been found in familial and sporadic PAH patients, it is important to elucidate the physiological role of the BMP signalling system in the regulation of normal paSMC, and to define the BMP-mediated effects on paSMC from PAH patients.

The role of BMPs in pulmonary vascular remodelling is not easy to predict, because members of the TGFβ superfamily of ligands exert complex effects on vascular cell function, which vary depending on the cell phenotype and context. The main reported effects of the TGFβ on vascular cells are growth inhibition, cell differentiation and stimulation of collagen synthesis (McCaffrey 2000). The BMPs have been less extensively studied, but BMP7 has been shown to inhibit proliferation of human aortic SMC and increased expression of smooth muscle differentiation markers, and BMP2 inhibited vascular SMC proliferation after balloon injury in rats (Nakaoka et al., 1997; Dorai et al., 2000). Morrell *et al.* also demonstrated that BMP2, 4, and 7 inhibited the proliferation of SMC derived from normal pulmonary arteries and from patients with secondary PAH to congenital heart disease, but failed to suppress proliferation of cells

from patients with PAH. An attractive hypothesis is that a failure of the growth-inhibitory effects of BMPs of cells from PAH patients could contribute to the vascular obliteration and remodelling that characterise this condition. Interestingly, the failure to suppress growth of cells from PAH patients was observed in all cells from PAH patients, whether or not specific BMPRII mutations were identified, suggesting that defective BMP-mediated signalling might be a common factor in PAH (Morrell et al., 2001).

4.5   Conclusions and future perspectives

This study tested the hypothesis that novel interaction partners of BMPRII are essential regulators of smooth muscle cell proliferation, a key finding in PAH. The basis of this hypothesis was the observation that up to 50% of patients with familial PAH exhibit germline mutations in *BMPR*2, the gene locus encoding BMPRII. Despite this overwhelming genetic evidence for a causal involvement of *BMPR2* mutations in PAH pathogenesis, it is still unclear about the precise mechanisms that give rise to such a localised disease in the setting of a germline mutation, which leads to the expression of the mutant BMPRII protein throughout the body. As most mutations described thus far are localised to the intracellular domain and predicted to lead to a truncation of the BMPRII protein, a loss and/or gain of function due to the specific mutations is proposed to be involved in PAH pathogenesis. Indeed, several recent publications have indicated that BMPRII mutations can alter intracellular signaling by p38 kinase or Smad proteins (Yang et al., 2005; Yu et al., 2005), although there is considerable discussion on whether BMPRII mutations or its allelic loss increases or decreases Smad signalling. In addition to this idea, truncations of BMPRII could also result in the gain/loss of interaction of an as yet unknown binding partner of BMPRII, in a ligand-dependent or-independent manner. Therefore, the aim of this study was to uncover novel BMPRII-interacting proteins, elucidate their function in paSMC, and investigate their localisation and expression in healthy and diseased lungs.

In summary, the present study identified RACK1 as a novel interaction partner for BMPRII using the yeast two-hybrid system. This novel interaction was confirmed by GST pull-down and co-immunoprecipitation in mammalian cells and occurred in a BMP2-independent manner, suggesting a constitutive interaction involved in basal maintenance of the smooth muscle phenotype. Further, it was also reported that the ability of RACK1 to bind to BMPRII is significantly reduced by mutations associated with PAH, which cause a truncation of the protein in the kinase domain. Finally, co-localisation of both BMPRII and RACK1 within paSMC, a prominent site of pathological remodelling in PAH,

was demonstrated, together with the functional relevance of RACK1 expression on cell proliferation.

The plethora of cellular functions in which RACK1 has been implicated reflects the ability of this scaffolding protein to interact with a wide range of signalling proteins. Analogous to Cpc2 in yeast cells, mammalian RACK1 seems to direct cross-pathway-control by integrating communication from different signalling pathways.

These data lay the foundation for future investigations into the link between the BMP system, RACK1 and PAH and provides a new dimension to the complexity of BMP signalling and PAH which must be further elucidated.

In conclusions genetic association studies and functional genetic analyses strongly support *BMPR2* as a key genetic determinant of PAH, and other genetic factors undoubtedly play a role in the pathobiology of the disease, and its phenotypic expression. The incomplete penetrence of the disease and its genetic anticipation in families bearing mutations suggest that other genetic factors and, or environmental exposure contribute to the disease pathogenesis. Carrying a mutation in *BMPR2* does not ensure that one will invariably develop the disease: other factors appear to be required that are determined by other genes or environmental factors. While these investigations have all led to an increased understanding of BMPRII functions, we are now at a stage where novel BMPRII interaction partners play a role in pathologic smooth muscle cell funtions such as proliferation, with direct relevance to disease.

To further study the aetiology of PAH, the detailed analyses of the functional interaction of BMPRII with a novel partner, RACK1, and its potential role in PAH has to be performed, together with the whole genome expression studies in paSMC with targeted overexpression or knock-down of RACK1 (using mammalian expression vectors and siRNA technology, respectively). These studies should be complemented by whole genome location analysis using chromatin immunoprecipitation, thus identifying direct target genes of the BMP-Smads1/5. To combine state-of-the-art molecular biological and cell biological methods to analyse *in vitro* and *in vivo* roles of the aforementioned system constituts our future directions.

5   Appendix

Table 5.1   List of *BMPR2* gene polymorpisms identified in PAH patients to date
Abbreviations: **ECD**; extracellular domain, **TM**; transmembrane domain, **KD**; kinase domain, **CD**; cytoplasmic domain (after Machado et al., 2006).

Location	Domain	Amino acid change	Comments
Exon1		L5fsX29	
Exon1		P8fsX27	
Exon1		W9X	
Exon1		P15fsX31	
Exon1		W16X	
Exon2	ECD	A26Q82del	
Exon2	ECD	E31X	
Exon2	ECD	C34R	
Exon2	ECD	Y40X	
Exon2	ECD	Q42R	
Exon2	ECD	G47N	
Exon2	ECD	H53fsX	
Exon2	ECD	T57fsX20	
Exon2	ECD	C60Y	
Exon2	ECD	S64W70 del	
Exon2	ECD	C66Y	
Exon2	ECD	C66R	
Exon2	ECD	Y67C	
Exon2	ECD	G68D	
Exon2	ECD	S73X	
Exon2	ECD	Q82X	
Exon2	ECD	Q82H	
Exon2	ECD	W85X	
Exon3	ECD	Q92X	
Exon3	ECD	C94R	
Exon3	ECD	C99R	
Exon3	ECD	T102A	
Exon3	ECD	S107P	
Exon3	ECD	C117Y	
Exon3	ECD	C117S	
Exon3	ECD	C118Y	
Exon3	ECD	C118W	
Exon3	ECD	S119fsX132	
Exon3	ECD	P120fsX	
Exon3	ECD	C123S	
Exon3	ECD	C123R	
Exon4	**ECD**	**R147X**	
Exon4	TM	P169fsX12	
Exon5	TM	G182D	
Exon5	TM	M186V	
Exon6	**KD**	**R211X**	
Exon6	**KD**	**R213X**	
Exon6	KD	S221fsX3	
Exon6	KD	L222fsX7	
Exon6	KD	K230fsX25	
Exon6	KD	KK230fsX21	
Exon6	KD	E243X	
Exon6	KD	R259fsX2	
Exon6	KD	G263fsX2	
Exon6	KD	D265fsX13	
Exon6	KD	R266T	
Exon6	KD	M273R	
Exon7	KD	G285fsX5	
Exon7	KD	S301P	
Exon7	KD	R303H	
Exon7	KD	A313P	
Exon7	KD	R321X	
Exon7	KD	D323fsX	
Exon8	KD	P327X7	
Exon8	**KD**	**R332X**	
Exon8	KD	L334X	
Exon8	KD	C347R	
Exon8	KD	C347Y	
Exon8	KD	T359fsX15	
Exon8	KD	G367fsX3	
Exon8	KD	N371fsX3	
Exon8	KD	I374fsX	
Exon9	KD	C397fsX	
Exon9	KD	S399X	
Exon9	KD	L401S	
Exon9	KD	Q403X	
Exon9	KD	W414X	
Exon9	KD	I416fsX3	
Exon9	KD	F417fsX1	
Exon9	KD	R419S	
Exon9	KD	C420R	
Exon9	**KD**	**C420Y**	
Exon9	KD	P425fsX22	
Exon10	KD	T438fsX34	
Exon10	KD	Q450X	
Exon10	KD	R459fsX9	
Exon10	KD	E459fsX10	
Exon10	KD	E464fsX6	

Exon10	KD	W466X
Exon10	KD	E468fsX5
Exon11	KD	L476fsX29
Exon11	KD	C483R
Exon11	KD	D485G
Exon11	KD	A490V
Exon11	**KD**	**R491W**
Exon11	**KD**	**R491Q**
Exon11	KD	Q495X
Exon11	KD	C496Y
Exon11	CD	E503D
Exon11	CD	K512T
Exon11	CD	N519K
Exon11	CD	R529fsX34
Exon12	CD	V563M
Exon12	CD	R584X
Exon12	CD	T652fsX6
Exon12	CD	V654fsX5
Exon12	CD	L658fsX48
Exon12	CD	Y708X
Exon12	CD	N764fsX48
Exon12	CD	T766fsX5
Exon12	CD	A796fsX6
Exon12	CD	V804fsX3
Exon12	CD	T836fsX
Exon12	CD	A846fsX15
Exon12	CD	N861fsX10
Exon12	**CD**	**R873X**
Exon12	CD	E874X
Exon12	**CD**	**R899X**
Exon12	CD	R899P
Exon12	CD	N903S
Exon12	CD	S930X

Table 5.2   List of primers used for PCR amplification.
M; mouse, **H**; human, **KD**; kinase domain, **CD**; cytoplasmic domain, **ID**; intracellular domain, **T**; temperature, **bp**; base pair, bold nucleotides represent restriction sites incorporated to the primers.

GenBank™ (Accesion number)	Forward Primer (5′ to 3′)	Reverse Primer (5′ to 3′)	Annealing T (ºC)	Amplicon Size (bp)
mBMPRII (NM_007561)	TAC AGA ATG TTG ACG ACA GGA GAC CGG	TCA CAG ACA CAA TTC ATT CCT ATA TC	58	3180
mBMPRII KD (P1,P2) (NM_007561)	GAC CTG **GAA TTC** CTG AAG CTG CTG GAG	CTC CCA **GGA TCC** TCA GAG TTC AGC CAT CCT	60	900
mBMPRII CD (P3,P4) (NM_007561)	AAT GAA **GAA TTC** CTG TCA CAT AAT AAG	CTT GAA **GGA TCC** TCA CAG ACA ATT CAT	60	1500
mBMPRII ID (P5,P4) (NM_007561)	TTA TGT **GAA TTC** TAC AGA ATG TTG ACA	CTT GAA **GGA TCC** TCA CAG ACA ATT CAT	58	2500
mPIASy (NM_021501)	CAA GAT GGC GGC AGA GCT GGT	CGA GGG AAT GAT GGA CGG GTG	60	1500
mPIASy (NM_021501)	G**GA ATT C**GG ATG GCG GCA GAG CTG GTG	**CTG CTC** GAG CTA CTT GTC CTG CAT	60	1500
mRACK1 (NM_008143)	TAT CCG GTG CCA TCC TTG TCG	CC AGG GAC TCA GCT TCC AGG ACT	58	950
mRACK1 (NM_008143)	**GAATTC**GGATGACCGAGC AGATGACCCTT	**AAGCTT**GCGGGTACCAATAGTTA CC	60	950
mRACK1 (NM_008143)	**CC ATG G**GG ATG ACC GAG CAG ATG ACC CTT	**GAA TTC** TTA GCG GGT ACC AAT AGT TAC	60	950
mRACK1 (1-154aa) (NM_008143)	**G AAT TC**A TGA CCG AGC AGA TGA CCC	**A AGC TT**G ACC GAG CAG ATG ACC	57	460
mRACK1 (154-317aa) (NM_008143)	**GAA TTC** ATG CGC TTC TCC CCG AAC ACG	**AAG CTT** GCG GGT ACC AAT AGT TAC CTG	60	490
mRACK2	AT GAC GGC AGC CGA GAA GTG	TAG ACT AGT CTT CTT TTG AGA	56	2500
hRACK1 (NM_008143)	AA CCC AGA TCG CTA CTA CCG	CC CAG GAG CCT GAG AGG GCA	58	200
mRACK1 (NM_008143)	CT CAA GGG CCA TAA TGG ATG	TC GAA GAG CAC GTT GTA	60	150

Table 5.3   List of primers used for site-directed mutagenesis.
T; temperature, bold nucleotides represent exchanged nucleotides incorporated to the primers.

Primer name	Forward primer sequence 5´-3´	Reverse primer sequence 5´-3´	Annealing T (℃)
Q495X	GCT CGG CTC ACT GCA **T**AG TGT GCT GAG GAG AGG	CCT CTC CTC AGC ACA CT**A** TGC AGT GAG CCG AGC	60
W466X	AAG TTC CCA GAA GCC T**A**G AAA GAA AAT AGC CTG	CAG GCT ATT TTC TTT C**T**A GGC TTC TGG GAA CTT	60
Q450X	ACA TTT GAG GAT ATG **T**AG GTT CTT GTG TCC AGA	TCT GGA CAC AAG AAC CT**A** CAT ATC CTC AAA TTT	60
R332X	CCC GCA ATC TCC CAC **T**GA GAT TTA AAC AGC AGG	CCT GCT GTT TAA ATC TC**A** GTG GGA GAT GGC GGG	60

Table 5.4   List of siRNA sequences designed against *RACK1*.

siRNA name	Sense sequence 5´-3´	Antisense sequence 5´-3´
si #1	CAA AUA CAC UGU CCA GGA UUU	AUC CUG GAC AGU GUA UUU GUU
si #2	GAU AAG ACC AUC AUC AUG UUU	ACA UGA UGA UGG UCU UAU CUU
si #3	CCA AGG AUG UGC UGA GUG UUU	ACA CUC AGC ACA UCC UUG GUU
si #4	GAG AUA AGA CCA UCA UCA UUU	AUG AUG AUG GUC UUA UCU CUU

Table 5.5   Table of vectors and restriction sites used for cloning.

Construct name	Gene name	Vector name, Company	Restriction sites
RACK1Myc	RACK1	pCMV5A;Stratagene, USA	*EcoRI; HindIII*
RACK1	RACK1	pcDNA(-);	*EcoRI; HindIII*
R1-154	RACK1	pCMV5A;Stratagene,USA	*EcoRI; HindIII*
R154-317	RACK1	pCMV5A; Stratagene,USA	*EcoRI; HindIII*
AD-RACK1	RACK1	pACT2; Clontech; USA	*NcoI;EcoRI*
BD-BMPRII kinase	BMPRII	pGBKT7;Clontech,USA	*EcoRI; BamHI*
BD-BMPRII tail	BMPRII	pGBKT7;Clontech,USA	*EcoRI; BamHI*
BD-BMPRII total	BMPRII	pGBKT7;Clontech,USA	*EcoRI; BamHI*
GST-BMPRII kinase	BMPRII	pGEX4T1;Amersham,Germany	*BamHI;EcoRI*
BMPRII Full-length	BMPRII	pCMV-HA, Stratagene;USA	*ApaI*
Flag-PIASY	PIASy	pCMV2C; Stratagen,USA	*EcoRI;*

Table 5.6   List of antibodies used for immunoblot (IB), immunohistochemistry (IHCH), and immunocytochemistry (ICCH).

Antibodies	Host	Dilution			Company
		IB	IHCH	ICCH	
Primary antibody					
anti-BMPRII	goat	1:1000	1:50	1:50	Santa-Cruz Biotech
anti-Flag	rabbit	1:2500			Sigma-Aldrich
anti-GFP	mouse	1:1000			Santa-Cruz Biotech
anti-HA Tag	mouse	1:1000			Cell Signaling
anti-HA Tag	mouse	1:2500			Sigma-Aldrich
anti-HA Tag	rabbit	1:2500			Sigma-Aldrich
anti-Lamin A/C	rabbit	1:10000			Santa-Cruz Biotech
anti-Myc Tag	mouse	1:4000			Sigma-Aldrich
anti-Pias Y	goat	1:1000			Santa-Cruz Biotech
anti-RACK 1	mouse	1:1000	1: 50	1:50	BD
anti-phospho Smad 1/5/8	rabbit	1:1000			Cell Signaling
anti-Smad 1/2/3	mouse	1:1000			Santa-Cruz Biotech
anti-SMA	mouse	1:2500	1:300	1:300	Sigma-Aldrich
anti-Tubulin	mouse	1:1000			Santa-Cruz Biotech
Secondary antibody					
Alexa Fluor 546 anti-rabbit IgG	goat			1:250	Molecular Probes
Alexa Fluor 546 anti-mouse IgG	goat			1:250	Molecular Probes
FITC-conjugated anti-mouse IgG	goat			1:300	ZyMax
FITC-conjugated anti-rabbit IgG	goat			1:300	ZyMax
FITC-conjugated anti-goat IgG	rabbit			1:300	ZyMax
POD-conjugated anti-rabbit IgG	goat	1:10000			Pierce
POD-conjugated anti-goat IgG	rabbit	1:10000			Pierce
POD-conjugated anti-mouse IgG	goat	1:10000			Pierce

6   References

Akiyama, S., T. Katagiri, M. Namiki, N. Yamaji, N. Yamamoto, K. Miyama, H. Shibuya, N. Ueno, J. M. Wozney and T. Suda (1997). Constitutively active BMP type I receptors transduce BMP-2 signals without the ligand in C2C12 myoblasts. *Exp Cell Res* **235**(2): 362-9.

Aoki, H., M. Fujii, T. Imamura, K. Yagi, K. Takehara, M. Kato and K. Miyazono (2001). Synergistic effects of different bone morphogenetic protein type I receptors on alkaline phosphatase induction. *J Cell Sci* **114**(Pt 8): 1483-9.

Atkinson, C., S. Stewart, P. D. Upton, R. Machado, J. R. Thomson, R. C. Trembath and N. W. Morrell (2002). Primary pulmonary hypertension is associated with reduced pulmonary vascular expression of type II bone morphogenetic protein receptor. *Circulation* **105**(14): 1672-8.

Bellusci, S., R. Henderson, G. Winnier, T. Oikawa and B. L. Hogan (1996). Evidence from normal expression and targeted misexpression that bone morphogenetic protein (Bmp-4) plays a role in mouse embryonic lung morphogenesis. *Development* **122**(6): 1693-702.

Beppu, H., M. Kawabata, T. Hamamoto, A. Chytil, O. Minowa, T. Noda and K. Miyazono (2000). BMP type II receptor is required for gastrulation and early development of mouse embryos. *Dev Biol* **221**(1): 249-58.

Beppu, H., O. Minowa, K. Miyazono and M. Kawabata (1997). cDNA cloning and genomic organization of the mouse BMP type II receptor. *Biochem Biophys Res Commun* **235**(3): 499-504.

Berns, H., R. Humar, B. Hengerer, F. N. Kiefer and E. J. Battegay (2000). RACK1 is up-regulated in angiogenesis and human carcinomas. *FASEB J* **14**(15): 2549-58.

Buensuceso, C. S., D. Woodside, J. L. Huff, G. E. Plopper and T. E. O'Toole (2001). The WD protein Rack1 mediates protein kinase C and integrin-dependent cell migration. *J Cell Sci* **114**(Pt 9): 1691-8.

Chang, B. Y., M. Chiang and C. A. Cartwright (2001). The interaction of Src and RACK1 is enhanced by activation of protein kinase C and tyrosine phosphorylation of RACK1. *J Biol Chem* **276**(23): 20346-56.

Chang, B. Y., K. B. Conroy, E. M. Machleder and C. A. Cartwright (1998). RACK1, a receptor for activated C kinase and a homolog of the beta subunit of G proteins, inhibits activity of src tyrosine kinases and growth of NIH 3T3 cells. *Mol Cell Biol* **18**(6): 3245-56.

Cheever, K. H. (2005). An overview of pulmonary arterial hypertension: risks, pathogenesis, clinical manifestations, and management. *J Cardiovasc Nurs* **20**(2): 108-16; quiz 117-8.

Chen, D., M. Zhao and G. R. Mundy (2004). Bone morphogenetic proteins. *Growth Factors* **22**(4): 233-41.

Chun, T. H., H. Itoh, L. Subramanian, J. A. Iniguez-Lluhi and K. Nakao (2003). Modification of GATA-2 transcriptional activity in endothelial cells by the SUMO E3 ligase PIASy. *Circ Res* **92**(11): 1201-8.

Cox, E. A., D. Bennin, A. T. Doan, T. O'Toole and A. Huttenlocher (2003). RACK1 regulates integrin-mediated adhesion, protrusion, and chemotactic cell migration via its Src-binding site. *Mol Biol Cell* **14**(2): 658-69.

Deng, Z., J. H. Morse, S. L. Slager, N. Cuervo, K. J. Moore, G. Venetos, S. Kalachikov, E. Cayanis, S. G. Fischer, R. J. Barst, S. E. Hodge and J. A. Knowles (2000). Familial primary pulmonary hypertension (gene PPH1) is caused by mutations in the bone morphogenetic protein receptor-II gene. *Am J Hum Genet* **67**(3): 737-44.

Dorai, H., S. Vukicevic and T. K. Sampath (2000). Bone morphogenetic protein-7 (osteogenic protein-1) inhibits smooth muscle cell proliferation and stimulates the expression of markers that are characteristic of SMC phenotype in vitro. *J Cell Physiol* **184**(1): 37-45.

Durmowicz, A. G. and K. R. Stenmark (1999). Mechanisms of structural remodeling in chronic pulmonary hypertension. *Pediatr Rev* **20**(11): e91-e102.

Ebisawa, T., K. Tada, I. Kitajima, K. Tojo, T. K. Sampath, M. Kawabata, K. Miyazono and T. Imamura (1999). Characterization of bone morphogenetic protein-6 signaling pathways in osteoblast differentiation. *J Cell Sci* **112 (Pt 20)**: 3519-27.

Eddahibi, S., N. Morrell, M. P. d'Ortho, R. Naeije and S. Adnot (2002). Pathobiology of pulmonary arterial hypertension. *Eur Respir J* **20**(6): 1559-72.

Eickelberg, O., M. E. Yeager and F. Grimminger (2003). The tantalizing triplet of pulmonary hypertension-BMP receptors, serotonin receptors, and angiopoietins. *Cardiovasc Res* **60**(3): 465-7.

Fields, S. and O. Song (1989). A novel genetic system to detect protein-protein interactions. *Nature* **340**(6230): 245-6.

Foletta, V. C., M. A. Lim, J. Soosairajah, A. P. Kelly, E. G. Stanley, M. Shannon, W. He, S. Das, J. Massague and O. Bernard (2003). Direct signaling by the BMP type II receptor via the cytoskeletal regulator LIMK1. *J Cell Biol* **162**(6): 1089-98.

Foletta, V. C., N. Moussi, P. D. Sarmiere, J. R. Bamburg and O. Bernard (2004). LIM kinase 1, a key regulator of actin dynamics, is widely expressed in embryonic and adult tissues. *Exp Cell Res* **294**(2): 392-405.

Fujii, M., K. Takeda, T. Imamura, H. Aoki, T. K. Sampath, S. Enomoto, M. Kawabata, M. Kato, H. Ichijo and K. Miyazono (1999). Roles of bone morphogenetic protein type I receptors and Smad proteins in osteoblast and chondroblast differentiation. *Mol Biol Cell* **10**(11): 3801-13.

Gaine, S. P. and L. J. Rubin (1998). Primary pulmonary hypertension. *Lancet* **352**(9129): 719-25.

Galleguillos, D., A. Vecchiola, J. A. Fuentealba, V. Ojeda, K. Alvarez, A. Gomez and M. E. Andres (2004). PIASgamma represses the transcriptional activation induced by the nuclear receptor Nurr1. *J Biol Chem* **279**(3): 2005-11.

Geijsen, N., M. Spaargaren, J. A. Raaijmakers, J. W. Lammers, L. Koenderman and P. J. Coffer (1999). Association of RACK1 and PKCbeta with the common beta-chain of the IL-5/IL-3/GM-CSF receptor. *Oncogene* **18**(36): 5126-30.

Geraci, M. W., B. Gao, Y. Hoshikawa, M. E. Yeager, R. M. Tuder and N. F. Voelkel (2001). Genomic approaches to research in pulmonary hypertension. *Respir Res* **2**(4): 210-5.

Gerlach-Bank, L. M., A. D. Ellis, B. Noonen and K. F. Barald (2002). Cloning and expression analysis of the chick DAN gene, an antagonist of the BMP family of growth factors. *Dev Dyn* **224**(1): 109-15.

Harrison, R. E., J. A. Flanagan, M. Sankelo, S. A. Abdalla, J. Rowell, R. D. Machado, C. G. Elliott, I. M. Robbins, H. Olschewski, V. McLaughlin, E. Gruenig, F. Kermeen, M. Halme, A. Raisanen-Sokolowski, T. Laitinen, N. W. Morrell and R. C. Trembath (2003). Molecular and functional analysis identifies ALK-1 as the predominant cause of pulmonary hypertension related to hereditary haemorrhagic telangiectasia. *J Med Genet* **40**(12): 865-71.

Hassel, S., S. Schmitt, A. Hartung, M. Roth, A. Nohe, N. Petersen, M. Ehrlich, Y. I. Henis, W. Sebald and P. Knaus (2003). Initiation of Smad-dependent and Smad-independent signaling via distinct BMP-receptor complexes. *J Bone Joint Surg Am* **85-A Suppl 3**: 44-51.

Hata, A., G. Lagna, J. Massague and A. Hemmati-Brivanlou (1998). Smad6 inhibits BMP/Smad1 signaling by specifically competing with the Smad4 tumor suppressor. *Genes Dev* **12**(2): 186-97.

Heldin, C. H., K. Miyazono and P. ten Dijke (1997). TGF-beta signalling from cell membrane to nucleus through SMAD proteins. *Nature* **390**(6659): 465-71.

Humbert, M., N. W. Morrell, S. L. Archer, K. R. Stenmark, M. R. MacLean, I. M. Lang, B. W. Christman, E. K. Weir, O. Eickelberg, N. F. Voelkel and M. Rabinovitch (2004). Cellular and molecular pathobiology of pulmonary arterial hypertension. *J Am Coll Cardiol* **43**(12 Suppl S): 13S-24S.

Imoto, S., K. Sugiyama, R. Muromoto, N. Sato, T. Yamamoto and T. Matsuda (2003). Regulation of transforming growth factor-beta signaling by protein inhibitor of activated STAT, PIASy through Smad3. *J Biol Chem* **278**(36): 34253-8.

Iwasaki, S., M. Iguchi, K. Watanabe, R. Hoshino, M. Tsujimoto and M. Kohno (1999). Specific activation of the p38 mitogen-activated protein kinase signaling pathway and induction of neurite outgrowth in PC12 cells by bone morphogenetic protein-2. *J Biol Chem* **274**(37): 26503-10.

Jeffery, T. K. and N. W. Morrell (2002). Molecular and cellular basis of pulmonary vascular remodeling in pulmonary hypertension. *Prog Cardiovasc Dis* **45**(3): 173-202.

Kawabata, M., T. Imamura and K. Miyazono (1998). Signal transduction by bone morphogenetic proteins. *Cytokine Growth Factor Rev* **9**(1): 49-61.

Kawabata, M., H. Inoue, A. Hanyu, T. Imamura and K. Miyazono (1998). Smad proteins exist as monomers in vivo and undergo homo- and hetero-oligomerization upon activation by serine/threonine kinase receptors. *EMBO J* **17**(14): 4056-65.

Kimura, N., R. Matsuo, H. Shibuya, K. Nakashima and T. Taga (2000). BMP2-induced apoptosis is mediated by activation of the TAK1-p38 kinase pathway that is negatively regulated by Smad6. *J Biol Chem* **275**(23): 17647-52.

Kobs, R. W., N. E. Muvarak, J. C. Eickhoff and N. C. Chesler (2005). Linked mechanical and biological aspects of remodeling in mouse pulmonary arteries with hypoxia-induced hypertension. *Am J Physiol Heart Circ Physiol* **288**(3): H1209-17.

Lame, M. W., A. D. Jones, D. W. Wilson, S. K. Dunston and H. J. Segall (2000). Protein targets of monocrotaline pyrrole in pulmonary artery endothelial cells. *J Biol Chem* **275**(37): 29091-9.

Lane, K. B., R. D. Machado, M. W. Pauciulo, J. R. Thomson, J. A. Phillips, 3rd, J. E. Loyd, W. C. Nichols and R. C. Trembath (2000). Heterozygous germline mutations in BMPR2, encoding a TGF-beta receptor, cause familial primary pulmonary hypertension. The International PPH Consortium. *Nat Genet* **26**(1): 81-4.

Liliental, J. and D. D. Chang (1998). Rack1, a receptor for activated protein kinase C, interacts with integrin beta subunit. *J Biol Chem* **273**(4): 2379-83.

Liu, F., F. Ventura, J. Doody and J. Massague (1995). Human type II receptor for bone morphogenic proteins (BMPs): extension of the two-kinase receptor model to the BMPs. *Mol Cell Biol* **15**(7): 3479-86.

Machado, R. D., M. A. Aldred, V. James, R. E. Harrison, B. Patel, E. C. Schwalbe, E. Gruenig, B. Janssen, R. Koehler, W. Seeger, O. Eickelberg, H. Olschewski, C. G. Elliott, E. Glissmeyer, J. Carlquist, M. Kim, A. Torbicki, A. Fijalkowska, G. Szewczyk, J. Parma, M. J. Abramowicz, N. Galie, H. Morisaki, S. Kyotani, N. Nakanishi, T. Morisaki, M. Humbert, G. Simonneau, O. Sitbon, F. Soubrier, F. Coulet, N. W. Morrell and R. C. Trembath (2006). Mutations of the TGF-beta type II receptor BMPR2 in pulmonary arterial hypertension. *Hum Mutat* **27**(2): 121-32.

Machado, R. D., M. W. Pauciulo, J. R. Thomson, K. B. Lane, N. V. Morgan, L. Wheeler, J. A. Phillips, 3rd, J. Newman, D. Williams, N. Galie, A. Manes, K. McNeil, M. Yacoub, G. Mikhail, P. Rogers, P. Corris, M. Humbert, D. Donnai, G. Martensson, L. Tranebjaerg, J. E. Loyd, R. C. Trembath and W. C. Nichols (2001). BMPR2 haploinsufficiency as the inherited molecular mechanism for primary pulmonary hypertension. *Am J Hum Genet* **68**(1): 92-102.

Machado, R. D., N. Rudarakanchana, C. Atkinson, J. A. Flanagan, R. Harrison, N. W. Morrell and R. C. Trembath (2003). Functional interaction between BMPR-II and Tctex-1, a light chain of Dynein, is isoform-specific and disrupted by mutations underlying primary pulmonary hypertension. *Hum Mol Genet* **12**(24): 3277-86.

Maeno, M., R. C. Ong, A. Suzuki, N. Ueno and H. F. Kung (1994). A truncated bone morphogenetic protein 4 receptor alters the fate of ventral mesoderm to dorsal mesoderm: roles of animal pole tissue in the development of ventral mesoderm. *Proc Natl Acad Sci U S A* **91**(22): 10260-4.

Mamidipudi, V., J. Zhang, K. C. Lee and C. A. Cartwright (2004). RACK1 regulates G1/S progression by suppressing Src kinase activity. *Mol Cell Biol* **24**(15): 6788-98.

Mandegar, M., Y. C. Fung, W. Huang, C. V. Remillard, L. J. Rubin and J. X. Yuan (2004). Cellular and molecular mechanisms of pulmonary vascular remodeling: role in the development of pulmonary hypertension. *Microvasc Res* **68**(2): 75-103.

Massague, J. (2003). Integration of Smad and MAPK pathways: a link and a linker revisited. *Genes Dev* **17**(24): 2993-7.

Massague, J. and Y. G. Chen (2000). Controlling TGF-beta signaling. *Genes Dev* **14**(6): 627-44.

Massague, J., J. Seoane and D. Wotton (2005). Smad transcription factors. *Genes Dev* **19**(23): 2783-810.

Massague, J. and D. Wotton (2000). Transcriptional control by the TGF-beta/Smad signaling system. *EMBO J* **19**(8): 1745-54.

McCaffrey, T. A. (2000). TGF-betas and TGF-beta receptors in atherosclerosis. *Cytokine Growth Factor Rev* **11**(1-2): 103-14.

McCahill, A., J. Warwicker, G. B. Bolger, M. D. Houslay and S. J. Yarwood (2002). The RACK1 scaffold protein: a dynamic cog in cell response mechanisms. *Mol Pharmacol* **62**(6): 1261-73.

McLaughlin, V. V., A. Shillington and S. Rich (2002). Survival in primary pulmonary hypertension: the impact of epoprostenol therapy. *Circulation* **106**(12): 1477-82.

Mehra, A., L. Attisano and J. L. Wrana (2000). Characterization of Smad phosphorylation and Smad-receptor interaction. *Methods Mol Biol* **142**: 67-78.

Miyazono, K., K. Kusanagi and H. Inoue (2001). Divergence and convergence of TGF-beta/BMP signaling. *J Cell Physiol* **187**(3): 265-76.

Miyazono, K., S. Maeda and T. Imamura (2005). BMP receptor signaling: transcriptional targets, regulation of signals, and signaling cross-talk. *Cytokine Growth Factor Rev* **16**(3): 251-63.

Miyazono, K., P. ten Dijke and C. H. Heldin (2000). TGF-beta signaling by Smad proteins. *Adv Immunol* **75**: 115-57.

Mochly-Rosen, D., B. L. Smith, C. H. Chen, M. H. Disatnik and D. Ron (1995). Interaction of protein kinase C with RACK1, a receptor for activated C-kinase: a role in beta protein kinase C mediated signal transduction. *Biochem Soc Trans* **23**(3): 596-600.

Moore, R. K., F. Otsuka and S. Shimasaki (2003). Molecular basis of bone morphogenetic protein-15 signaling in granulosa cells. *J Biol Chem* **278**(1): 304-10.

Morisaki, H., N. Nakanishi, S. Kyotani, A. Takashima, H. Tomoike and T. Morisaki (2004). BMPR2 mutations found in Japanese patients with familial and sporadic primary pulmonary hypertension. *Hum Mutat* **23**(6): 632.

Morrell, N. W., X. Yang, P. D. Upton, K. B. Jourdan, N. Morgan, K. K. Sheares and R. C. Trembath (2001). Altered growth responses of pulmonary artery smooth muscle cells from patients with primary pulmonary hypertension to transforming growth factor-beta(1) and bone morphogenetic proteins. *Circulation* **104**(7): 790-5.

Mourton, T., C. B. Hellberg, S. M. Burden-Gulley, J. Hinman, A. Rhee and S. M. Brady-Kalnay (2001). The PTPmu protein-tyrosine phosphatase binds and recruits the scaffolding protein RACK1 to cell-cell contacts. *J Biol Chem* **276**(18): 14896-901.

Murakami, G., T. Watabe, K. Takaoka, K. Miyazono and T. Imamura (2003). Cooperative inhibition of bone morphogenetic protein signaling by Smurf1 and inhibitory Smads. *Mol Biol Cell* **14**(7): 2809-17.

Nakaoka, T., K. Gonda, T. Ogita, Y. Otawara-Hamamoto, F. Okabe, Y. Kira, K. Harii, K. Miyazono, Y. Takuwa and T. Fujita (1997). Inhibition of rat vascular smooth muscle proliferation in vitro and in vivo by bone morphogenetic protein-2. *J Clin Invest* **100**(11): 2824-32.

Namiki, M., S. Akiyama, T. Katagiri, A. Suzuki, N. Ueno, N. Yamaji, V. Rosen, J. M. Wozney and T. Suda (1997). A kinase domain-truncated type I receptor blocks bone morphogenetic protein-2-induced signal transduction in C2C12 myoblasts. *J Biol Chem* **272**(35): 22046-52.

Newman, J. H., R. C. Trembath, J. A. Morse, E. Grunig, J. E. Loyd, S. Adnot, F. Coccolo, C. Ventura, J. A. Phillips, 3rd, J. A. Knowles, B. Janssen, O. Eickelberg, S. Eddahibi, P. Herve, W. C. Nichols and G. Elliott (2004). Genetic basis of pulmonary arterial hypertension: current understanding and future directions. *J Am Coll Cardiol* **43**(12 Suppl S): 33S-39S.

Newman, J. H., L. Wheeler, K. B. Lane, E. Loyd, R. Gaddipati, J. A. Phillips, 3rd and J. E. Loyd (2001). Mutation in the gene for bone morphogenetic protein receptor II as a cause of primary pulmonary hypertension in a large kindred. *N Engl J Med* **345**(5): 319-24.

Nishihara, A., T. Watabe, T. Imamura and K. Miyazono (2002). Functional heterogeneity of bone morphogenetic protein receptor-II mutants found in patients with primary pulmonary hypertension. *Mol Biol Cell* **13**(9): 3055-63.

Nishimura, T., L. T. Vaszar, J. L. Faul, G. Zhao, G. J. Berry, L. Shi, D. Qiu, G. Benson, R. G. Pearl and P. N. Kao (2003). Simvastatin rescues rats from fatal pulmonary hypertension by inducing apoptosis of neointimal smooth muscle cells. *Circulation* **108**(13): 1640-5.

Nishitoh, H., H. Ichijo, M. Kimura, T. Matsumoto, F. Makishima, A. Yamaguchi, H. Yamashita, S. Enomoto and K. Miyazono (1996). Identification of type I and type II serine/threonine kinase receptors for growth/differentiation factor-5. *J Biol Chem* **271**(35): 21345-52.

Nohe, A., S. Hassel, M. Ehrlich, F. Neubauer, W. Sebald, Y. I. Henis and P. Knaus (2002). The mode of bone morphogenetic protein (BMP) receptor oligomerization determines different BMP-2 signaling pathways. *J Biol Chem* **277**(7): 5330-8.

Onichtchouk, D., Y. G. Chen, R. Dosch, V. Gawantka, H. Delius, J. Massague and C. Niehrs (1999). Silencing of TGF-beta signalling by the pseudoreceptor BAMBI. *Nature* **401**(6752): 480-5.

Padanilam, B. J. and M. R. Hammerman (1997). Ischemia-induced receptor for activated C kinase (RACK1) expression in rat kidneys. *Am J Physiol* **272**(2 Pt 2): F160-6.

Pietra, G. G. (1994). Histopathology of primary pulmonary hypertension. *Chest* **105**(2 Suppl): 2S-6S.

Pietra, G. G., F. Capron, S. Stewart, O. Leone, M. Humbert, I. M. Robbins, L. M. Reid and R. M. Tuder (2004). Pathologic assessment of vasculopathies in pulmonary hypertension. *J Am Coll Cardiol* **43**(12 Suppl S): 25S-32S.

Rich, S., D. R. Dantzker, S. M. Ayres, E. H. Bergofsky, B. H. Brundage, K. M. Detre, A. P. Fishman, R. M. Goldring, B. M. Groves, S. K. Koerner and et al. (1987). Primary pulmonary hypertension. A national prospective study. *Ann Intern Med* **107**(2): 216-23.

Robbins, I. M. (2004). Advancing therapy for pulmonary arterial hypertension: can animal models help? *Am J Respir Crit Care Med* **169**(1): 5-6.

Rodriguez, M. M., D. Ron, K. Touhara, C. H. Chen and D. Mochly-Rosen (1999). RACK1, a protein kinase C anchoring protein, coordinates the binding of activated protein kinase C and select pleckstrin homology domains in vitro. *Biochemistry* **38**(42): 13787-94.

Ron, D., C. H. Chen, J. Caldwell, L. Jamieson, E. Orr and D. Mochly-Rosen (1994). Cloning of an intracellular receptor for protein kinase C: a homolog of the beta subunit of G proteins. *Proc Natl Acad Sci U S A* **91**(3): 839-43.

Rosenzweig, B. L., T. Imamura, T. Okadome, G. N. Cox, H. Yamashita, P. ten Dijke, C. H. Heldin and K. Miyazono (1995). Cloning and characterization of a human type II receptor for bone morphogenetic proteins. *Proc Natl Acad Sci U S A* **92**(17): 7632-6.

Rudarakanchana, N., J. A. Flanagan, H. Chen, P. D. Upton, R. Machado, D. Patel, R. C. Trembath and N. W. Morrell (2002). Functional analysis of bone morphogenetic protein type II receptor mutations underlying primary pulmonary hypertension. *Hum Mol Genet* **11**(13): 1517-25.

Sakou, T. (1998). Bone morphogenetic proteins: from basic studies to clinical approaches. *Bone* **22**(6): 591-603.

Seay, U., D. Sedding, S. Krick, M. Hecker, W. Seeger and O. Eickelberg (2005). Transforming growth factor-beta-dependent growth inhibition in primary vascular smooth muscle cells is p38-dependent. *J Pharmacol Exp Ther* **315**(3): 1005-12.

Sekiya, T., S. Adachi, K. Kohu, T. Yamada, O. Higuchi, Y. Furukawa, Y. Nakamura, T. Nakamura, K. Tashiro, S. Kuhara, S. Ohwada and T. Akiyama (2004). Identification of BMP and activin membrane-bound inhibitor (BAMBI), an inhibitor of transforming growth factor-beta signaling, as a target of the beta-catenin pathway in colorectal tumor cells. *J Biol Chem* **279**(8): 6840-6.

Shimasaki, S., R. K. Moore, F. Otsuka and G. F. Erickson (2004). The bone morphogenetic protein system in mammalian reproduction. *Endocr Rev* **25**(1): 72-101.

Simonneau, G., N. Galie, L. J. Rubin, D. Langleben, W. Seeger, G. Domenighetti, S. Gibbs, D. Lebrec, R. Speich, M. Beghetti, S. Rich and A. Fishman (2004). Clinical classification of pulmonary hypertension. *J Am Coll Cardiol* **43**(12 Suppl S): 5S-12S.

Souchelnytskyi, S., L. Ronnstrand, C. H. Heldin and P. ten Dijke (2001). Phosphorylation of Smad signaling proteins by receptor serine/threonine kinases. *Methods Mol Biol* **124**: 107-20.

Strange, J. W., J. Wharton, P. G. Phillips and M. R. Wilkins (2002). Recent insights into the pathogenesis and therapeutics of pulmonary hypertension. *Clin Sci (Lond)* **102**(3): 253-68.

Sturm, S., M. Koch and F. A. White (2000). Cloning and analysis of a murine PIAS family member, PIASgamma, in developing skin and neurons. *J Mol Neurosci* **14**(1-2): 107-21.

Sugiyama, S., H. Hirota, M. Yoshida, Y. Takemura, Y. Nakaoka, Y. Oshima, K. Terai, M. Izumi, Y. Fujio, S. Hasegawa, T. Mano, Y. Nakatsuchi, M. Hori, K. Yamauchi-Takihara and I. Kawase (2004). Novel insertional mutation in the bone morphogenetic protein receptor type II associated with sporadic primary pulmonary hypertension. *Circ J* **68**(6): 592-4.

Suzuki, A., R. S. Thies, N. Yamaji, J. J. Song, J. M. Wozney, K. Murakami and N. Ueno (1994). A truncated bone morphogenetic protein receptor affects dorsal-ventral patterning in the early Xenopus embryo. *Proc Natl Acad Sci U S A* **91**(22): 10255-9.

Takahashi, H., N. Goto, Y. Kojima, Y. Tsuda, Y. Morio, M. Muramatsu and Y. Fukuchi (2006). Downregulation of type II bone morphogenetic protein receptor in hypoxic pulmonary hypertension. *Am J Physiol Lung Cell Mol Physiol* **290**(3): L450-8.

ten Dijke, P. and C. S. Hill (2004). New insights into TGF-beta-Smad signalling. *Trends Biochem Sci* **29**(5): 265-73.

ten Dijke, P., K. Miyazono and C. H. Heldin (1996). Signaling via hetero-oligomeric complexes of type I and type II serine/threonine kinase receptors. *Curr Opin Cell Biol* **8**(2): 139-45.

Thomson, J., R. Machado, M. Pauciulo, N. Morgan, M. Yacoub, P. Corris, K. McNeil, J. Loyd, W. Nichols and R. Trembath (2001). Familial and sporadic primary pulmonary hypertension is caused by BMPR2 gene mutations resulting in haploinsufficiency of the bone morphogenetic protein type II receptor. *J Heart Lung Transplant* **20**(2): 149.

Thomson, J. R., R. D. Machado, M. W. Pauciulo, N. V. Morgan, M. Humbert, G. C. Elliott, K. Ward, M. Yacoub, G. Mikhail, P. Rogers, J. Newman, L. Wheeler, T. Higenbottam, J. S. Gibbs, J. Egan, A. Crozier, A. Peacock, R. Allcock, P. Corris, J. E. Loyd, R. C. Trembath and W. C. Nichols (2000). Sporadic primary pulmonary hypertension is associated with germline mutations of the gene encoding BMPR-II, a receptor member of the TGF-beta family. *J Med Genet* **37**(10): 741-5.

Trembath, R. C. (2001). Mutations in the TGF-beta type 1 receptor, ALK1, in combined primary pulmonary hypertension and hereditary haemorrhagic telangiectasia, implies pathway specificity. *J Heart Lung Transplant* **20**(2): 175.

Tuder, R. M., B. Groves, D. B. Badesch and N. F. Voelkel (1994). Exuberant endothelial cell growth and elements of inflammation are present in plexiform lesions of pulmonary hypertension. *Am J Pathol* **144**(2): 275-85.

Uehara, R., H. Suzuki, N. Kurokawa, T. Urashima, M. Fujiwara, M. Matoba and Y. Eto (2002). Novel nonsense mutation of the BMPR-II gene in a Japanese patient with familial primary pulmonary hypertension. *Pediatr Int* **44**(4): 433-5.

Vani, K., G. Yang and J. Mohler (1997). Isolation and cloning of a Drosophila homolog to the mammalian RACK1 gene, implicated in PKC-mediated signalling. *Biochim Biophys Acta* **1358**(1): 67-71.

Ventura, F., J. Doody, F. Liu, J. L. Wrana and J. Massague (1994). Reconstitution and transphosphorylation of TGF-beta receptor complexes. *EMBO J* **13**(23): 5581-9.

Vitt, U. A., S. Y. Hsu and A. J. Hsueh (2001). Evolution and classification of cystine knot-containing hormones and related extracellular signaling molecules. *Mol Endocrinol* **15**(5): 681-94.

Vitt, U. A., S. Mazerbourg, C. Klein and A. J. Hsueh (2002). Bone morphogenetic protein receptor type II is a receptor for growth differentiation factor-9. *Biol Reprod* **67**(2): 473-80.

Warburton, D., S. Bellusci, P. M. Del Moral, V. Kaartinen, M. Lee, D. Tefft and W. Shi (2003). Growth factor signaling in lung morphogenetic centers: automaticity, stereotypy and symmetry. *Respir Res* **4**(1): 5.

West, J., K. Fagan, W. Steudel, B. Fouty, K. Lane, J. Harral, M. Hoedt-Miller, Y. Tada, J. Ozimek, R. Tuder and D. M. Rodman (2004). Pulmonary hypertension in transgenic mice expressing a dominant-negative BMPRII gene in smooth muscle. *Circ Res* **94**(8): 1109-14.

Wieser, R., J. L. Wrana and J. Massague (1995). GS domain mutations that constitutively activate T beta R-I, the downstream signaling component in the TGF-beta receptor complex. *EMBO J* **14**(10): 2199-208.

Wong, W. K., J. A. Knowles and J. H. Morse (2005). Bone morphogenetic protein receptor type II C-terminus interacts with c-Src: implication for a role in pulmonary arterial hypertension. *Am J Respir Cell Mol Biol* **33**(5): 438-46.

Wozney, J. M., V. Rosen, A. J. Celeste, L. M. Mitsock, M. J. Whitters, R. W. Kriz, R. M. Hewick and E. A. Wang (1988). Novel regulators of bone formation: molecular clones and activities. *Science* **242**(4885): 1528-34.

Wrana, J. L. (2000). Crossing Smads. *Sci STKE* **2000**(23): RE1.

Wrana, J. L. (2000). Regulation of Smad activity. *Cell* **100**(2): 189-92.

Wrana, J. L. and L. Attisano (2000). The Smad pathway. *Cytokine Growth Factor Rev* **11**(1-2): 5-13.

Wrana, J. L., L. Attisano, R. Wieser, F. Ventura and J. Massague (1994). Mechanism of activation of the TGF-beta receptor. *Nature* **370**(6488): 341-7.

Xenarios, I. and D. Eisenberg (2001). Protein interaction databases. *Curr Opin Biotechnol* **12**(4): 334-9.

Yamashita, H. and K. Miyazono (1999). [Bone morphogenetic protein (BMP) receptors and signal transduction]. *Nippon Rinsho* **57**(1): 220-6.

Yamashita, H., P. Ten Dijke, C. H. Heldin and K. Miyazono (1996). Bone morphogenetic protein receptors. *Bone* **19**(6): 569-74.

Yang, X., L. Long, M. Southwood, N. Rudarakanchana, P. D. Upton, T. K. Jeffery, C. Atkinson, H. Chen, R. C. Trembath and N. W. Morrell (2005). Dysfunctional Smad signaling contributes to abnormal smooth muscle cell proliferation in familial pulmonary arterial hypertension. *Circ Res* **96**(10): 1053-63.

Yarwood, S. J., M. R. Steele, G. Scotland, M. D. Houslay and G. B. Bolger (1999). The RACK1 signaling scaffold protein selectively interacts with the cAMP-specific phosphodiesterase PDE4D5 isoform. *J Biol Chem* **274**(21): 14909-17.

Yoshida, Y., S. Tanaka, H. Umemori, O. Minowa, M. Usui, N. Ikematsu, E. Hosoda, T. Imamura, J. Kuno, T. Yamashita, K. Miyazono, M. Noda, T. Noda and T. Yamamoto (2000). Negative regulation of BMP/Smad signaling by Tob in osteoblasts. *Cell* **103**(7): 1085-97.

Yu, P. B., H. Beppu, N. Kawai, E. Li and K. D. Bloch (2005). Bone morphogenetic protein (BMP) type II receptor deletion reveals BMP ligand-specific gain of signaling in pulmonary artery smooth muscle cells. *J Biol Chem* **280**(26): 24443-50.

7 Declaration

Ich erkläre: „Ich habe die vorgelegte Dissertation selbständig, ohne unerlaubte fremde Hilfe und nur mit den Hilfen angefertigt, die ich in der Dissertation angegeben habe. Alle Textstellen, die wörtlich oder sinngemäß aus veröffentlichten oder nicht veröffentlichten Schriften entnommen sind, und alle Angaben, die auf mündlichen Auskünften beruhen, sind als solche kenntlich gemacht. Bei den von mir durchgeführten und in der Dissertation erwähnten Untersuchungen habe ich die Grundsätze guter wissenschaftlicher Praxis, wie sie in der „Satzung der Justus-Liebig-Universität Gießen zur Sicherung guter wissenschaftlicher Praxis" niedergelegt sind, eingehalten".

8   *Curriculum vitae*

PERSONAL DATA:

Name: Anna Zakrzewicz (née Krecisz)
Date of birth: 28.11.1977
Place of birth: Kielce, Poland
Nationality: Polish

EDUCATION AND QUALIFICATION:

2002 - 2004   PhD student within *„Molecular Biology and Medicine of the Lung"* (MBML). An International Graduate Program of the Justus Liebig University of Giessen, Germany.

2002 - 2006   PhD thesis at the University of Giessen Lung Center, Giessen, Germany.
                      Project: *„Functional analysis of RACK1 as a novel interaction partner of BMPRII in pulmonary arterial hypertension".*

1999 - 2001   Master Degree Program in the Department of Molecular Biology and Biotechnology, Adam Mickiewicz University, Poznan, Poland.
                      Project: *„Investigation of Le-ACS4 gene polymorphism in polish cultivars of tomatoes".*

1998 - 2000   Students' Scientific Research Group in the Department of Molecular Biology and Biotechnology, Adam Mickiewicz University, Poznan, Poland.
                      Project: *„SSCP method for genetic variability analysis of ACC synthase gene".*

1996 - 2001   Adam Mickiewicz University, Poznan, Poland.
                      Faculty of biology
                      Specialisation – Biotechnology

PRIZES:

2006   Pneumology Posterprize of the Annual Meeting of the German Society of Internal Medicine.

ORAL PRESENTATIONS:

2006   A. Zakrzewicz, M. Hecker, G. Kwapiszewska, B. Nejman, R. E. Morty, W. Seeger, W. Klepetko, and O. Eickelberg. *„Functional analyses of RACK1 as a novel interacting partner of BMPRII in PAH"* Proceedings of the American Thoracic Society 2006;3:A532.
101st International Conference of The American Thoracic Society in San Diego.

2005   A. Krecisz, R. E. Morty, W. Seeger, W. Klepetko, and O. Eickelberg. *„Identification of PIASy as a novel interaction partner of BMPRII"* Proceedings of the American Thoracic Society 2005;2:A526.
100th International Conference of The American Thoracic Society in San Diego.

POSTER PRESENTATIONS:

2006   A. Zakrzewicz, M. Hecker, G. Kwapiszewska, R.E. Morty, W. Seeger, R.T. Schermuly, O. Eickelberg. *"Receptor of Activated C Kinase (RACK)1: „Funktionelle Bedeutung als neuer Interaktionspartner des BMPRII bei Pulmonaler Hypertonie"* Medizinisce Klinik 2006;101:866.
112th Annual Meeting of the German Society of Internal Medicine in Wiesbaden.

2006   A. Zakrzewicz, M. Hecker, B. Nejmann, N. Büchner, G Kwapiszewska, R. Sandu, R.E. Morty, W. Seeger, R.T. Schermuly, O. Eickelberg. *„Bedeutung von RACK1 als neuer Interaktionspartner des BMPRII bei Pulmonaler Hypertonie".*
47th Annual Meeting of the German Society of Pneumology in Nürnberg.

2005   R. Schwappacher, S. Hassel, <u>A. Krecisz</u>, J.K. Schnitzer, M. Roth, S. Souchelnytskyi, Eickelberg O., P. Knaus. *„Characterisation of BMP Type II Receptor associated proteins"* European Journal of Cell Biology 2005;83.

18th Annual Meeting of the German Society for Cell Biology, DGZ, Heidelberg.

2001   <u>A. Krecisz</u>, G. Kwapiszewska, M. Jakubowicz. *„Polymorphism of Le-ACS4 genes in polish cultivares ot tomatoes".*

9th International Scientific Students Conference for Students and Young Doctors, Gdansk, Poland.

2000   <u>A. Krecisz,</u> G. Kwapiszewska, M. Jakubowicz. *„SSCP method for genetic variability analysis of ACC synthase genes".*

8th International Scientific Students Conference for Students and Young Doctors, Gdansk, Poland.

PUBLICATIONS:

2007   <u>Anna Zakrzewicz</u>, Matthias Hecker, Leigh M. Marsh, Grazyna Kwapiszewska, Bozena Nejman, Werner Seeger, Ralph T. Schermuly, Rory E. Morty, and Oliver Eickelberg. *„RACK1, a novel interaction partner of BMPRII, regulates smooth muscle cell proliferation in pulmonary arterial hypertension"* Circulation. 2007 Jun 12;115(23):2957-68.

2007   <u>Anna Zakrzewicz</u>, Fotini M. Kouri, Bozena Nejman, Grazyna Kwapiszewska, Matthias Hecker, Roxana Sandu, Eva Dony, Werner Seeger, Ralph T. Schermuly, Oliver Eickelberg, and Rory E. Morty. *„The TGF-β/Smad2,3 signalling axis is impaired in experimental pulmonary hypertension"* Eur Respir J. 2007 Jun;29(6):1094-104.

2007   Rory E. Morty, Bozena Nejman, Grazyna Kwapiszewska, Matthias Hecker, <u>Anna Zakrzewicz</u>, Fotini M. Kouri, Dorothea M. Peters, Rio Dumitrascu, Werner Seeger, Petra Knaus, Ralph T. Schermuly, and Oliver Eickelberg *„Dysregulated bone morphogenetic protein signaling*

in monocrotaline-induced pulmonary arterial hypertension" Arterioscler Thromb Vasc Biol. 2007 May;27(5):1072-8.

2007   Grazyna Kwapiszewska, Roger Trösner, Leigh Marsh, Sigrid Schmitt, Jochen Wilhelm, <u>Anna Zakrzewicz</u>, Monica Linder, Ardeschir Ghofrani, Ralph Theo Schermuly, Rainer Maria Bohle, Werner Seeger, Oliver Eickelberg, Ludger Fink, Norbert Weissmann *"Fhl-1, a new key protein in hypoxia-induced and idiopathic pulmonary hypertension"* (in revision).

2002   Malgorzata Jakubowicz, Jolanta Jolkowska, Grazyna Kwapiszewska, <u>Anna Krecisz</u>, Piotr Czerski *"RFLP analysis of 1-aminocyclopropane-1-carboxylate synthase ACC2 and ACC4 genes from Polish cultivars of tomato"* Acta Biochim Pol. 2002;49(4):1037-42.

9   Publications related to the thesis

2007   Anna Zakrzewicz, Matthias Hecker, Leigh M. Marsh, Grazyna
                Kwapiszewska, Bozena Nejman, Werner Seeger, Ralph T.
                Schermuly, Rory E. Morty, and Oliver Eickelberg *„RACK1, a novel
                interaction partner of BMPRII, regulates smooth muscle cell
                proliferation in pulmonary arterial hypertension"* Circulation. 2007 Jun
                12;115(23):2957-68.

2007   Rory E. Morty, Bozena Nejman, Grazyna Kwapiszewska, Matthias
                Hecker, Anna Zakrzewicz, Fotini M. Kouri, Dorothea M. Peters, Rio
                Dumitrascu, Werner Seeger, Petra Knaus, Ralph T. Schermuly, and
                Oliver Eickelberg *„Dysregulated bone morphogenetic protein signaling
                in monocrotaline-induced pulmonary arterial hypertension"* Arterioscler
                Thromb Vasc Biol. 2007 May;27(5):1072-8.

10   Acknowledgements

In the last chapter of my thesis, I want to express my sincere acknowledgments to all those who have encouraged me, with their support and suggestions, all the long way of my PhD.

My first words go to Prof. Dr. Werner Seeger and Dr. Oliver Eickelberg for providing me a great learning experience and giving me the opportunity to be a part of the international student's group, and Dr. Rory Morty, especially for sharing all his secrets about yeast-two hybrid technology and great help and patients during reading of my thesis.

Special thanks, I address to Dr. Matthias Hecker for his great help, motivation, and positive spirit obtained during my experimental work and writing time, and of course for always being on my side...

Dr. Leigh Marsh I thank for performing flow cytometric analysis.

All members of the Eickelberg group and MBML students, I thank for this time together, for stimulating discussions (not only scientifical), and support given during this time.

Polish community from Giessen, I thank for being abroad together part of my country, sharing good and bad times and perfect understanding.

My husband, Darek, I would like to thank for his support (especially during fights with all machines), encouragement during long hours of thesis writing and always being my best friend.

At the end, I would like to thank my family in Poland: mother, grandmother, and brother for their care and protection and for amazing love and support.

Finally, my deepest gratitude goes to the departed soul of my father for his unconditional love and his spiritual support throughout the last years of his life. The work I have done on this thesis I would like to dedicate to Him.